Plate buckling

Stiffened plates subjected to in-plane and out-of-plane loading

P.C.B. Zeelenberg

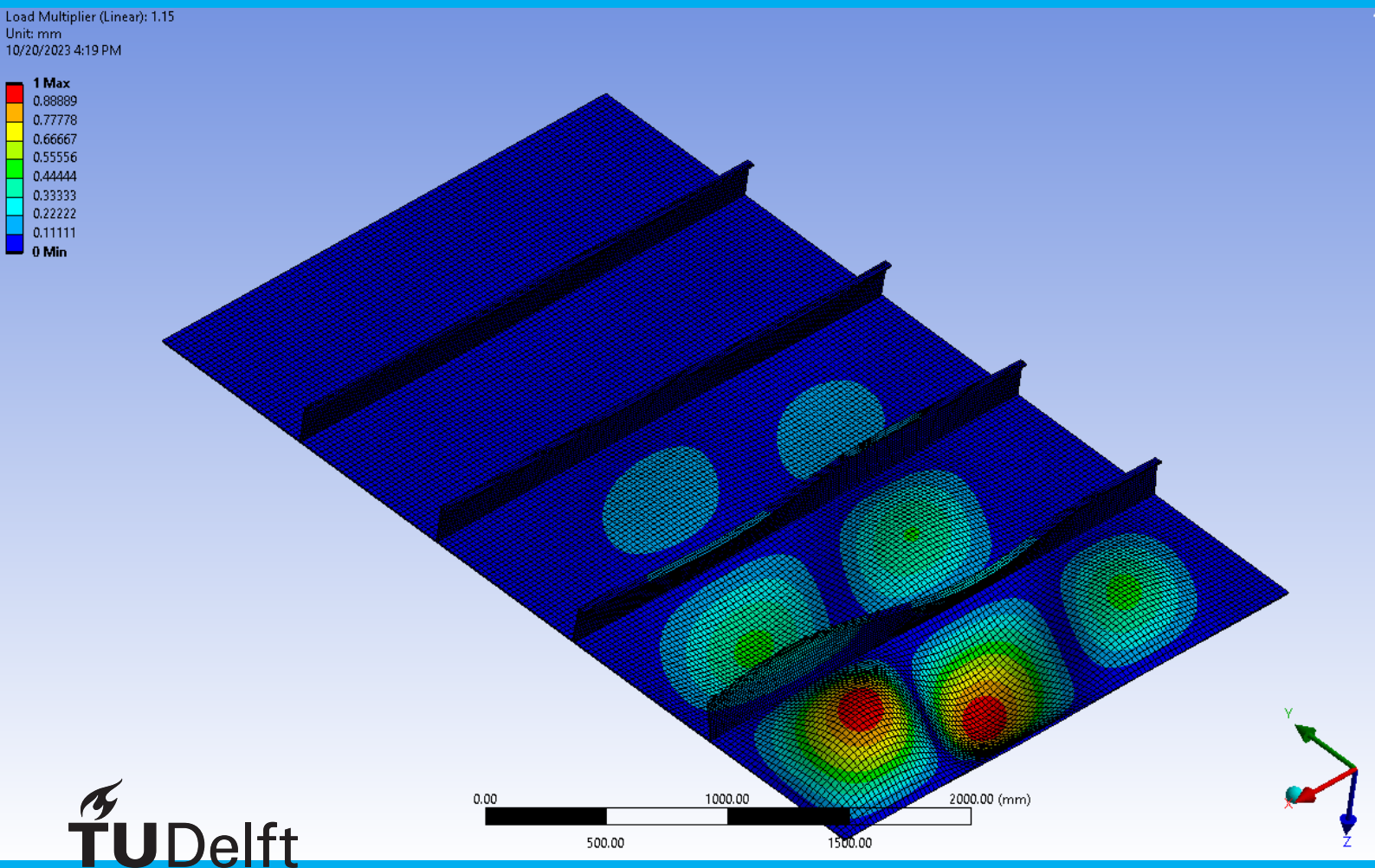

TU Delft

Plate buckling

Stiffened plates subjected to in-plane and out-of-plane loading

by

P.C.B. Zeelenberg

Report of internship conducted at McDermott International
as student of Delft University of Technology,

Student number:	4697936
Project duration:	September 4, 2023 – November 10, 2023
Supervision:	Dr. T. Tankova, TU Delft, university supervisor
	Ir. R. Kapoor, McDermott International, company supervisor

TU Delft Delft University of Technology

MCDERMOTT

Preface

This report is written in the context of the course ”CIEM020 Research Internship” as an elective in the curriculum of the MSc programme Civil Engineering at Delft University of Technology. The subject of the internship is the buckling behaviour of stiffened steel plated structures, which are intended to be used in the newest generation topsides of HVDC converter stations engineered and built by McDermott International. I would like to thank Dr. Tankova for her help and support provided as my university supervisor. Also, I would like to thank Rajat Kapoor, Mohammad Shariat Ahmadi, Budi Tjitrowirjo and Menno de Vor for their assistance and supervision at McDermott International.

P.C.B. Zeelenberg, the Hague November 2023

Summary

In the report the plate buckling verification for stiffened plates subjected to combinations of biaxial in-plane normal stress, in-plane shear stress and out-of-plane loads is performed based on Eurocodes and relevant literature. A normative panel is selected from the structure to go through the calculations step-by-step. As not much literature or information is available for the combination of in-plane stress and out-of-plane load, the main objective is to develop a reliable verification analysis for this load combination.

It was found that by combining the reduced stress method as given in EN-1993-1-5 and the simplified design method as given in EN-1993-1-7 (section 5.2.3.4) for the combination of in-plane stress and out-of-plane load, a verification is possible.

The obtained results were compared to the unity checks given by another design code (DNV-RP-C201) that has a validated design approach for this load combination for stiffened plates. The results showed large similarities in unity checks found for plates subjected to longitudinal in-plane normal stress and out-of-plane loads. In cases with high values of shear stress and for large plate thicknesses, the results for the unity check for out-of-plane loads showed less similarity.

It was recommended to perform the verification of panels subjected a combination of in-plane longitudinal normal stress, in-plane shear stress and out-of-plane loads according to the standard verification analysis given in EN-1993-1-5 (reduced stress method) and EN-1993-1-7 (simplified design method, section 5.2.3.4). For plates subjected to combinations of biaxial in-plane normal stress, in-plane shear stress and out of plane loads, it is recommended to verify the stiffeners according to EN-1993-1-5 section 9, and to check the local buckling according to the reduced stress method, as the local buckling should be normative in case the stiffeners comply with section EN-1993-1-5 section 9.

Contents

1 Introduction

1.1. Company and internship background

Mcdermott International is a globally operating contracting company active in the energy sector. Originally founded in the United States, its early enterprises consisted of the construction of oil rigs used in the Texas oil boom in the 1930s. Mcdermott delivers integrated solutions in the energy field, from engineering to procurement and construction in their yards.

As the earth's natural resources deplete and global warming as a result of the use of fossil fuels becomes increasingly problematic, the energy sector is shifting its focus towards renewable energy projects. In this context, Mcdermott is involved in an increasing number of projects related to the energy transition. Among these are hydrogen or offshore wind projects.

One of these projects is the BorWin 6 project. This project was awarded to a consortium of McDermott and Global Energy Interconnection Research Institute Co. Ltd. and C-EPRI Electric Power Engineering (GEIRI/C-EPRI) in February 2022 (renews.biz, 2023). The project consists of a 235-kilometre-long cable route to transport power from offshore wind parks off the coast of Germany to the extra-high-voltage grid in Buttel, Germany (renews.biz, 2023). The power from wind turbines is delivered as three-phase current in the BorWin Kappa platform, where it is converted into direct current. It is then transported via cables to Büttel (renews.biz, 2023).

Figure 1.1: Render of an HVDC platform. (source: internal presentation

1.2. Topsides

The term topside is used for the part of an offshore structure that is located above the waterline, out of the splash zone. In offshore engineering, topsides traditionally housed the equipment used for oil and gas extraction. However, they can also be used to house the equipment for power conversion in offshore windparks, as is the case in the Borwin 6 project. These kinds of topsides are often referred to as HVDC platforms. Next to equipment, topsides often house the living quarters for staff.

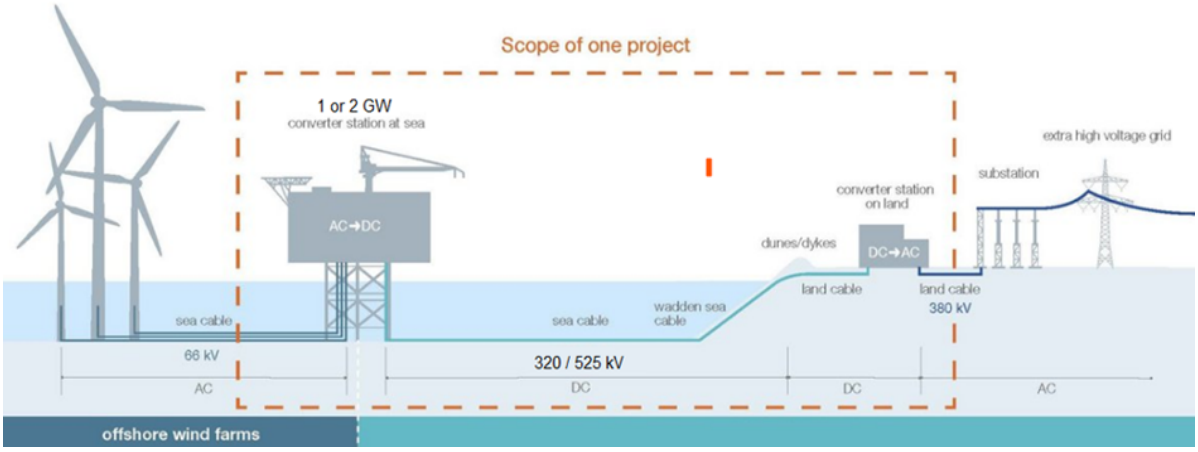

Figure 1.2: The Borwin 6 project shown. The topside is left in the red box. (van Dijk, 2023)

Topsides are traditionally constructed by making use of a post-and-beam structure. If needed, this post and beam structure can be covered with non-structural plating. Especially in the case of converter stations, it is often desired to make use of this cladding, as the equipment used for the power conversion is sensitive to the influence of (sea)water and temperature. Although relatively simple to construct, this traditional way of constructing topsides has the disadvantage that the structure is prone to leaks, endangering the cool and dry air conditions inside the topside needed for the converter equipment. For this reason, newer generations of HVDC topsides are designed to make use of a structural skin. This structural skin consists of reinforced steel plates, also referred to as a “stressed skins”. The concept of reinforced plates is already widely used in other industries, such as the airplane or shipbuilding industries. Reinforced steel plate structures are also often used as the deck of steel bridges.

These stressed skins can be checked using design codes. Examples of these are “DNV-RP-C201” and “Eurocode 3 – Design of steel structures- part 1-5: Plated structural elements” (EN-1993-1-5), and “Eurocode 3 - Design of steel structures - Part 1-7: Plated structures subject to out of plane loading” (EN-1993-1-7).

Due to the fact that topsides are subjected to high environmental loads from sea waves and strong winds, they are checked for many criteria. Among these are yielding, fatigue, buckling, and deformations. Because of the slender nature of the skins of topsides and the fact that stressed skins are required to have a structural function, they are prone to buckling behaviour. The buckling behaviour is studied in this internship report.

1.3. Research question and goal

Stressed skins on topsides are subjected to both in-plane loads and out-of-plane loads. In-plane loads may result from decks that transfer their loads to the skin or the dead weight of the stressed skin itself. Examples of out-of-plane loads are wind pressure or overpressure from the inside of the structure. The most suitable design code to use for these loadcases is the DNV-RP-C201 code. In the verification of stiffened panels, a part of the panel is examined. Both in-plane and out-of-plane loads can be checked under different structural dimensions and boundary conditions.

For the Borwin 6 project, one of the demands is that the structure complies with Eurocode. Therefore,

DNV-RP-C201 cannot be used to design the structure. Eurocode, however, does not provide such a practical approach to checking stiffened steel panels subjected to both in- and out of plane loads as DNV-RP-C201 does. EN-1993-1-5 describes plated structural elements subject to in-plane loading. Especially steel bridges and their stiffened decks have a prominent role in EN-1993-1-5. EN-1993-1-7 describes steel-plated structures subjected to out-of-plane loading and only very briefly touches upon the combination of in- and out-of-plane loading.

This leads to the following research question:

How can Eurocode be used to verify the buckling strength of a stiffened steel panel subjected to biaxial in-plane normal stress, shear stress, and out-of-plane loading?

And the following sub-questions:

- Which eurocode checks and failure modes are relevant?
- How to validate the acquired results?
- To what extent do the ground truth results and the acquired results compare?

1.4. Methodology

In order to find answers to the research question, one of the panels in the Borwin6 HVDC converter station is zoomed in on. For this panel including its loads and boundary conditions an extensive verification is carried out according to EN-1993-1-5 and EN-1993-1-7 and additional information given in relevant literature. Finally, this verification approach of the panel based on Eurocodes is compared to DNV-RP-C201 for multiple loadcases in order to validate the obtained results.

1.5. Reading guide

An overview of general plate buckling theory and the relevant design rules are given in chapter 2. Chapter 3 further specifies the structural details and load situation for the analysed panel. An extensive verification analysis according to Eurocode is performed in chapter 5. Chapter 6 thereafter performs a validation method of a crucial parameter used in the verification. A validation of the obtained unity checks is performed in chapter 6, after which a conclusion is drawn and a recommendation is made to McDermott International.

2

Plate buckling theory

Buckling is a failure mode of structures that have a high stiffness in one direction compared to another direction. In the event that a load is applied in the stiff direction, the structure may show sudden failure behaviour in the other direction. This failure mode is often observed in slender columns or plates.

Plate buckling is a failure mode of plates under compressive load in which the plate shows an out-of-plane deformation. A plate is defined as a three-dimensional structure with a certain width, length, and thickness, but with a thickness significantly smaller than both the width and length, which are of comparable size. Some fundamental principles of plate buckling theory are discussed, as well as column-like and plate-like buckling behaviour. Two verification methods are described, and their potential for verification of the analysed case.

2.1. Cross-section classification

In EN-1993-1-5 different cross-section classes are considered in order to subdivide these sections according to their slenderness. Four classes are distinguished:

- ”Class 1: cross-sections are those which can form a plastic hinge with the rotation capacity required from plastic analysis without reduction of the resistance.”
- ”Class 2: cross-sections are those which can develop their plastic moment resistance, but have limited rotation capacity because of local buckling.”
- ”Class 3 cross-sections are those in which the stress in the extreme compression fibre of the steel member assuming an elastic distribution of stresses can reach the yield strength, but local buckling is liable to prevent development of the plastic moment resistance.”
- ”Class 4 cross-sections are those in which local buckling will occur before the attainment of yield stress in one or more parts of the cross-section.”

(*Eurocode 3: Design of steel structures — Part 1-1: General rules and rules for buildings*, 2005, p. 40).

The classification can be understood as an increased risk for local buckling with higher classes and less bending capacity (Ahlstrand, 2021, p. 7). Class 4 cross sections are assumed to be thin-walled. Local buckling in these sections occurs before the most compressed fibre starts yielding; therefore, local buckling will occur even before the elastic bending moment is reached (Ahlstrand, 2021, p. 7). Members in class 4 are reduced to account for local and global buckling. These methods can be divided into two main groups: the reduced stress methods and the effective width methods.

2.2. Effective width method versus reduced stress method

The effective width method and the reduced stress method differ fundamentally in their approaches to approximating the real stress distribution in a member. In the reduced stress method, the part of the cross section with the lowest critical buckling stress is governing. It is assumed that if one element buckles, the entire cross section buckles. In case the stress in the normative element does not exceed the critical stress of the normative element, cross-section class 3 properties are assumed, and the verification can be performed as a class 3 section, multiplying the yield stress with a reduction factor (van der Burg, 2011, p. 14).

The effective width method reduces the cross-sectional area of the parts of the plate that are subject to compression (van der Burg, 2011, p. 14). In contrast to the reduced stress method, the method assumes that load shedding between cross-section elements is possible (Beg et al., 2011, p. 161). Load shedding can be understood as a buckled plate part that retains its capacity. Because of this, other parts of the plate can also reach their buckled state (van der Burg, 2011, p. 14). Because of load shedding, the plate buckling capacity found is usually slightly larger when the effective width method is used in comparison to the reduced stress method (van der Burg, 2011, p. 14).

2.3. plates loaded in compression

Plated structures can show plate-like buckling behaviour and column-like buckling behaviour. The difference between these is that a plate must be supported on at least three edges in order for plate-like behaviour to be considered (Ahlstrand, 2021, p. 10). In plate-like buckling behaviour, there is also a so-called post-buckling reserve.

This buckling reserve means that plates can still carry load of axial compressive force, bending moment, and shear force after initial buckling. A large part of this behaviour is governed by the boundary conditions of the plate. When, for instance, subjected to compressive stress, the plate will start to buckle in the center. However, the out-of-plane motion is restricted to a certain degree by the boundaries of both sides perpendicular to the compressive stresses, acting as ties. This phenomenon is shown in figure 2.1. Apart from the boundary conditions, the aspect ratio a/b also plays a role in whether a plate will show column-like or plate-like buckling behaviour. Plates with a small aspect ratio will will show more column-like behaviour.

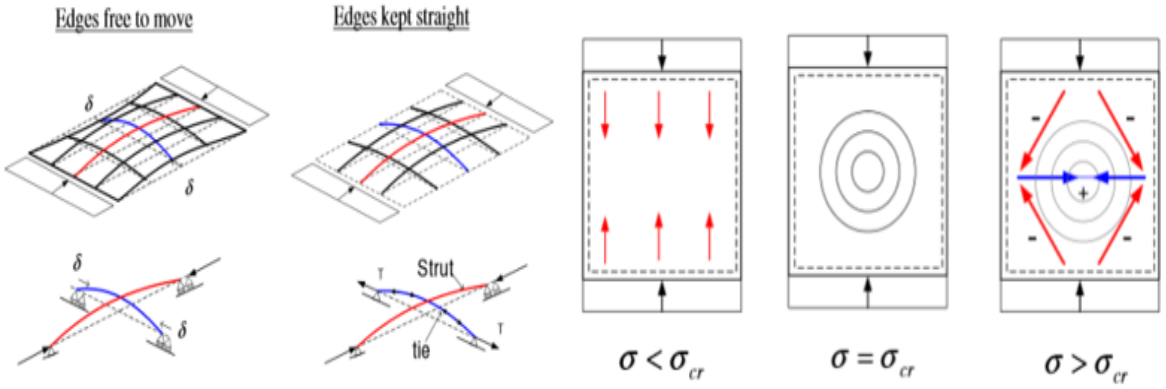

Figure 2.1: Influence of boundary conditions on the buckling behaviour (Indriðason & Sigmundsson, 2015, p. 5)

2.3.1. Euler plate buckling

Plate-like buckling behaviour is first considered. The most basic case is the so-called Euler plate buckling. The critical stress for Euler plate buckling is given by 2.1, for the case in 2.2. The factor k_σ is called the buckling factor, and depends on the support condition, load case (or stress ratio ψ), and the aspect ratio a/b (van der Burg, 2011, p. 20).

$$\sigma_{cr} = k_\sigma * \sigma_E = \frac{k_\sigma * \pi^2 * E}{12 * (1 - \nu^2)} * (\frac{t}{b})^2 \quad (2.1)$$

In which:

- σ_{crit} the critical plate buckling stress [N/mm^2]
- k_σ the buckling factor [-]
- E the Young's modulus [N/mm^2]
- ν the poisson's ratio (=0.3), [-]
- t the thickness of the plate [mm]
- b the width of the compressed edge of the plate [mm]

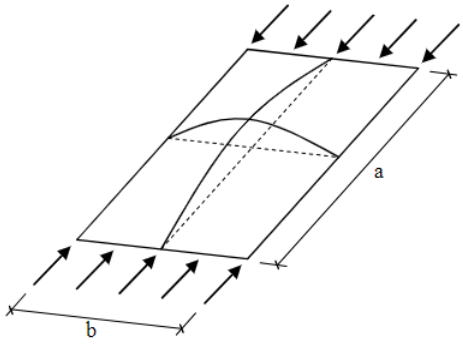

Figure 2.2: Definition of a single plate loaded in compression (Tankova, 2023, sl. 11)

The influence of the aspect ratio on the buckling factor is given by equation 2.2.

$$k_\sigma = (\frac{m}{\alpha} + \frac{\alpha}{m})^2 \quad (2.2)$$

(van der Burg, 2011, p. 20)

In which:

- m the amount of half sine waves in the element
- α the aspect ratio a/b, a=plate length, b=plate width

In most design codes, including Eurocode, the aspect ratio of plated elements is not taken into account and taken as its minimum value of 4. This is a conservative assumption, as for rather low or high aspect ratios, the buckling factor can be significantly higher, as visualised by figure 2.3.

The influence of the combination of the aspect ratio α and the support conditions on the buckling factor k_σ is visualised in figure 2.4. The red values of k_σ = 4.0 and k_σ = 0.43 are the minimum values (i.e. for large aspect ratios) obtained for support conditions referred to as "internal compression element" and "outstand compression element".

The stress ratio ψ is defined according to equation 2.3. In Eurocode the stress ratio is taken into account in combination with the support conditions by table 4.1 and 4.2.

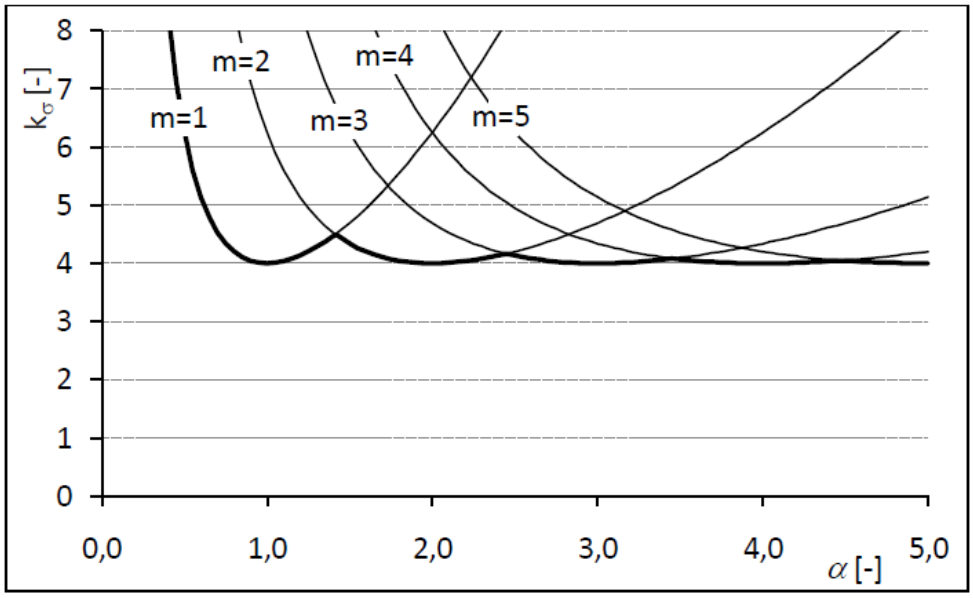

Figure 2.3: Buckling factor as function of aspect ratio. (van der Burg, 2011, p. 21)

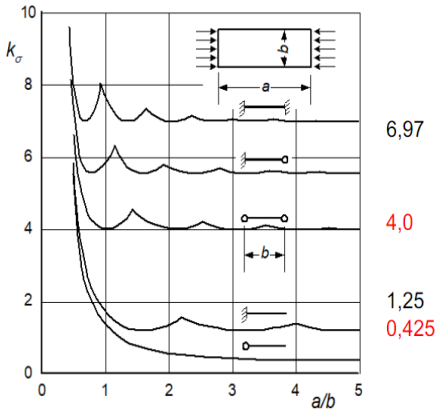

Figure 2.4: Buckling factor as function of combination of aspect ratio and support conditions. (Tankova, 2023, sl. 15)

$$\psi = \frac{max(\sigma_1, \sigma_2)}{min(\sigma_1, \sigma_2)} \tag{2.3}$$

Formula 2.1 can directly be used in a reduced stress verification. The formula can be expressed in a reduction factor, as a function of the relative plate slenderness $\lambda_{rel} = \sqrt{\frac{f_y}{\sigma_{cr}}}$:

$$N_{cr} = \sigma_{cr} * b * t = \rho * f_y * b * t$$
$$\sigma_{cr} = \rho * f_y$$
$$\rho = \frac{\sigma_{cr}}{f_y} = \frac{1}{\lambda_{rel}^2}$$

2.3.2. Von Kármán plate buckling

The elastic critical buckling stress is an approximation that assumes that the stress distribution stays linear when the stress increases. In reality, the stress at the edges of the plate becomes higher and thus moves away from the part(s) that first start to show local buckling behaviour. This real stress

distribution is a complex combined action in which the bending stresses as a result of buckling, the membrane stresses as a result of the load, and the shear stresses as a result of the rotation of the corners of the plate play a role (van der Burg, 2011, p. 22).

To account for this phenomenon of redistribution of stresses, the effective width concept was introduced by Theodore von Kármán in 1932 (van der Burg, 2011, p. 22). The effective width method assumes that a fictitious plate with an effective width and given thickness has a critical stress equal to the yield strength of the steel. In this method, the real stress distribution in the plate under compression is approximated by two strips of yield stress. The width of these two strips added is equal to the effective width of the plate, as shown in figure 2.5. The reduction factor ρ that is obtained by this method can be derived by:

$$f_y = \frac{k_\sigma * \pi^2 * E}{12*(1-\nu^2)} * (\frac{t}{b_{eff}})^2$$
$$\sigma_{cr} = \frac{k_\sigma * \pi^2 * E}{12*(1-\nu^2)} * (\frac{t}{b})^2$$
$$f_y * (\frac{b_{eff}}{t})^2 = \frac{k_\sigma * \pi^2 * E}{12*(1-\nu^2)} = \sigma_{cr} * (\frac{b}{t})^2$$
$$f_y * b_{eff}^2 = \sigma_{cr} * b^2$$
$$\frac{b_{eff}}{b} = \sqrt{\frac{\sigma_{cr}}{\lambda_{rel}}}$$
$$\rho = \frac{1}{\lambda_{rel}}$$

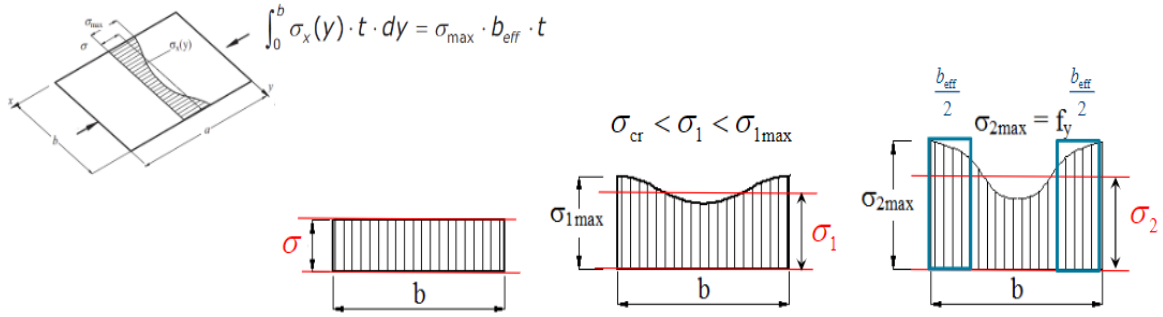

Figure 2.5: Effective width concept. (Tankova, 2023, sl. 23)

2.3.3. Winter plate buckling

The effective width method proposed by von Kármán did not yet take into account the effect of initial imperfections of plates, such as residual stresses (van der Burg, 2011, p. 23). When the method was compared to tests, it proved only valid for plates with large b/t ratios, in which initial imperfections have only a marginal impact on the buckling behaviour (van der Burg, 2011, p. 22).

For this reason, George Winter introduced a formula to calculate the effective width, taking into account initial imperfections, in 1947 (van der Burg, 2011, p. 23). The reduction factor proposed by Winter is given in equation 2.4. The Winter reduction factor is the reduction used in Eurocode to verify (un)stiffened panels.

$$\rho = \frac{b_{eff}}{b} = \frac{\lambda_{rel} - 0.22}{\lambda_{rel}^2} \tag{2.4}$$

2.4. Reduced width method in Eurocode

Eurocode describes the reduced width method in great detail. Since the choice is made to verify the final plated element using the reduced stress method, this explanation of the Eurocode approach is limited to normal force and bending moment. First the unstiffened case is described, and subsequently the stiffened case.

2.4.1. Global buckling and local buckling

In case a panel is stiffened, a distinction is made between two buckling phenomena, local buckling and global buckling. Local buckling is defined as the buckling of the panel between two stiffeners. Global buckling is defined as the buckling of the stiffener.

2.4.2. Unstiffened case

If a cross section is classified as a class 4 member, a reduction has to be made in order to account for local buckling, as described in section 2.1.

As mentioned, plated structures can show either plate-like buckling behaviour, column-like buckling behaviour, or something in between. In Eurocode, the verification of stiffened and unstiffened plated structures depends on this interaction. Plate-like buckling behaviour is described above. Eurocode uses the Winter reduced width method to determine the critical plate-like buckling stress.

Plate-like behaviour

The column-like critical buckling stress is given in equation 2.5, where a distinction is made between stiffened and unstiffened plates. The reduction is done making use of the Winter reduction, which is done making use of tables 4.1 and 4.2 and formula 2.5.

$$\rho = \begin{cases} 1, & \text{if } \lambda_p \leq 0673 \\ \frac{\bar{\lambda}_p - 0.055*(3+\psi)}{\lambda_p^2}, & \text{if } \lambda_p > 0673. \end{cases} \tag{2.5}$$

$$\overline{\lambda}_p = \sqrt{\frac{f_y}{\sigma_{cr,p}}} = \frac{\frac{b}{t}}{28.4 * \epsilon * \sqrt{k_\sigma}} \tag{2.6}$$

Using this reduction factor, the effective area of the plate can be calculated as the area in compression A_c multiplied with ρ. With this effective area, the critical plate buckling stress can be directly calculated using formula 2.1.

$$A_{c,eff} = \rho * A_c \tag{2.7}$$

column-like behaviour

In case the aspect ratio is smaller than 1, column-like buckling does not need to be taken into account, and thus also the interaction between column-like and plate-like behaviour is not needed. In case the aspect ratio does not fulfill the above requirement, the critical column-like buckling stress is calculated according to 2.8. For the interaction between column-like and plate-like buckling, the column buckling reduction factor χ_c must be calculated.

$$\sigma_{cr,c} = \frac{\pi^2 * E * t^2}{12 * (1 - \nu^2) * a^2} \tag{2.8}$$

$$\chi_c = \frac{1}{\phi + \sqrt{\phi^2 - \overline{\lambda}_c^2}} \tag{2.9}$$

Table 4.1: Internal compression elements

Stress distribution (compression positive)	Effective[p] width b_{eff}
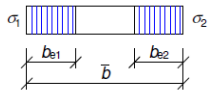	$\psi = 1$: $b_{eff} = \rho\ \bar{b}$ $b_{e1} = 0,5\ b_{eff}$ $b_{e2} = 0,5\ b_{eff}$
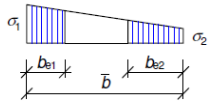	$1 > \psi \geq 0$: $b_{eff} = \rho\ \bar{b}$ $b_{e1} = \frac{2}{5-\psi} b_{eff}$ $b_{e2} = b_{eff} - b_{e1}$
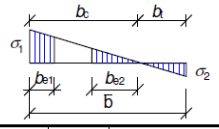	$\psi < 0$: $b_{eff} = \rho\ b_c = \rho\ \bar{b} / (1-\psi)$ $b_{e1} = 0,4\ b_{eff}$ $b_{e2} = 0,6\ b_{eff}$

$\psi = \sigma_2/\sigma_1$	1	$1 > \psi > 0$	0	$0 > \psi > -1$	-1	$-1 > \psi > -3$
Buckling factor k_σ	4,0	$8,2 / (1,05 + \psi)$	7,81	$7,81 - 6,29\psi + 9,78\psi^2$	23,9	$5,98\ (1 - \psi)^2$

Figure 2.6: Table 4.1 as given in EN-1993-1-5 (p. 17). (*Eurocode 3 — Design of steel structures — Part 1-5: Plated structural elements*, 2006)

$$\phi = 0.5[1 + 0.21 * (\bar{\lambda}_c - 0.2) + \bar{\lambda}_c^2] \tag{2.10}$$

$$\bar{\lambda}_c = \sqrt{\frac{\beta_{A,c} * f_y}{\sigma_{cr,c}}} \tag{2.11}$$

2.4.3. Stiffened case

For stiffened plates, both column-like and plate-like behaviour have to be taken into account. Also, local buckling of plates between stiffeners must be taken into account. The approach depends on whether a plate is stiffened with one, two, or multiple stiffeners in longitudinal direction.

Local Buckling

The first step is to calculate the reduction factors ρ for all the individual plate elements in between stiffeners. These panels are assumed to be unstiffened panels, and their reduction factors are therefore calculated in the same way as in the unstiffened case, as described in 2.4.2. This also holds for the individual plated elements of the stiffeners, taking into account the distinction between internal compression elements for webs and outstand compression elements for flanges. Using these reduction factors, $A_{c,eff,loc}$ is calculated. This is the effective area of the stiffeners in compression added to the effective area of the adjacent plating of these stiffeners.

$$A_{c,eff,loc} = A_{sl,eff} + \sum_c \rho_{loc} * b_{c,loc} * t \tag{2.12}$$

In which:

- $A_{sl,eff}$ the effective area of only the stiffeners
- ρ_{loc} the reduction factors for local buckling of the panels adjacent to the stiffeners
- $b_{c,loc}$ the width of the panels adjacent to the stiffeners
- t the thickness of the stiffened plate

Plate-like behaviour

Now the reduction factor for plate buckling ρ_p can be calculated using 2.5. The difference with the unstiffened case is that now the relative plate slenderness is calculated in a different way, given by 2.13.

$$\lambda_p = \sqrt{\frac{\beta_{A,c} * f_y}{\sigma_{cr,p}}} \tag{2.13}$$

$$\beta_{A,c} = \frac{A_{c,eff,loc}}{A_c} \tag{2.14}$$

In which:

- $\sigma_{cr,p}$ ciritical plate-like buckling stress, calculation depends on number of longitudinal stiffeners
- A_c The gross area of the compression zone of the stiffened plate, except the parts of subpanels that are supported by an adjacent plate, see figure 2.7

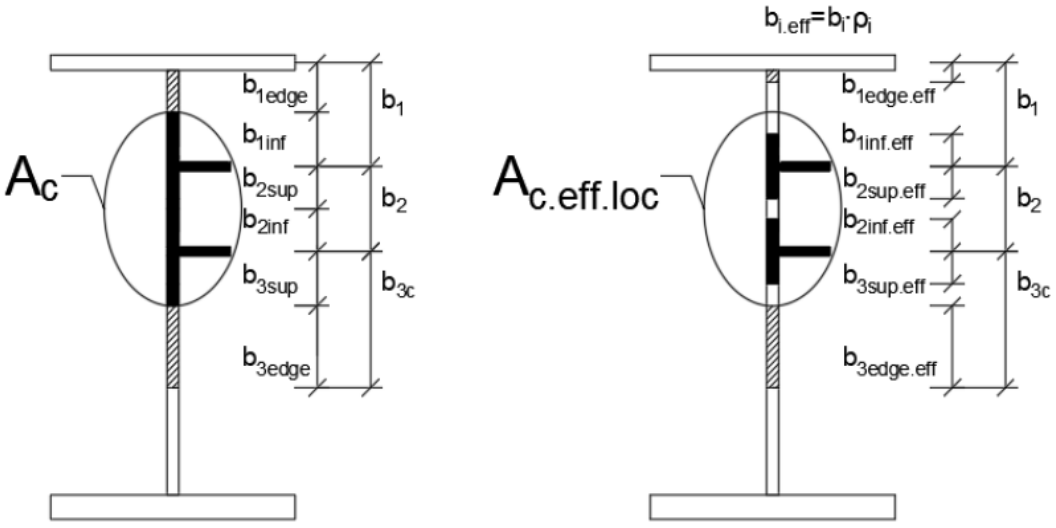

Figure 2.7: Definition of $A_{c,eff,loc}$ and A_c for a stiffened plate stiffened with two longitudinal stiffeners (Ahlstrand, 2021, p. 17)

The critical plate-like buckling stress σ_p depends on the amount of stiffeners in longitudinal direction. In cases where this amount is greater than two, the equivalent orthotropic assumption is used, in which the critical plate-like buckling stress is calculated with 2.1. The buckling coefficient $k_{\sigma,p}$ is in this case determined according to 2.15.

$$k_{\sigma,p} = \begin{cases} \frac{2*((1+\alpha^2)^2+\gamma-1)}{\alpha^2*(\psi+1)*(1+\delta)}, & \text{if } \alpha \leq \sqrt[4]{\gamma} \\ \frac{4*(1+\sqrt{\gamma})}{(\psi+1)*(1+\delta}, & \text{if } \alpha > \sqrt[4]{\gamma}. \end{cases} \tag{2.15}$$

In which:

- $\psi = \frac{\sigma_2}{\sigma_1} \geq 0.5$
- $\gamma = \frac{I_{sl}}{I_p}$
- $\delta = \frac{\sum A_{sl}}{A_p}$

- $\alpha = \frac{a}{b} \leq 0.5$

With:

- I_{sl} the second moment of area of the whole stiffened plate
- I_p the second moment of area for bending of the plate $= \frac{bt^3}{12(1-\nu^2)}$
- $\sum A_{sl}$ the sum of gross areas of the individual longitudinal stiffeners
- A_p the gross area of the plate $= bt$
- σ_1 the larger edge stress
- σ_2 the smaller edge stress

width	Gross width	Effective width	Condition for ψ_i
$b_{1,inf}$	$\frac{3-\psi_1}{5-\psi_1} b_1$	$\frac{3-\psi_1}{5-\psi_1} b_{1,eff}$	$\psi_1 = \frac{\sigma_{cr,sl,1}}{\sigma_{cr,p}} \geq 0$
$b_{2,sup}$	$\frac{2}{5-\psi_2} b_2$	$\frac{2}{5-\psi_2} b_{2,eff}$	$\psi_2 = \frac{\sigma_2}{\sigma_{cr,sl,1}} \geq 0$
$b_{2,inf}$	$\frac{3-\psi_2}{5-\psi_2} b_2$	$\frac{3-\psi_2}{5-\psi_2} b_{2,eff}$	$\psi \leq 0$
$b_{3,sup}$	$0.4 b_{3c}$	$0.4 b_{3c,eff}$	$\psi_3 = \frac{\sigma_3}{\sigma_2} \leq 0$

Table 2.1: Contributing parts of the subpanels adjacent to stiffeners for linearly distributed stresses, see figure 2.7

In case the panel is stiffened with one or two longitudinal stiffeners, a simplification may be made. Eurocode simplifies this case to a fictitious isolated strut supported on an elastic foundation, as shown in figure 2.8. The critical plate-buckling stress can in this case directly be determined as the elastic critical buckling stress of the most compressed stiffener extrapolated to the most compressed edge of the plate (see equation 2.19).

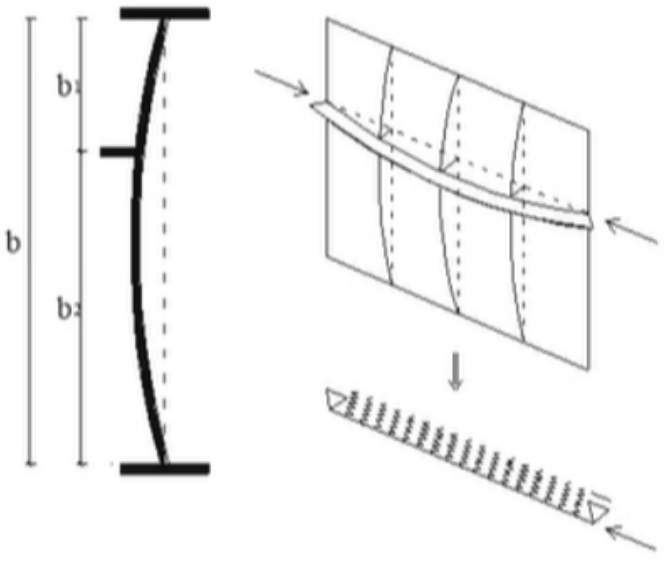

Figure 2.8: Strut on elastic foundation model for plate with single longitudinal stiffener (Pavlovic, 2019, p. 14)

$$\sigma_{cr,sl} = \frac{1.05E}{A_{sl,1}} \frac{\sqrt{I_{sl,1} t^3 b}}{b_1 b_2}, \text{if } a \geq a_c \tag{2.16}$$

$$\sigma_{cr,sl} = \frac{\pi^2 E I_{sl,1}}{A_{sl,1} a^2} + \frac{E t^3 b a^2}{4\pi^2 (1-\nu^2) A_{sl,1} b_1^2 b_2^2}, \text{if } a \leq a_c \tag{2.17}$$

with

$$a_c = 4.33 \sqrt[4]{\frac{I_{sl,1} b_1^2 b_2^2}{t^3 b}} \tag{2.18}$$

and

$$\sigma_{cr,p} = \frac{\sigma_1}{\sigma_{cr,sl,1}} \tag{2.19}$$

In which

- $A_{sl,1}$ the gross area of the column obtained from 2.7 and 2.1
- $I_{sl,1}$ the second moment of area of the gross cross-section of the column obtained from figure 2.7 and table 2.1 about an axis through the centroid of this column parallel to the plate
- b_1 and b_1 the distances from the longitudinal edges of the web to the stiffener ($b_1 + b_1 = b$)

For plates with two stiffeners, formulas 2.17 and 2.18 may be used, however in this case multiple combinations of stiffeners that buckle have to be taken into account. Both stiffeners may individually buckle, or both stiffeners may buckle at the same instance. In the last case Eurocode considers a single lumped stiffener that is substituted for both individual stiffeners, such that the position of the lumped stiffener is at the location of the respective forces in the individual stiffeners and that its second moment of area and cross-sectional area are the sum of the two individual stiffeners.

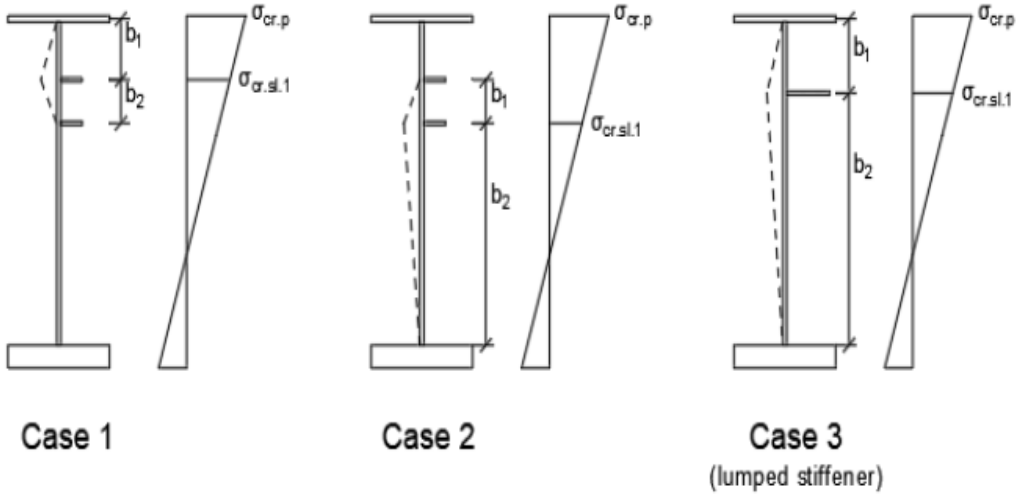

Figure 2.9: The three distinct cases for stiffener buckling for a stiffened plate with two stiffeners (Ahlstrand, 2021, p. 19)

Column-like buckling behaviour

For the column-like behaviour of stiffened plates, the critical column buckling stress can be calculated making use of equation 2.20.

$$\sigma_{cr,sl,c} = \frac{\pi^2 E I_{sl,1}}{A_{sl,1} a^2} \tag{2.20}$$

$$\sigma_{cr,c} = \sigma_{cr,sl,c} * \frac{\sigma_1}{\sigma_{sl,1}} \tag{2.21}$$

In equation 2.20 the same areas of the stiffener and the adjacent plating are used as in the plate-like buckling, for the determination of $I_{sl,1}$ and $A_{sl,1}$. Instead of the calculation of a plate buckling reduction factor ρ, a column-like reduction factor χ_c is calculated, as given in equation 2.22.

$$\chi_c = \frac{1}{\phi + \sqrt{\phi^2 - \bar{\lambda}_c^2}} \tag{2.22}$$

$$\phi = 0.5[1 + \alpha_e * (\bar{\lambda}_c - 0.2) + \bar{\lambda}_c^2] \tag{2.23}$$

$$\bar{\lambda}_c = \sqrt{\frac{\beta_{A,c} * f_y}{\sigma_{cr,c}}} \tag{2.24}$$

$$\beta_{A,c} = \frac{A_{sl,eff,loc}}{A_s l, 1} \tag{2.25}$$

$$\alpha_e = \alpha + \frac{0.09}{i/e} \tag{2.26}$$

with:

- $\alpha = 0.34$ (buckling curve b) for closed section stiffeners
- $\alpha = 0.49$ (buckling curve c) for open section stiffeners

and radius of gyration i

$$i = \sqrt{\frac{I_{sl,1}}{A_s l, 1}} \tag{2.27}$$

and coefficient e:

$$e = max(e_1, e2) \tag{2.28}$$

Coefficient e is defined as the largest distance from the centroid of the entire column (consisting of the stiffener itself and its adjacent plating) to either:

- the centroid of only the stiffener (e_1)
- the centroid of only the adjacent plating (e_2)

Interaction plate-like and column-like buckling
As described, plates can show plate-like behaviour, column-like behaviour, and everything in between. In Eurocode this is taken into account making use of an interaction formula 2.29.

$$\rho_c = \xi(2 - \xi)(\rho - \chi_c) + \chi_c \tag{2.29}$$

$$\xi = \frac{\sigma_{cr,p}}{\sigma_{cr,c}} \quad \text{but} \quad 0 \leq \xi \leq 1 \tag{2.30}$$

The value ρ_c can be interpreted as a reduction of the cross section $A_{c,eff,loc}$. Then the effective compressed area $A_{c,eff}$ can be found as 2.31.

$$A_{c,eff} = \rho_c A_{c,eff,loc} + \sum b_{edge,eff} t \tag{2.31}$$

Using the effective compressed area $A_{c,eff,loc}$ effective properties of the cross section can be found, among which A_{eff}, W_{eff} and I_{eff}.

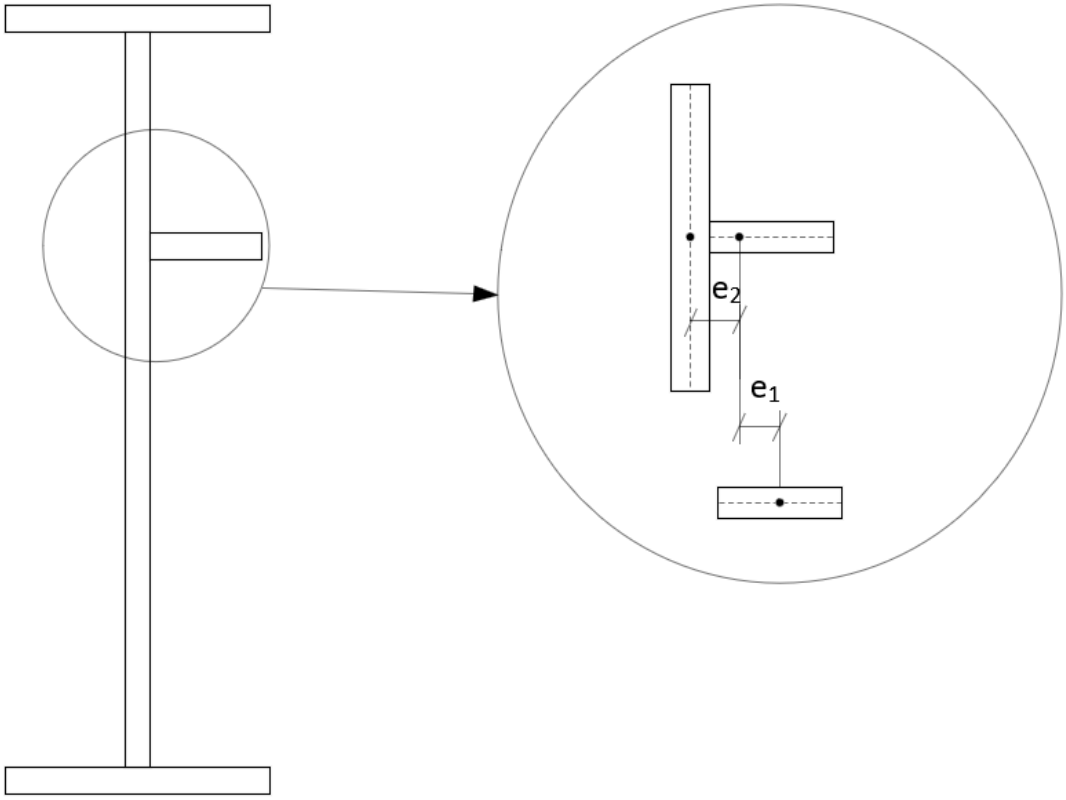

Figure 2.10: The definition of distance e_1 and e_2. Source: own figure

Verification
Finally the cross section can be verified according to 2.32.

$$\eta_1 = \frac{N_{Ed}}{\frac{f_y A_{eff}}{\gamma_{M0}}} + \frac{M_{y,Ed} + N_{Ed} e_{y,N}}{\frac{f_y W_{y,eff}}{\gamma_{M0}}} + \frac{M_{z,Ed} + N_{Ed} e_{z,N}}{\frac{f_y W_{z,eff}}{\gamma_{M0}}} \leq 1 \tag{2.32}$$

In which:

- A_{eff} the effective cross-sectional area calculated making use of ρ_c
- W_{eff} the effective cross-sectional area calculated making use of ρ_c
- $e_{y,N}$, $e_{z,N}$ the eccentricities with respect to the neutral axis
- $M_{y,Ed}$, $M_{z,Ed}$ the design bending moments with respect to the y-y and z-z axes, respectively
- N_{Ed} the design axial force
- γ_{M0} the partial factor

2.5. Reduced stress method in Eurocode

As described in section 2.3.1, equation 2.1 can be directly used in a reduced stress method. The reduced stress method in Eurocode is given by

$$\sqrt{\left(\frac{\sigma_{x,Ed}}{\rho_x f_y/\gamma_{M1}}\right)^2 + \left(\frac{\sigma_{z,Ed}}{\rho_z f_y/\gamma_{M1}}\right)^2 - \left(\frac{\sigma_{x,Ed}}{\rho_x f_y/\gamma_{M1}}\right)\left(\frac{\sigma_{z,Ed}}{\rho_z f_y/\gamma_{M1}}\right) + 3\left(\frac{\tau_{Ed}}{\chi_w f_y/\gamma_{M1}}\right)^2} \leq 1 \tag{2.33}$$

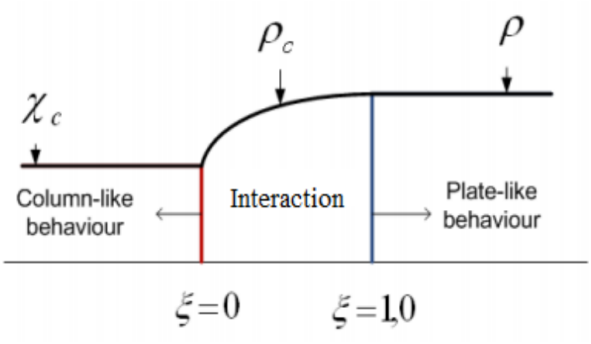

Figure 2.11: The interaction formula for ρ_c plotted (Ahlstrand, 2021, p. 22)

In which:

- ρ_x ,ρ_z the reduction factor for longitudinal and transverse stresses respectively
- $\sigma_{x,Ed}$ $\sigma_{z,Ed}$ the design longitudinal and transverse stresses respectively
- τ_{Ed} the design shear stress
- χ_w the reduction factor for shear stress
- γ_1 the partial factor
- f_y the yield stress

The reduction factors ρ_x and ρ_z are determined, taking column-like buckling into account where relevant. This can be done in exactly the same manner as in the reduced width method, with one crucial difference in the way $\bar{\lambda}_p$ is found. The formula for $\bar{\lambda}_p$ in the reduced stress method is given in equation 2.34.

$$\bar{\lambda}_p = \sqrt{\frac{\alpha_{ult,k}}{\alpha_{cr}}} \tag{2.34}$$

with:

- α_{cr} the minimum load amplifier for the design loads to to reach the elastic critical load of the plate, under the complete stress field
- $\alpha_{ult,k}$ the minimum load amplifier for the design loads to reach the characteristic value of resistance of the most critical point of the plate

The value for $\alpha_{ult,k}$ can be obtained via the Von Mises yield criterion, as given in 2.35

$$\frac{1}{\alpha_{ult}^2} = (\frac{\sigma_{x,Ed}}{f_y})^2 + (\frac{\sigma_{z,Ed}}{f_y})^2 - (\frac{\sigma_{x,Ed}}{f_y})(\frac{\sigma_{z,Ed}}{f_y}) + 3(\frac{\tau_{Ed}}{f_y})^2 \tag{2.35}$$

The value for α_{cr} is given by equation 2.36.

$$\frac{1}{\alpha_{cr}} = \frac{1+\psi_x}{4\alpha_{cr,x}} + \frac{1+\psi_z}{4\alpha_{cr,z}} + \sqrt{(\frac{1+\psi_x}{4\alpha_{cr,x}} + \frac{1+\psi_z}{4\alpha_{cr,z}})^2 + \frac{1-\psi_x}{2\alpha_{cr,x}^2} + \frac{1-\psi_z}{2\alpha_{cr,z}^2} + \frac{1}{\alpha_{cr,\tau}^2}} \tag{2.36}$$

with:

- $\alpha_{cr,x} = \frac{\sigma_{cr,x}}{\sigma_{x,Ed}}$
- $\alpha_{cr,z} = \frac{\sigma_{cr,z}}{\sigma_{z,Ed}}$

- $\alpha_{cr,\tau} = \frac{\tau_{cr,\tau}}{\tau_{\tau,Ed}}$

The values for $\sigma_{cr,x}$ and $\sigma_{cr,z}$ can be obtained via equation 2.1. The values for ψ_x and ψ_z are obtained in the same way as for the reduced width method, as given in equation 2.3. The critical shear stress may be obtained from equation 2.37.

$$\tau_{cr} = k_\tau \sigma_E \tag{2.37}$$

With:

- σ_E the Euler's stress as given in 2.1
- k_τ the shear buckling coefficient

Eurocode gives the shear buckling coefficient for plates as 2.38.

$$k_\tau = \begin{cases} 5.34 + 4.00(h_w/a)^2 + k_{\tau,sl}, & \text{if } a/h_w \geq 1 \\ 4.00 + 5.34(h_w/a)^2 + k_{\tau,sl}, & \text{if } a/h_w < 1 \end{cases} \tag{2.38}$$

$$k_{\tau,sl} = 9\left(\frac{h_w}{a}\right)^2 \sqrt[4]{\left(\frac{I_{sl}}{t^3 h_w}\right)^3} \geq \frac{2.1}{t}\sqrt[3]{\frac{I_{sl}}{h_w}} \tag{2.39}$$

with

- a the distance between transverse stiffeners
- I_{sl} the second moment of area of the longitudinal stiffener about the z-z axis. For plates with more than one longitudinal stiffener, I_{sl} is the sum of the second moment of area of all longitudinal stiffeners.
- The second moment of area stated above is calculated of the stiffener itself plus a width of the surrounding plated area equal to $15\epsilon t$, as shown in figure 2.12

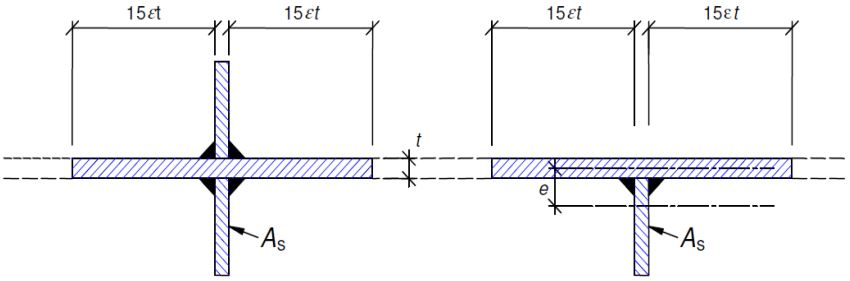

Figure 9.1: Effective cross-section of stiffener

Figure 2.12: The effective cross section that may be used for the shear force (*Eurocode 3 — Design of steel structures — Part 1-5: Plated structural elements*, 2006, p. 30)

Equation 2.38 only holds for plates with rigid transverse stiffeners and without longitudinal stiffeners, or for plates with more than two longitudinal stiffeners. It may also be used for plates with one or two longitudinal stiffeners, as long as $\alpha = \frac{a}{h_w} \geq 3$. For plates with one or two longitudinal stiffeners and $\alpha < 3$, the shear buckling coefficient is given by 2.40.

$$k_\tau = 4.1 + \frac{6.3 + 0.18 * \frac{I_{sl}}{t^3 h_w}}{\alpha^2} + 2.2\sqrt[3]{\frac{I_{sl}}{t^3 h_w}} \tag{2.40}$$

When the value for $\overline{\lambda}_p$ is found making use of equation 2.34, the calculations performed to obtain rho_c are the same as for the reduced width method. Separate values for ρ_c for the longitudinal direction and the transverse direction are obtained. The only missing value to perform a unity check is now χ_w. With the value of $\overline{\lambda}_p$, the reduction factor for the shear stress χ_w can be obtained by using $\overline{\lambda}_p$ for $\overline{\lambda}_w$ in table 2.2.

$\overline{\lambda}_w < 0.83/\eta$	Rigid end post η	Non-rigid end post η
$0.83/\eta \leq \overline{\lambda}_w < 1.08$	$0.83/\overline{\lambda}_w$	$0.83/\overline{\lambda}_w$
$\overline{\lambda}_w \geq 1.08$	$1.37/(0.7 + \overline{\lambda}_w)$	$0.83/\overline{\lambda}_w$

Table 2.2: reduction factor for shear stress χ_w

2.6. Out-of-plane loading

In EN-1993-1-5 only plated structural elements subjected to in-plane loading are considered. Plated structural elements subjected to out-of-plane loading are discussed in EN-1993-1-7, in which comments are included on structures subjected to a combination of in- and out-of-plane loading. For this combined loading, Eurocode gives a simplified design approach that gives conservative estimates.

This simplified approach consists of 9 points, which are:

1. A stiffened plate or a stiffened plate segment may be modeled as a grillage if it is regularly stiffened in the transverse and longitudinal direction.
2. In determining the cross-sectional area A_i of the cooperating plate of an individual member i of the grillage the effects of shear lag should be taken into account by the reduction factor β according to EN 1993-1-5.
3. For a member i of the grillage which is arranged in parallel to the direction of in-plane compression forces, the cross-sectional area A_i should also be determined taking account of the effective width of the adjacent subpanels due to plate buckling according to EN 1993-1-5.
4. The interaction between shear lag effects and plate buckling effects, see Figure 5.2, should be considered by the effective area A_i from the following equation:

$$A_i = [\rho_c (A_{L,eff} + \sum \rho_{pan,i} b_{pan,i} t_{pan,i})] \beta^{\kappa} \tag{2.41}$$

   - $A_{L,eff}$ the effective area of the stiffener considering the local plate buckling of the stiffener
   - ρ_c the reduction factor due to global plate buckling of the stiffened plate segment
   - $\rho_{pan,i}$ the reduction factor due to local plate buckling of subpanel i
   - $b_{pan,i}$ the width of the subpanel i
   - $t_{pan,i}$ the thickness of the subpanel i
   - β the effective width factor for the effect of shear lag
   - κ ratio for effect of shear lag

5. The verification of a member i of the grillage may be performed using the interaction formula in EN 1993-1-1, section 6.3.3 taking into account the following loading conditions:
   - effects of out of plane loadings
   - equivalent axial force in the cross section Ai due to normal stresses in the plate
   - eccentricity e of the equivalent axial force N_{Ed} with respect to the centre of gravity of the cross-sectional area A_i

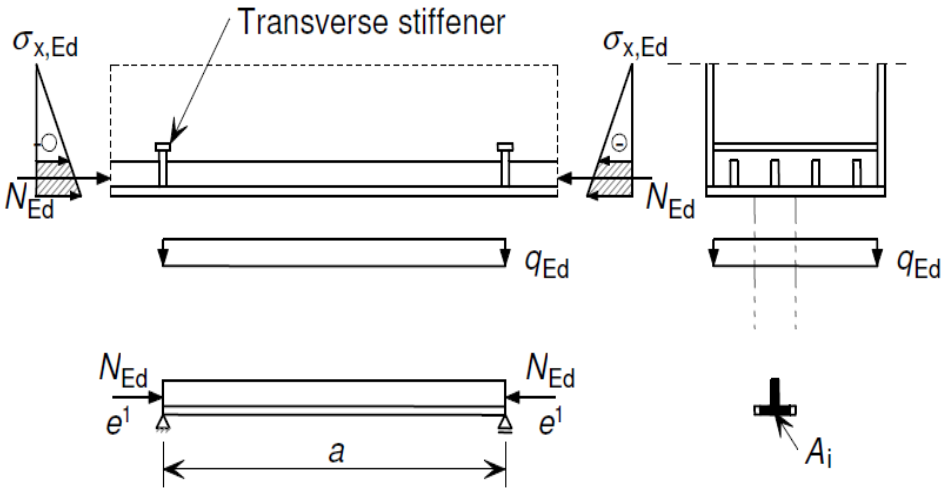

Figure 2.13: The definition of the grillage with surface area A_i (*Eurocode 3 — Design of steel structures — Part 1-7: Plated structures subject to out of plane loading*, 2007)

6. If the stiffeners of a plate or a plate segment are only arranged in parallel to the direction of in-plane compression forces, the stiffened plate may be modeled as an equivalent beam on elastic springs, see EN 1993-1-5.
7. If the stiffeners of a stiffened plate segment are positioned in the transverse direction to the compression forces, the interaction between the compression forces and bending moments in the unstiffened plate segments between the stiffeners should be verified according to 5.2.3.4.2(4).
8. The longitudinal stiffeners should fulfill the requirements given in section 9 of EN 1993-1-5.
9. The transverse stiffeners should fulfill the requirements given in section 9 of EN 1993-1-5.

Shear lag does not play a role in this verification, as there is no bending moment around the y-axis. Therefore formula 2.41 may be reduced to:

$$A_i = \rho_c(A_{L,eff} + \sum \rho_{pan,i} b_{pan,i} t_{pan,i}) \tag{2.42}$$

Concerning points 8 and 9, it is assumed in this case that the stiffeners indeed fulfill the requirements given in section 9 of EN 1993-1-5.

3

Analysed panel

This section further specifies the stiffened panel and the loads and boundary conditions relevant for the verification analysis.

3.1. Panel location

The specific panel that is analysed is a panel stiffened in the vertical direction. As stiffener profile a bulb flat is used, which is a customary profile in the offshore and shipbuilding industry. The specific panel analysed is a part of the northwall of the platform, referred to as ”bay-4-1”.

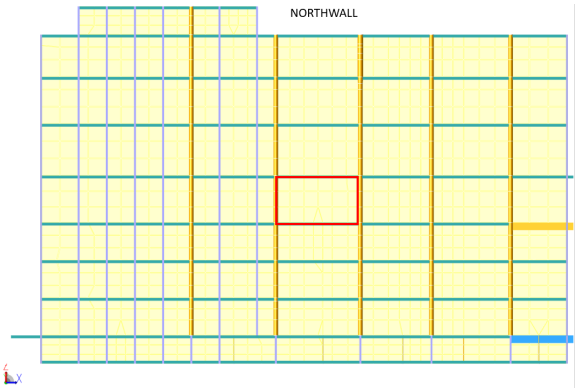

(a) The bay-4-1 panel located in the northwall.

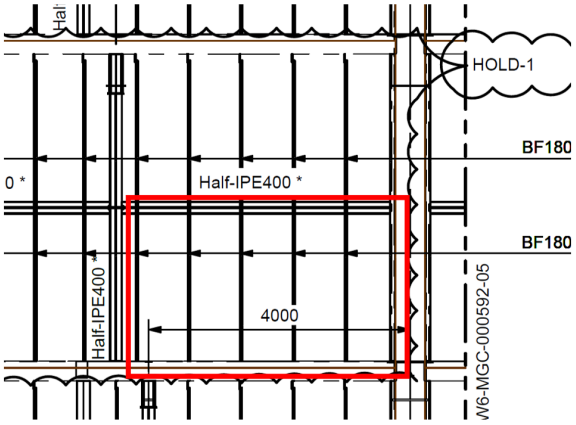

(b) The bay-4-1 panel in more detail.

Figure 3.1

3.2. Boundary conditions and dimensions

It is assumed that the panel is hinged on its four edges. This is a conservative assumption, as the panel is more prone to buckling with hinged boundary conditions than with clamped boundaries. Also, the verification analysis in EN-1993-1-5 assumes hinged boundaries for the stiffened and unstiffened plates. Relevant dimensions are the stiffener spacing, global width and length, plate thickness and stiffener details. The global width and length of the panel are 4000 [mm] and 2600 [mm], respectively. There are 4 stiffeners so that the panels intermediate panel have a width of 800 [mm]. The plate thickness is 8 [mm].

3.3. Loads

There are three distinct in-plane loads that the panel is subjected to, which are longitudinal in-plane stress σ_x, transverse in-plane stress σy and a shear stress τ. Besides these there is also out-of-plane stress which is assumed to work on the unstiffened face of the panel denoted by P_{sd}. The magnitudes of the stresses are given in table 3.1. They are also indicated in figure 3.2a.

Stress	Magnitude	Unit
$\sigma_{x,A}$	34	[MPa]
$\sigma_{x,B}$	55.1	[MPa]
$\sigma_{y,A}$	2.2	[MPa]
$\sigma_{y,C}$	10.6	[MPa]
τ	62.3	[MPa]
P_{sd}	0.002	[MPa]

Table 3.1: Stresses in the analysed panel

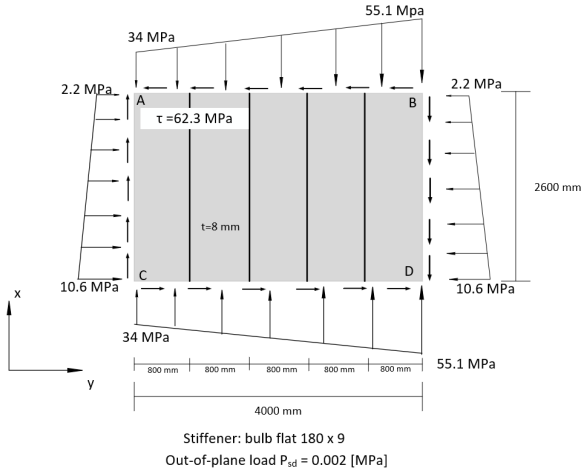

(a) Loads and dimensions of the analysed panel

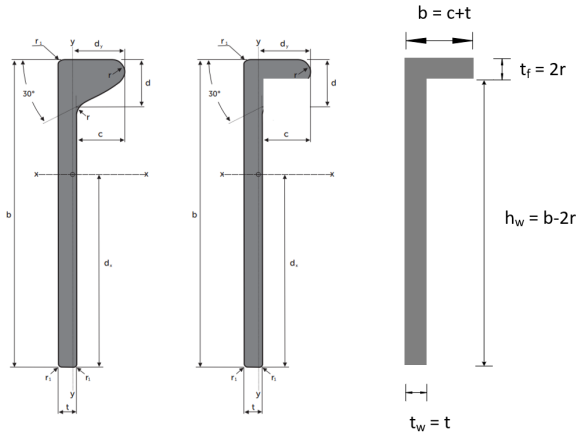

(b) Reduction performed on bulb flat profile

Figure 3.2

3.4. Stiffeners

For the stiffener a so-called bulb flat profile is used. Because in the verification method in EN-1993-1-7 the thicknesses of elements of the structure must be reduced by a certain amount, a bulb flat is very impractical to verify. Therefore the bulb flat is reduced to an angle profile, as shown in figure 3.2b. For some calculations the stiffener properties of the original bulb flat are used as given in appendix E, for these details it is advised to study the hand calculations given in the appendices.

4

Verification according to EN-1993-1-5 and EN-1993-1-7

4.1. Comparison of Eurocode methods

The objective is to describe the buckling for the in- and out-of-plane buckling according to Eurocode. To do this, first a calculation sheet was set up in Excel for the effective width method for a snippet of the analysed panel. This snippet is a panel that has only one stiffener, a width of 800 [mm] a length of 2600 [mm] and a thickness of 8 [mm]. The stiffener used in this snippet is a bulb flat ”180x11.5”. Figure 4.1 shows a schematic representation of this snippet.

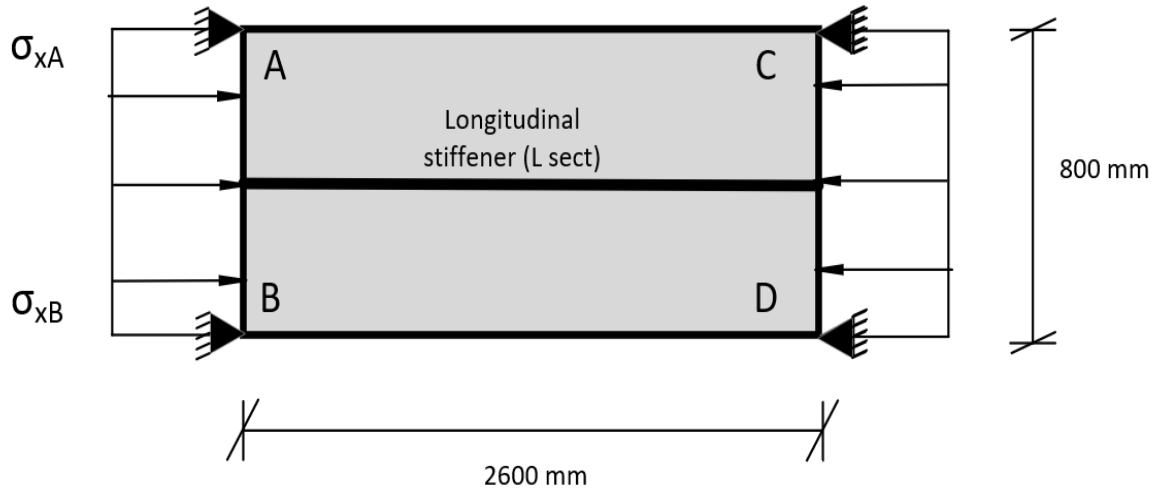

Figure 4.1: The snippet of the plate used for the effective width method

This snippet is not representative for the true buckling behaviour of the analysed panel, as the analysed panel has a larger width than 800 [mm], and therefore shows more column-like behaviour than the snippet. However, due to the fact that this snippet has only one longitudinal stiffener, it is relatively easy to perform the reduced width method on this plate structure.

Next to the Excel sheet in which the reduced width method is used, an Excel sheet was set up in which the reduced stress method is performed. Using the simplified case of the snippet of the analysed panel, a comparison can be made between the effective width method and the reduced width method.

For this comparison, the snippet is loaded with a uniform stress in the x-direction (parallel to the longitudinal stiffener). The uniform stress is increased in steps of 20 [MPa], until the unity checks of both methods have surpassed the value of 1.

The results obtained are plotted and given in figure 4.2.

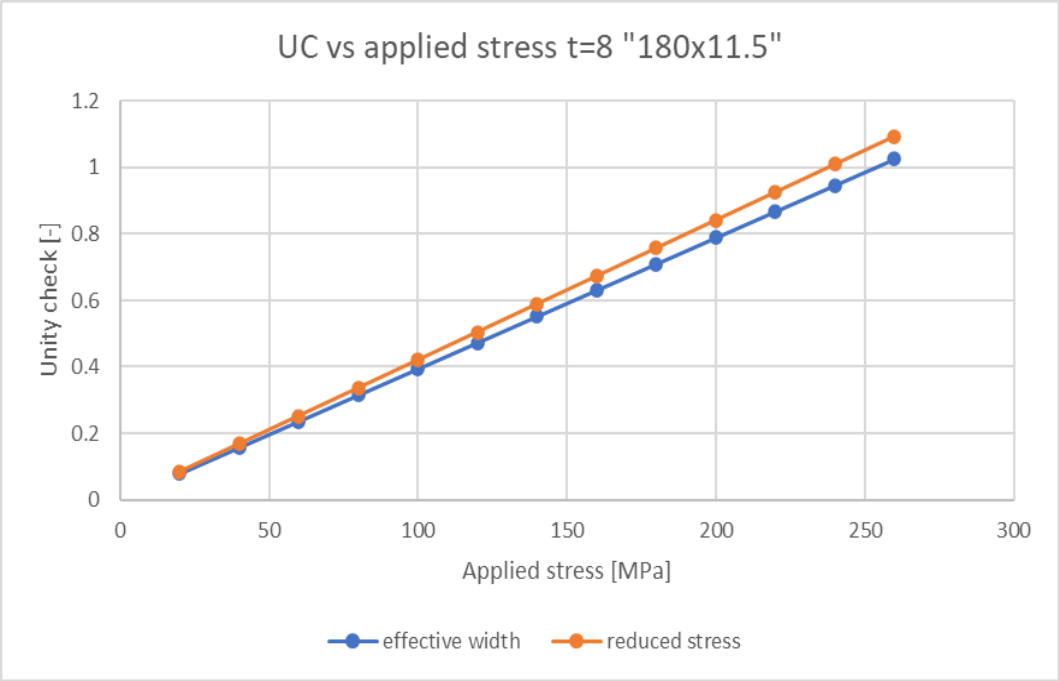

Figure 4.2: Unity check vs applied stress for effective width method and reduced stress method for a plate thickness of 8 [mm].

As mentioned in section 2.2, the plate buckling capacity found is usually higher for the effective width method. This is probably because the effective width method uses partial factor γ_{m0} (for which 1 is used), and the reduced stress method uses partial factor γ_{m1} (for which 1.1 is used). The higher unity checks for buckling capacity in the effective width method is supported by the outcomes of the comparison of the two excel calculation sheets, in which the effective width method indeed consistently gives a lower unity check for equal applied stress than the reduced stress method. The comparison was performed for 4 otherwise equal plates with thicknesses of 8 [mm], 10 [mm], 12 [mm] and 14 [mm]. The difference in unity check was calculated following equation 4.1.

$$Difference = \frac{UC_{reducedstress}}{UC_{effectivewidth}} \tag{4.1}$$

The difference found between the methods was very consistent for all applied stresses per plate thickness. The results are summarised in table 4.1.

Plate thickness [mm]	Difference [%]
8	6.61
10	1.96
12	7.26
14	9.37

Table 4.1: difference in unity check effective width method vs. reduced stress method

It is concluded that the reduced stress method and the effective width method are both options that may be used for the verification of plate buckling. As described in section2.5, the reduced stress method has one unity check in which the longitudinal in-plane normal stress (x-direction), transverse in-plane normal stress (y-direction), and in-plane shear stress are directly inserted. The effective width

method has distinct verification approaches for longitudinal stress, transverse stress, and shear stress. Because the reduced stress method is slightly conservative compared to the effective width method and because the verification is suitable for biaxial stress situations (σ_x and σ_y), the reduced stress method is chosen as the method to use for the verification analysis.

4.2. Reduced stress method

The first step in the verification of an element is to determine the cross-section class of the element. According to EN-1993-1-1, an internal compression element belongs to cross section class 4 when c/t > 124ϵ. The assumption is made that the stiffened plate to be verified is indeed a class 4 member.

4.2.1. Verification under longitudinal in-plane normal stress and shear stress

Because EN-1993-1-5 gives no way to take the stresses perpendicular to the stiffeners into account for global buckling, this verification disregards these stresses. Proposals to add stresses in the y-direction in the verification are given in section 4.2.2.

The general approach of the verification is to first consider the global plate buckling. Then the local plate buckling is considered. A brief example calculation is performed here, the total calculation can be found in appendix B.

geometry and loads

The geometry and loads on the stiffened panel are given by figure 4.3.

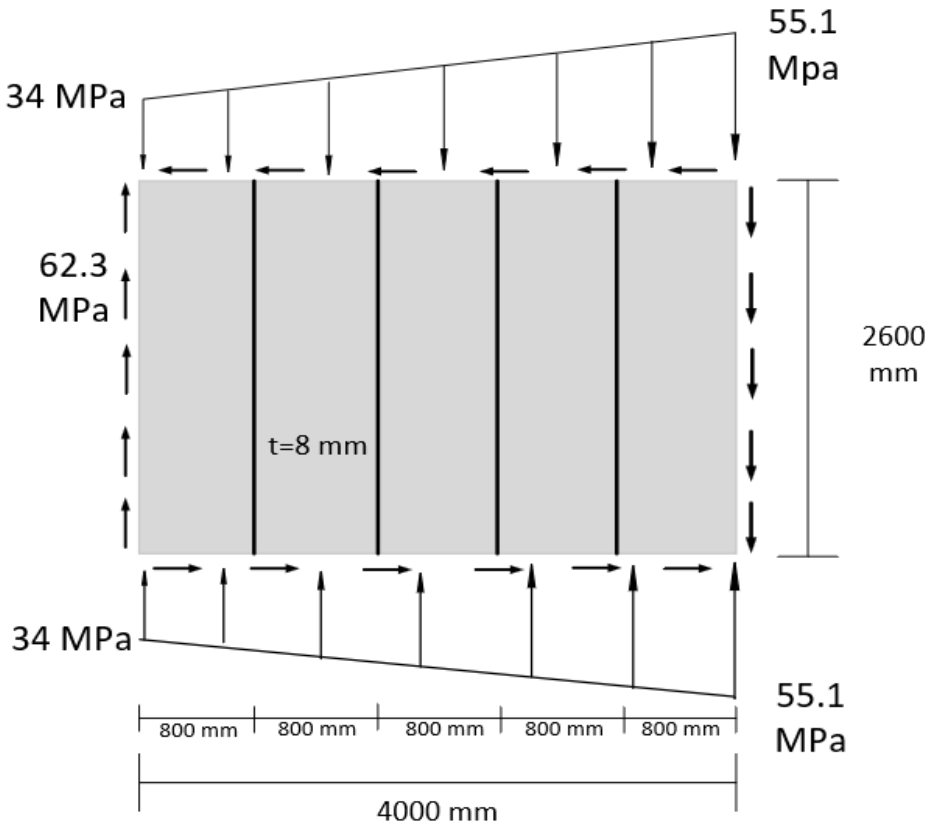

Figure 4.3: Structural system sketch including loads and dimensions

The stiffener in this case is a bulb flat of the type ”180x9”. The relevant parameters are given in table 4.2.

Parameter	symbol	value	unit
height of web	h_w	166	[mm]
thickness of web	t_w	9	[mm]
width of flange	b	34	[mm]
thickness of flange	t_f	14	[mm]
sec. moment of area strong axis	I_y	6610900	$[mm^4]$
distance center of gravity	dx	107.4	[mm]
area	A	2063	$[mm^2]$

Table 4.2: relevant stiffener parameters (see appendix E)

Load amplifier global buckling behaviour
The verification starts with the global buckling behaviour. The critical buckling factor is found according to equation 2.19. This results in:

$$k_{\sigma,p} = 1343.1[-]$$

With the critical buckling factor, the critical global plate-like buckling stress can be found according to equation 2.1:

$$\sigma_{cr} = k_\sigma * \sigma_E = \frac{k_\sigma * \pi^2 * E}{12*(1-\nu^2)} * (\frac{t}{b})^2 = 1343.1 * 190000 * (\frac{8}{4000})^2 = 1020.76\ [MPa]$$

The next step is to calculate the critical shear buckling stress τ_{crit}. Using the effective cross-section of a stiffener as given in figure 2.12 and the equations 2.38 and 2.39, the critical global shear buckling factor is calculated. This results in:

$$k_\tau = 323.365\ [-]$$

Critical global shear buckling stress can be calculated as:

$$\tau_{cr} = k_\tau * \sigma_E = \frac{k_\tau * \pi^2 * E}{12*(1-\nu^2)} * (\frac{t}{b})^2 = 323.365 * 190000 * (\frac{8}{4000})^2 = 245.76\ [MPa]$$

With the global critical plate buckling stress σ_{cr} and the global critical shear buckling stress τ_{cr} the load amplifiers $\alpha_{cr,x}$ and $\alpha_{cr,\tau}$ can be found by:

$$\alpha_{cr,x} = \frac{\sigma_{cr,x}}{\sigma_{x,Ed}} = \frac{1020.76}{55.1} = 18.525$$
$$\alpha_{cr,\tau} = \frac{\tau_{cr,\tau}}{\tau_{\tau,Ed}} = \frac{245.76}{62.3} = 3.9447$$

With the separate critical load amplifiers for x-direction and shear stress, the global critical load amplifier α_{cr} can be calculated using equation 2.36.

$$\frac{1}{\alpha_{cr}} = \frac{1+\psi_x}{4\alpha_{cr,x}} + \sqrt{(\frac{1+\psi_x}{4\alpha_{cr,x}})^2 + \frac{1-\psi_x}{2\alpha_{cr,x}^2} + \frac{1}{\alpha_{cr,\tau}^2}}$$

$$\frac{1}{\alpha_{cr}} = \frac{1+0.617}{4*18.525} + \sqrt{(\frac{1+0.617}{4*18.525})^2 + \frac{1-0.617}{2*18.525^2} + \frac{1}{3.9447^2}}$$

The value for α_{cr} is found to be 3.605.

Load amplifier local buckling behaviour
A similar approach is followed for the local buckling. The panel subjected to the highest compressive stresses is examined, as shown in figure 4.4

The critical buckling stress can be determined again by making use of equation 2.1. The critical buckling factor k_σ can in this case directly be obtained from table 4.1 from EN-1993-1-5, as given in figure 2.6.

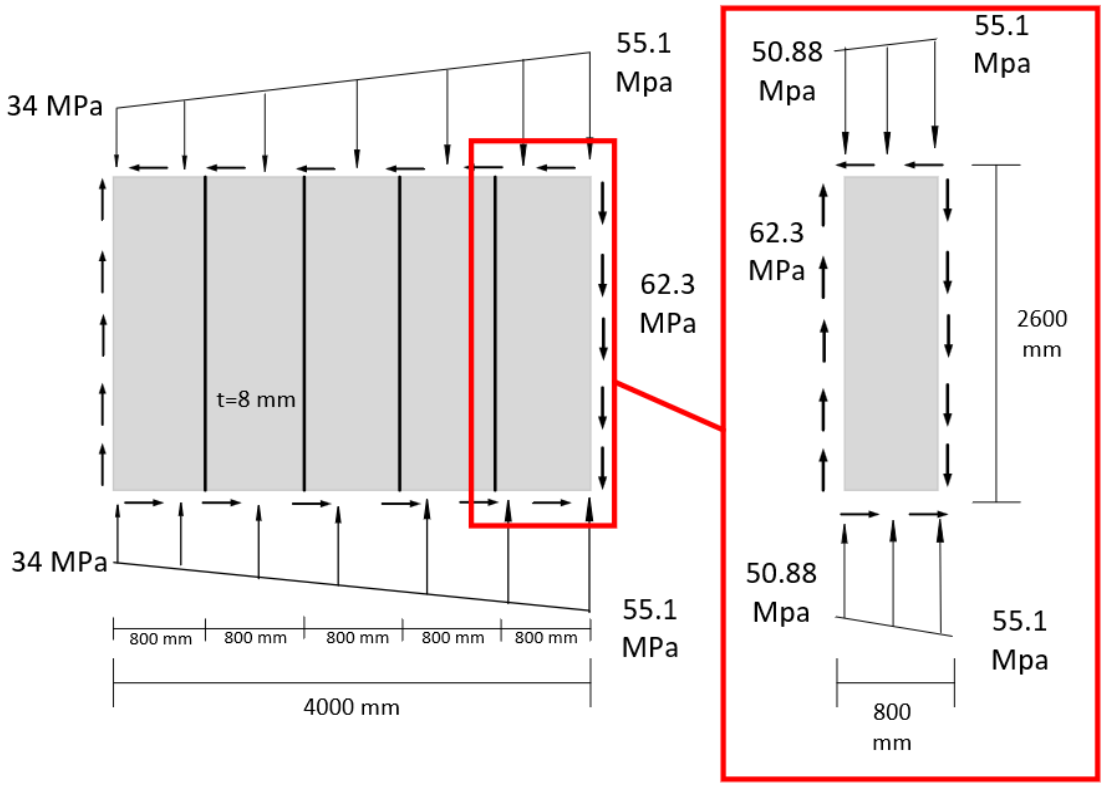

Figure 4.4: Panel to be verified for local buckling

$$\psi = \frac{\sigma_2}{\sigma_1} = \frac{-50.88}{-55.1} = 0.9234$$
$$k_\sigma = \frac{8.2}{1.05+\psi} = \frac{8.2}{1.05+0.9234} = 4.155$$
$$\sigma_{cr} = k_\sigma * \frac{\pi^2 * E}{12*(1-\nu^2)} * (\frac{t}{b})^2 = 4.155 * 190000 * (\frac{8}{800})^2 = 78.862\ [MPa]$$

The value for τ_{cr} is also calculated making use of equations 2.1 and 2.38. This results in:

$$\frac{a}{h_w} = \frac{2600}{800} = 3.25$$
$$k_{tau} = 5.34 + 4 * (\frac{h_w}{a})^2 + k_{\tau,sl} = 5.34 + 4 * (\frac{800}{2600})^2 + 0 = 5.7187$$
$$\tau_{cr} = k_\tau * \frac{\pi^2 * E}{12*(1-\nu^2)} * (\frac{t}{b})^2 = 5.7187 * 190000 * (\frac{8}{800})^2 = 108.54\ [MPa]$$

Analogue to the global buckling, the factors $\alpha_{cr,x}$ and $\alpha_{cr,\tau}$ can be found by:

$$\alpha_{cr,x} = \frac{\sigma_{cr,x}}{\sigma_{x,Ed}} = \frac{78.862}{55.1} = 1.4313$$
$$\alpha_{cr,\tau} = \frac{\tau_{cr,\tau}}{\tau_{\tau,Ed}} = \frac{108.54}{62.3} = 1.7422$$

Again the critical load amplifier can be found according to:

$$\frac{1}{\alpha_{cr}} = \frac{1+\psi_x}{4\alpha_{cr,x}} + \sqrt{(\frac{1+\psi_x}{4\alpha_{cr,x}})^2 + \frac{1-\psi_x}{2\alpha_{cr,x}^2} + \frac{1}{\alpha_{cr,\tau}^2}}$$
$$\frac{1}{\alpha_{cr}} = \frac{1+0.923}{4*1.4313} + \sqrt{(\frac{1+0.923}{4*1.4313})^2 + \frac{1-0.923}{2*1.4313^2} + \frac{1}{1.742^2}}$$
$$\alpha_{cr} = 0.9853$$

Utilization

The values for the minimum load amplifiers for both global buckling and local buckling are now known. Making use of these values, the unity check can be found. Again, first the unity check for the global buckling is found, and then the unity check for the local buckling.

$$\sigma_{v,Ed} = \sqrt{\sigma_{x,Ed}^2 + 3 * \tau_{Ed}^2} = \sqrt{55.1^2 + 3 * 62.3^2} = 121.16\ [MPa]$$

$$\alpha_{ult} = \frac{f_y}{\sigma_{v,Ed}} = \frac{355}{121.16} = 2.93$$

$$\overline{\lambda}_p = \overline{\lambda}_w = \sqrt{\frac{\alpha_{ult}}{\alpha_{cr}}} = \sqrt{\frac{2.93}{3.605}} = 0.901$$

The reduction factor for plate buckling ρ_p can be calculated as:

$$\rho_p = \frac{\overline{\lambda}_p - 0.055*(3+\psi}{\overline{\lambda}_p^2} = \frac{0.901 - 0.055*(3+0.617)}{0.901^2} = 0.864$$

The reduction factor for shear stress χ_w is obtained making use of table 2.2:

$$\chi_w = \frac{0.83}{\overline{\lambda}_w} = \frac{0.83}{0.901} = 0.921$$

The critical column buckling stress for global buckling is now needed in order to calculate the interaction factor ξ. The critical buckling stress for column-like behaviour is found by:

$$\sigma_{cr,c} = \frac{\pi^2 * E * I_{sl,1}}{A_{sl,1} * a^2} * \frac{\sigma_1}{\sigma_{sl,1}} \frac{\pi^2 * 210000 * 26002293}{8458.12 * 2600^2} * \frac{55.1}{50.88} = 1020.74\ [MPa]$$

The interaction factor is found as:

$$\xi = \frac{\sigma_{crit,p}}{\sigma_{crit,c}} - 1 = \frac{1020.76}{1020.74} - 1 = 0$$

To calculate the final reduction factor ρ_c, the reduction factor due to column buckling χ_c must be calculated according to:

$$\chi_c = \frac{1}{\phi_p + \sqrt{\phi_p^2 - \overline{\lambda}_p^2}} = 0.555$$

$$\phi_p = 0.5 * [1 + \alpha_e * (\overline{\lambda}_c - 0.2) + \overline{\lambda}_c^2] = 1.126$$

$$\alpha_e = \alpha + \frac{0.09}{i/e} = 0.49 + \frac{0.09}{55.446/84.229} = 0.6267$$

Finally the reduction factor $\rho_{c,glob}$ is calculated as:

$$\rho_c = (\rho_p - \chi_c) * \xi * (2 - \xi) + \chi_c = (0.864 - 0.555) * 0 * (2 - 0) + 0.555 = 0.555 \qquad (4.2)$$

For local buckling the plate slenderness $\overline{\lambda_p}$ is found as:

$$\overline{\lambda_p} = \overline{\lambda_w} = \sqrt{\frac{\alpha_{ult}}{\alpha_{cr}}} = \sqrt{\frac{2.93}{0.9853}} = 1.7244$$

And the reduction factor for plate buckling ρ_p as:

$$\rho_p = \frac{\overline{\lambda}_p - 0.055*(3+\psi}{\overline{\lambda}_p^2} = \frac{1.7244 - 0.055*(3+0.923)}{1.707^2} = 0.5073$$

Again the reduction factor for shear stress is obtained making use of table 2.2:

$$\chi_w = \frac{1.37}{0.7 + \overline{\lambda_w}} = \frac{1.37}{0.7 + 1.7244} = 0.565$$

as $\overline{\lambda_w} > 1.08$

Again, in order to find the interaction factor ξ, the critical buckling stress for column-like behaviour must be found. For an unstiffened plate the critical buckling stress for column-like behaviour is given by:

$$\sigma_{cr,c} = \frac{\pi^2 * E * t_p^2}{12*(1-\nu^2)*a^2} = \frac{\pi^2 * 210000 * 8^2}{12*(1-0.3^2)*2600^2} = 1.796\ [MPa]$$

And:

$$\xi = \frac{\sigma_{crit,p}}{\sigma_{crit,c}} - 1 = \frac{78.862}{1.796} - 1 = 1$$
$$\text{as } 0 \leq \xi \leq 1$$

For the final reduction factor ρ_p, only the reduction factor due to column buckling χ_c is needed, which can be obtained as:

$$\chi_c = \frac{1}{\phi_p + \sqrt{\phi_p^2 - \bar{\lambda}_p^2}} = 0.2919$$
$$\phi_p = 0.5 * [1 + \alpha * (\bar{\lambda}_c - 0.2) + \bar{\lambda}_c^2] = 2.1469$$
$$\alpha = 0.21$$

Finally, the reduction factor $\rho_{c,loc}$ is obtained by:

$$\rho_c = (\rho_p - \chi_c) * \xi * (2 - \xi) + \chi_c = (0.5073 - 0.2919) * 1 * (2 - 1) + 0.2919 = 0.5073$$

To find the utilization of the structure, the minimum values for both the reduction ρ_c and the reduction factor for shear buckling χ_c must be used (Beg et al., 2011, p. 265)

This then results in the following reduction factors:

$$\rho_x = min(\rho_{c,loc}, \rho_{c,glob}) = min(0.5073; 0.555) = 0.5073$$
$$\chi_x = min(\chi_{loc}, \chi_{glob}) = min(0.565; 0.921) = 0.565$$

The utilization can finally be obtained by:

$$\sqrt{(\frac{\sigma_{x,Ed}}{\rho_x * f_y/\gamma_{m1}})^2 + 3 * (\frac{\tau_{Ed}}{\chi_w * f_y/\gamma_{m1}})^2} \leq 1$$

$$\sqrt{(\frac{55.1}{0.5073*355/1.1})^2 + 3 * (\frac{62.3}{0.565*355/1.1})^2} = 0.681$$

It can be concluded that the panel fulfills the requirements given by EN-1993-1-5 for plate buckling.

4.2.2. Verification under biaxial in-plane normal stress and shear stress

Global buckling

In EN-1993-1-5, no method is given to find the global critical buckling stress for stress in the direction perpendicular to the stiffeners (σ_y). This means that for global buckling the value for $\alpha_{crit,y}$ can not be found, and thus the value of the global minimum load amplifier α_{crit} can not be found if transverse load is present, since α_{crit} is a function of $\alpha_{crit,x}$, $\alpha_{crit,y}$ and $\chi_{crit,\tau}$. It is therefore not possible to perform the standard verification given by the unity check formula 2.33 making use of:

- min($\rho_{cx,glob}$, $\rho_{cx,loc}$)
- min($\rho_{cy,glob}$, $\rho_{cy,loc}$)
- min($\chi_{w,glob}$, $\chi_{w,loc}$)

As the values for $\rho_{cx,glob}$ and $\chi_{w,glob}$ are not found accurately.

A logical alternative would be to find the value for $\alpha_{crit,glob}$ from FE analysis or from EBPlate. However this is also not possible, as EBPlate might give a local buckling mode for the given loads, and thus also gives only $\alpha_{crit,loc}$ and not $\alpha_{crit,glob}$, as only the minimum of the two is given by EBPlate. Finally, it is simply not justified to use only min($\alpha_{crit,loc}$, $\alpha_{crit,glob}$) to find the unity check (Zizza, 2016, p. 41). Instead, the values min($\rho_{cx,loc}$, $\rho_{cx,glob}$), min($\rho_{cy,loc}$, $\rho_{cy,glob}$) and min($\chi_{w,loc}$, $\chi_{w,glob}$) should be used (Beg et al., 2011, p. 265).

An option to determine a value for $\sigma_{crit,y}$ is to assume that no stiffeners are present, and to find the minimum value for k_σ by using formula 2.2 for n = 1 up to and including n = number of stiffeners. This would give a very conservative value for $\sigma_{crit,y}$. The stress in the direction perpendicular to the stiffeners σ_y is taken as uniformly distributed for the reason described in section 4.2.2.

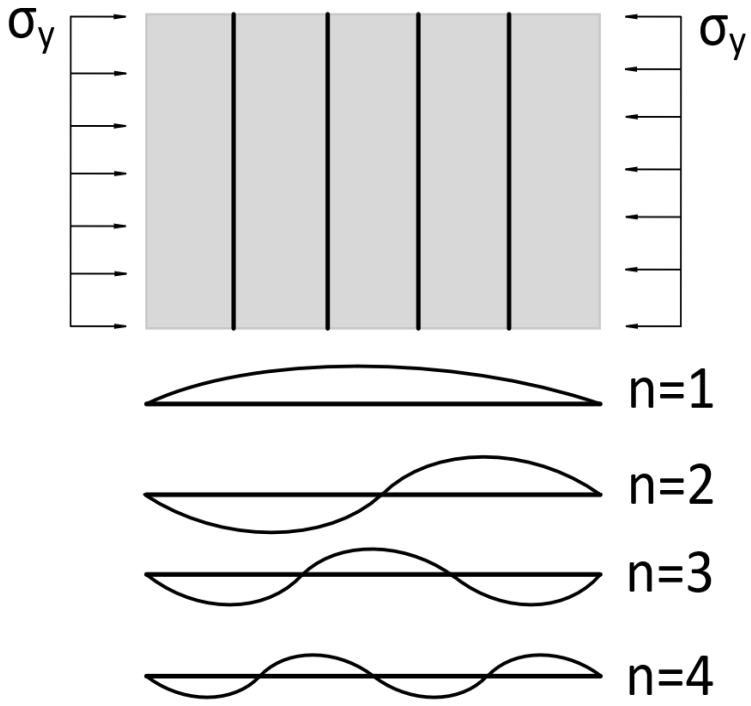

Figure 4.5: The number of half sine waves used to determine the minimum k_σ

The second option is to check the stiffener for the requirements given in EN-1993-1-5 section 9, so that local buckling is governing (which can be checked), as described by (Mensinger, 2016, p. 5). Unfortunately due to time restraints, EN-1993-1-5 section 9 has not been taken into account in the verification, and therefore the stress in y-direction is left out of the scope of this report.

Local buckling

In contrast to the global buckling case, the local minimum load amplifier $alpha_{crit,loc}$ can be found for panels subjected to bidirectional stresses, in very much the same way as for the unidirectional case. However, in this case the buckling factor k_{sigma} can not be found using table 4.1. The critical buckling factor depends on aspect ratio, support conditions and the stress distribution. EN-1993-1-5 does not take into account the aspect ratio as mentioned in section 2.3.1. It simply assumes a minimum plate buckling factor of 4. For plates with very small aspect ratio's (very wide plates), this is not accurate. Because the verification of critical local buckling stress for the transverse direction is in this case a very wide plate, the buckling factor k_σ is determined using equation 2.2 with m=1. This automatically means that the stress distribution must be constant, as equation 2.2 is only accurate for simply supported plates with uniformly distributed stresses. In case the transverse stress acting on the plate is linearly increasing, the maximum is taken and assumed to be uniformly distributed as a conservative

approach.

Another difference with the longitudinal case is the determination of the reduction factor ρ_y. According to EN-1993-1-5 section 10.5(a), this reduction factor may be determined in the same way as ρ_x. However, it is recommended by (Beg et al., 2011, p. 165) to use the equation given in EN-1993-1-5 B.1:

$$\rho = \frac{1}{\phi_p + \sqrt{\phi_p^2 - \overline{\lambda}_p}} \tag{4.3}$$

$$\phi_p = \frac{1}{2} * [1 + \alpha_p * (\overline{\lambda}_p - \overline{\lambda}_{p0}) + \overline{\lambda}_p] \tag{4.4}$$

In which:

- $\overline{\lambda}_{p0}$ = 0.8
- α_p = 0.34 (assuming welded/ cold formed product)

No calculation of the column-like buckling reduction is needed, as a generalized buckling curve is used (Derik, 2013, p. 51).

4.2.3. verification under longitudinal stress, shear stress and out-of-plane load

The verification of out-of-plane loading is done by taking the effective parts of the cross section and reducing them with the factor ρ_c as given in equation 2.42. The resulting grillage with the effective area A_i should be checked according to section 6.3.3 of EN-1993-1-1 (*Eurocode 3 — Design of steel structures — Part 1-7: Plated structures subject to out of plane loading*, 2007, p.14).

The reduction factor due to global plate buckling of the stiffened plate segment ρ_c only depends on longitudinal in-plane stress, as the effective width method has to be used and there the shear stress does not influence ρ_c. There is little information in the relevant Eurocodes (1-1,1-5,1-7) about the in-plane shear force (Kleppe et al., 2021, p. 10). A significant reduction for out-of-plane capacity due to the addition of in-plane shear stress is found from finite element simulations, but this reduction is not proportional to the shear stress utilization (Kleppe et al., 2021, p. 11).

For the verification, the first step is to find the factor ρ_c, resulting from the interaction between column-like and plate-like buckling.

Column-like buckling

The most compressed stiffener is governing for this verification:

$$\overline{\lambda}_c = \sqrt{\frac{\beta_{A,c} * f_y}{\sigma_{cr,c}}} = 0.41506$$

with:

$$\beta_{A,c} = \frac{A_{sl,eff}}{A_{sl,1}} = \frac{4189.7}{8458.11} = 0.4953$$

With the slenderness $\overline{\lambda}_c$ the reduction factor due to column buckling χ_c can be found:

$$\phi = 0.5 * [\alpha_e * (\overline{\lambda}_c - 0.2) + \overline{\lambda}_c^2] = 0.6535$$

$$\chi_c = \frac{1}{\phi - \sqrt{\phi^2 - \overline{\lambda}_c^2}} = 0.8633$$

Plate-like buckling
The whole compressed area of the plate must be examined in order to find the relative plate slenderness $\overline{\lambda}_p$:

$$\overline{\lambda}_p = \sqrt{\frac{\beta_{A,c} * f_y}{\sigma_{cr,c}}} = 0.4155$$

with:

$$\beta_{A,c} = \frac{A_{c,eff,loc}}{A_c} = \frac{16788.73}{33826.16} = 0.496$$

Because $\overline{\lambda}_p < 0.673$:

$$\rho_p = 1$$

It should be noted that because in this case there are multiple stiffeners, unlike in the simplified case used for the comparison between the effective width method and the reduced stress method in section 4.1, the values for $\beta_{A,c}$ in plate like buckling and column like buckling differ.

Interaction plate-like and column-like buckling

$$\xi = \frac{\sigma_{cr,p}}{\sigma_{cr,c}} - 1 = 0$$

$$\rho_c = (\rho_p - \chi_c) * \xi * (2 - \xi) + \chi_c = 0.8633$$

Check according to EN-1993-1-1 6.3.3
With reduction factor ρ_c known, the effective area can be calculated according to equation 2.42:

$$A_i = \rho_c(A_{L,eff} + \sum \rho_{pan,i} b_{pan,i} t_{pan,i}) =$$
$$\rho_c * (h_{w,eff} * t_w + b_{f,eff} * t_f + [b_{1,inf,eff} + b_{1,sup,eff}] * t_p) = 3617.015\ [mm^2]$$

And subsequently the second moment of area I_y and moment of resistance $W_{y,eff,min}$ can be found. According to EN-1993-1-1 the characteristic resistance for uniform compression can be found as:

$$N_{Rk} = A_{eff} * f_y = 3617.015\ [mm^2] * 355\ [N/mm^2] = 1284040.27\ [N]$$

and design resistance for bending:

$$M_{y,Rk} = W_{y,eff,min} * f_y = 43551631.7\ [Nmm]$$
$$M_{z,Rk} = W_{z,eff,min} * f_y = 46875116.9\ [Nmm]$$

The critical buckling forces can be found as:

$$N_{cr,y} = \frac{\pi^2 * E * I_y}{L_c r} = 5718089.835\ [N]$$

$$N_{cr,z} = \frac{\pi^2 * E * I_z}{L_c r} = 6885173.25\ [N]$$

The value χ_c from column-like buckling as described in EN-1993-1-5 can be used for the value of χ_y (Kleppe et al., 2021, p. 6).

$$\chi_c = \chi_y = 0.8634$$

$$\overline{\lambda}_z = \sqrt{\frac{N_{Rk}}{N_{cr,z}}} = 0.43185$$

$$\phi_z = 0.5 * [1 + 0.49 * (\overline{\lambda}_z - 0.2) + \overline{\lambda}_z^2] = 0.65$$

$$\chi_z = \frac{1}{\phi_z + \sqrt{\phi_z^2 - \overline{\lambda}_z^2}} = 0.88$$

To find the interaction factors k_{yy}, k_{yz}, k_{zy}, k_{zz} table A.1 is used from EN-1993-1-1, because table B.1 specifies only I-sections and RHS sections. First the values for C_{my}, C_{mz} (table A.2), μ_y and μ_z are found as:

$$C_{my} = 1 + 0.03 * \frac{N_{Ed}}{N_{cr,y}} = 1.0022$$

$$C_{mz} = 0.79 + 0.21 * \psi + 0.36 * (\psi - 0.33) * \frac{N_{Ed}}{N_{cr,z}} = 1.0149$$

(The equivalent uniform moment factor C_{mLT} is taken as 1)

$$\mu_y = \frac{1 - \frac{N_{Ed}}{N_{cr,y}}}{1 - \chi_y} = 0.989$$

$$\mu_z = \frac{1 - \frac{N_{Ed}}{N_{cr,z}}}{1 - \chi_z * \frac{N_{Ed}}{N_{cr,z}}} = 0.992$$

And with these the interaction factors can be found:

$$k_{yy} = C_{my} * C_{mLT} * \frac{\mu_y}{1 - \frac{N_{E,d}}{N_{cr,y}}} = 1.071$$

$$k_{yz} = C_{mz} * \frac{\mu_y}{1 - \frac{N_{E,d}}{N_{cr,z}}} = 1.070$$

$$k_{yy} = C_{my} * C_{mLT} * \frac{\mu_z}{1 - \frac{N_{E,d}}{N_{cr,y}}} = 1.074$$

$$k_{zz} = C_{mz} * \frac{\mu_z}{1 - \frac{N_{E,d}}{N_{cr,z}}} = 1.073$$

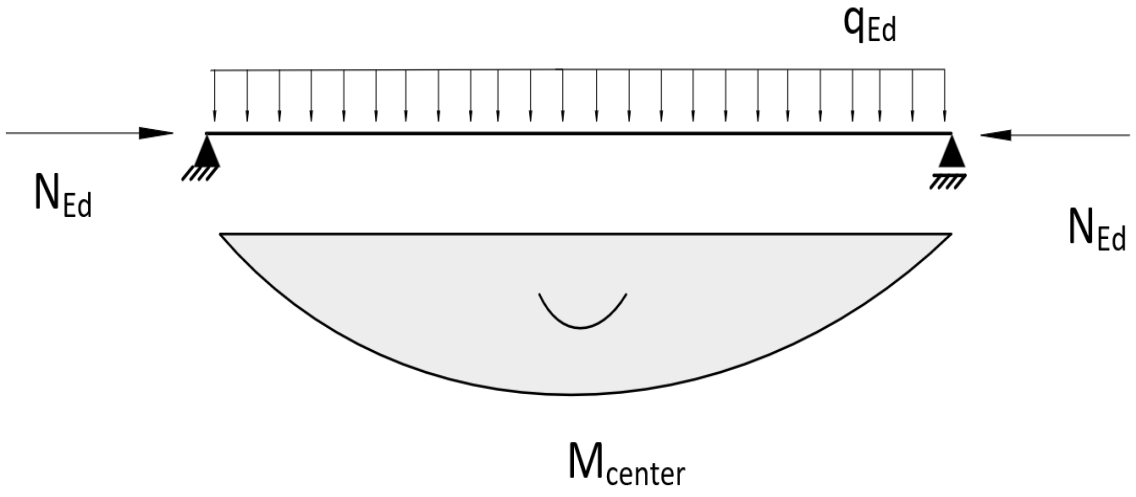

Figure 4.6: The equivalent beam under bending and axial compression

The equivalent beam under bending due to the out-of-plane load and normal force is given in figure 4.6. In the verification according to 6.3.3 EN-1993-1-1, an eccentricity moment $\Delta M_{y,Ed} = e_{N,z} * N_{Ed}$ is included to account for the shift in centroidal axis for a class 4 section. This moment is neglected in this case. In case it would be taken into account, a constant bending moment opposite in sign to M_{center} (or $M_{y,Ed}$) is placed on the beam. Therefore, M_{center} would be reduced, and not taking these moments into account is therefore assumed to be a conservative assumption. (Kleppe et al., 2021, p. 6) also suggest to neglect this eccentricity moment.

$$M_{y,Ed} = \frac{1}{8} * width * P_{sd} * l^2 = \frac{1}{8} * (391.875 + 407.515)\ [mm] * 0.002\ [N/mm^2] * (2600\ [mm])^2 = 1350969\ [Nmm]$$

In this case the panel is subjected to a linearly increasing longitudinal stress (-34 [MPa] to -55.1 [MPa]). This gives a constant bending moment around the z-axis of the equivalent beam:

$$M_{z,Ed} = \frac{1}{2} * (\sigma_{stiff} - \sigma_{inf}) * 407.515 * t_p * \frac{2}{3} * 407.515 + \frac{1}{2} * (\sigma_{sup} - \sigma_{stiff}) * 391.875 * t_p * \frac{2}{3} * 391.875 = 1798476.57[Nmm]$$

Utilization

The reduction factor for lateral torsion buckling χ_{LT} is not relevant in this verification (Kleppe et al., 2021, p. 6). It is thus taken to be equal to 1. The equivalent beam is isolated in this verification, but in reality it is part of the plate. The lateral torsion buckling effect of the equivalent beam is assumed to be taken into account in the plate buckling verification, and lateral torsion buckling of only the stiffener is assumed out of the scope of this verification.

The utilizations in 6.3.3 EN-1993-1-1 are given as:

$$\frac{N_{Ed}}{\frac{\chi_y * N_{Rk}}{\gamma_{m1}}} + k_{yy} * \frac{M_{y,Ed} + \Delta M_{y,Ed}}{\chi_{LT} * \frac{M_{y,Rk}}{\gamma_{m1}}} + k_{yz} * \frac{M_{z,Ed} + \Delta M_{z,Ed}}{\frac{M_{z,Rk}}{\gamma_{m1}}} \leq 1$$

$$\frac{N_{Ed}}{\frac{\chi_y * N_{Rk}}{\gamma_{m1}}} + k_{zy} * \frac{M_{y,Ed} + \Delta M_{y,Ed}}{\chi_{LT} * \frac{M_{y,Rk}}{\gamma_{m1}}} + \frac{M_{z,Ed} + k_{zz} * \Delta M_{z,Ed}}{\frac{M_{z,Rk}}{\gamma_{m1}}} \leq 1$$

This gives the utilizations of 0.504 and 0.496. It can be concluded that the panel fulfills the requirements given by EN-1993-1-7 for the combination of in-plane stress and out-of-plane stress.

5

Validation of minimum load amplifier

This chapter validates the accuracy of the minimum load amplifier obtained in chapter 4. For this, multiple tools are available. A finite element model of the analysed panel is used, as well as an online elastic buckling tool called EBPlate.

5.1. FE-model

A finite element model is set up of the analysed panel. For this model the software package ANSYS is used.

5.1.1. Geometry

The geometry of the FE model is exactly equal to the geometry of the analysed panel, except for the stiffeners. As explained in chapter 3, the bulb flat stiffener is converted to an angle profile with an equivalent conservative cross section. In this equivalent cross section the web thickness t_w and flange thickness t_f are not necessarily equal. In the elastic buckling tool EBPlate, angle profiles can only be inserted if these parameters are equal. In order to make an objective comparison between the results obtained from the FE-model and EBPlate, the stiffener in ANSYS was modeled with equal web thickness and flange thickness. The geometric properties of the FE-model are given in table 5.1. In EBPlate, the stiffener is inserted with h=18 [cm], b=3.4 [cm] and t=0.9 [cm] as shown in figure 5.3b.

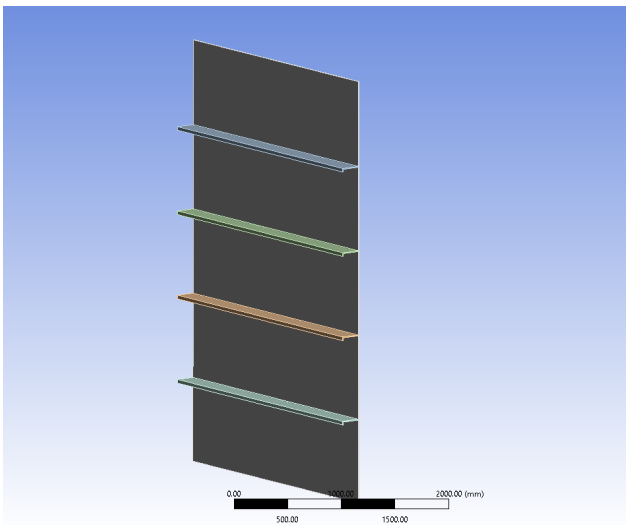

(a) stiffened side

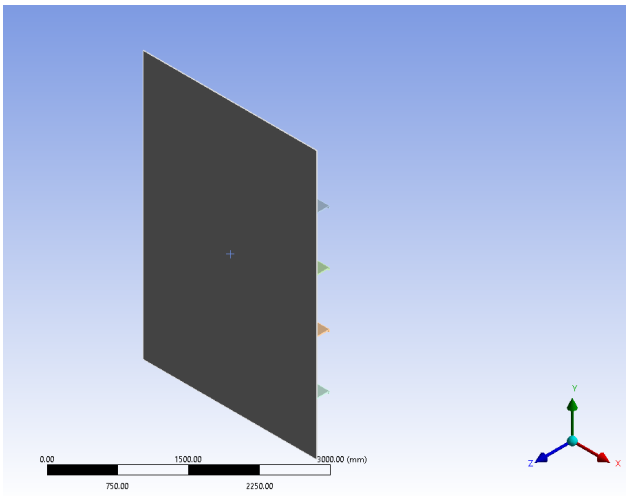

(b) Unstiffened side

Figure 5.1: Geometry of the FE-model

symbol	description	value	unit
h_w	height of stiffener web	171	[mm]
t_w	thickn. of stiffener web	9	[mm]
b	width of stiffener flange	34	[mm]
t_f	thickn. of stiffener flange	9	[mm]
r	fillet weld radius flange-web	4	[mm]
a	length of panel	2600	[mm]
b	width of panel	4000	[mm]
t_p	thickness of plate	8	[mm]
n	number of stiffeners	4	[-]

Table 5.1: Geometric properties of the FE-model

5.1.2. Mesh and analysis type

For the plate a mesh size of 24.0 [mm] is used. The stiffeners are given a smaller size of 12.0 [mm]. Altough not specified to the software explicitly, the mesh consists almost completely out of rectangular elements. This is the preferred element shape for the mesh for an element that consists out of rectangles itself as well. A static structural analysis and an eigenvalue buckling analysis are carried out.

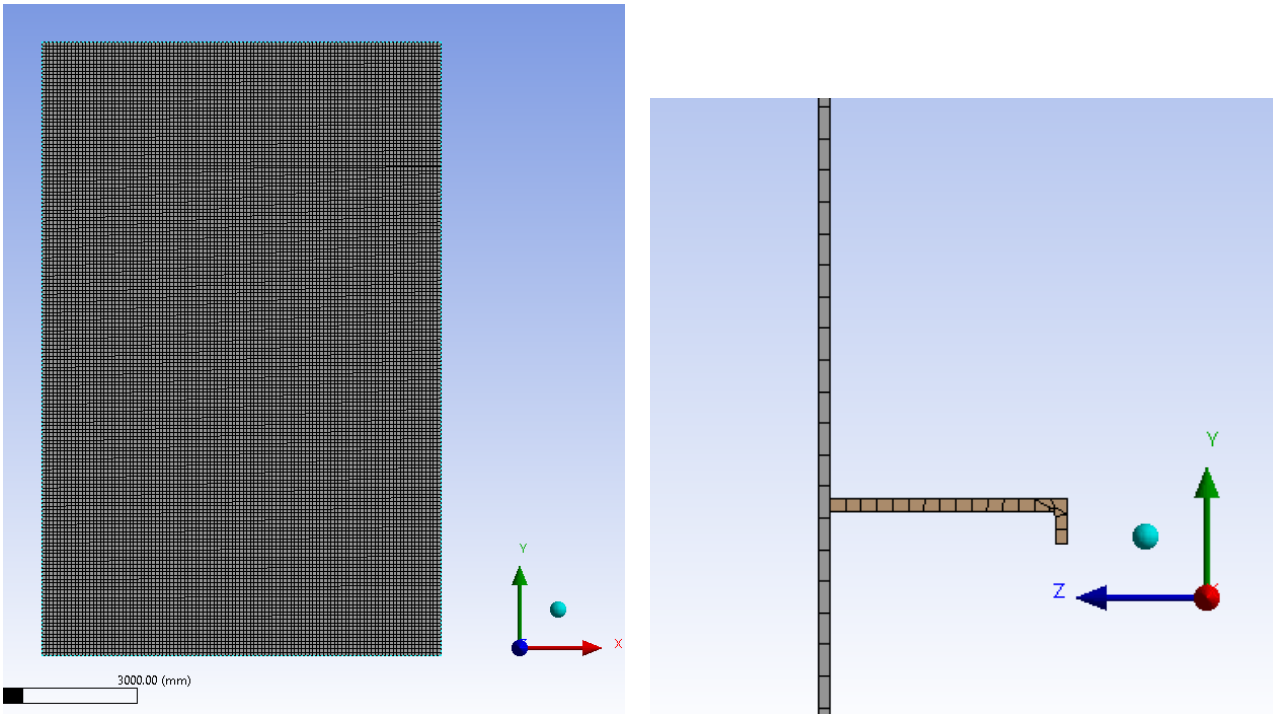

(a) stiffened side

(b) Meshing detail of the stiffener

Figure 5.2: Geometry of the FE-model

5.1.3. Boundary conditions and loads

Figure 5.3a shows the loads and boundary conditions imposed on the FE-model. Deformation in the z-direction is prevented along all the edges of the panel, labelled ”A” in figure 5.3a. Deformation in the x-direction is prevented on the right edge of the panel, labelled ”C” in figure 5.3a. Finally, deformation in the y-direction is prevented in the bottom right point labelled ”H”.

The left edge is loaded with the linearly increasing load, with 34 [MPa] at the top left point of the panel and 55.1 [MPa] at the bottom left point of the panel. All four edges of the panel are loaded with the

shear stress of 62.3 [MPa].

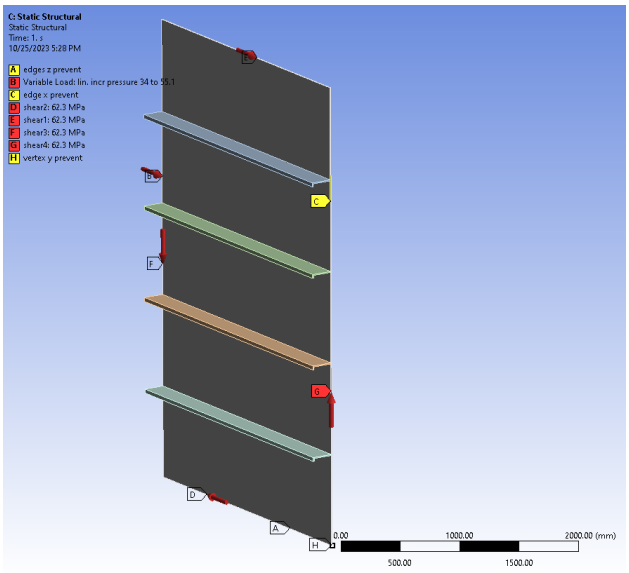

(a) Loads and boundary conditions imposed on the model

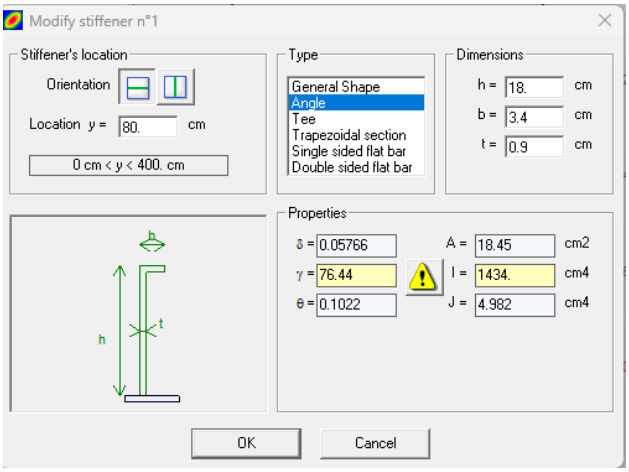

(b) Stiffener details as inserted in EBPlate

Figure 5.3

5.1.4. Stress distribution and deformation in the panel

The stress distribution and the deformations are checked after the static structural analysis is carried out. The stress distribution is given in figure 5.4. The average stress in the panel amounts to 68.6 [MPa]. A maximum of 511.1 [MPa] is found at the connection of the bottom stiffener and the plate.

The stresses after the static structural analysis seem in the right order of magnitude. To check whether the boundary conditions imposed on the model work as expected, the components of the deformation of the model are examined. These deformations are given in figure 5.5. The deformation in x direction is zero along the right edge as imposed by the boundary condition there. The deformation varies along the x-axis due to the stress in that direction, and in a smaller degree along the y-axis due to the shear stress. The deformation in y-direction is only due to the shear stresses. At the bottom right point the deformation in y direction is zero as imposed by the boundary condition. The deformation in z-direction is maximum in the bottom center of the panel, and zero around the edges. An important note for figure 5.5 is that the shape of the panel is the deformed shape under the influence of the loads. The skewedness is a result of the shear forces acting on the panel. The deformations are according to the expectations given the boundary conditions and loads.

5.1.5. Eigenvalue buckling analysis

An eigenvalue buckling analysis is carried out on the panel. This analysis is validated by comparing it to the outcomes of EBPlate. EBPlate is a tool which can be used to find critical buckling stresses and the corresponding buckling modes of (un)stiffened plates (Centre Technique Industriel de la Construction Metallique (CTICM)., n.d.). EBPlate gives a minimum load amplifier ϕ_{crit} of 1.14, which is almost the same as the load multiplier given by ANSYS of 1.15 for the first buckling mode. As a lower value for the load multiplier is more conservative, it can be concluded that EBPlate is slightly more conservative than the FE-model in this case. The buckling modes given by ANSYS and EBPlate look the same as shown in figures 5.6a and 5.6b.

It is clear that the panel buckles locally. Although the stiffener in the bottom right in figure 5.6a undergoes lateral torsion buckling, the panels between the stiffeners show buckling behaviour before the stiffener

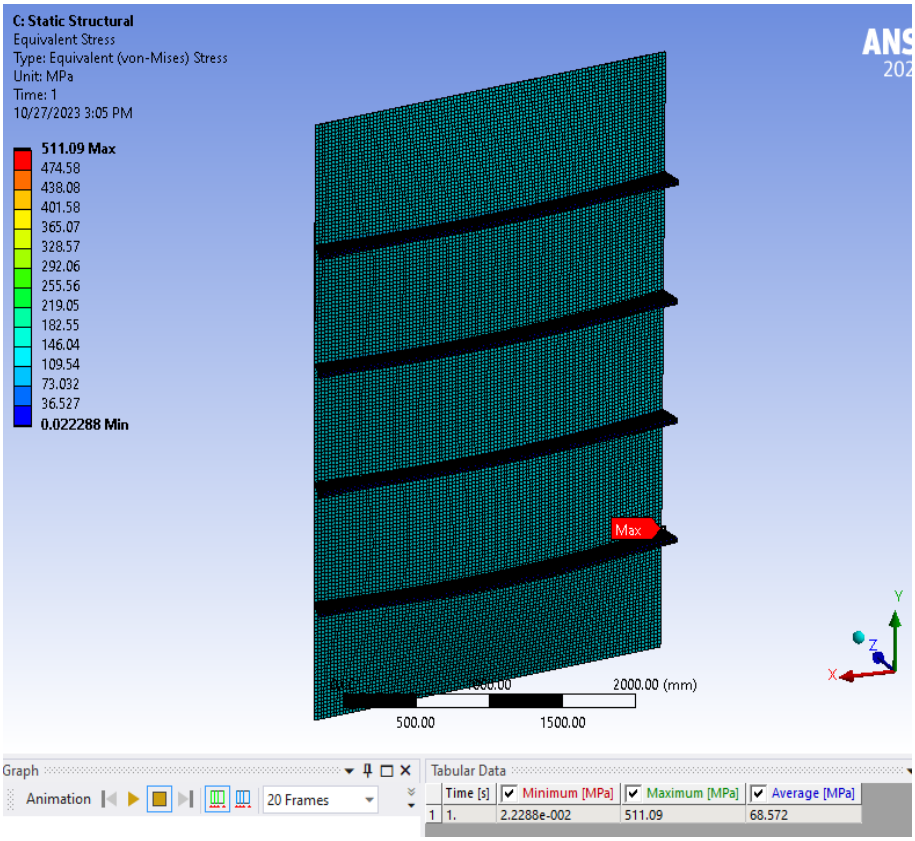

Figure 5.4: Stress distribution in the panel after static structural analysis

shows buckling behaviour. The calculation in section 4.2 gave a minimum load amplifier α_{crit} for local buckling of 0.9853, which is rather conservative compared to the FE-model and EBPlate. This is logical, as in the verification analysis in chapter4.2 the subpanel subjected to the highest stresses was checked as if being a seperate panel with all four edges being simply supported edges. If this separate case is analysed in EBPlate with simply supported edges, the minimum load amplifier obtained is 0.9927, as shown in figure 5.7. It can be concluded that the hand calculation gives a value for the load amplifier that is very close while slightly conservative compeared to EBPlate.

5.2. Validation of calculated load amplifier

The FE-model and EBPlate give the same result for the minimum load amplifier for the analysed panel under the stresses given in chapter 3. It is concluded therefore concluded that this is a reliable value for the minimum load amplifier. The next step is to compare values obtained from the calculation sheet and values from EBPlate. For this comparison, the minimum load amplifier α_{crit} is calculated for the panel with geometry as described in section 5.1.1, for increasing plate thicknesses. The stiffener in EBPlate is again inserted with h=18 [cm], b=3.4 [cm], t=0.9 [cm]. In the excel calculation, the real properties of the 180x9 bulb flat are used. The plate thickness is increased from t_p = 6 [mm] to t_p = 40 [mm] with steps of 2 [mm]. The procedure is done for three load cases:

1. Uniformly distributed longitudinal stress σ_x of 100 $[N/mm^2]$
2. Uniformly distributed longitudinal stress σ_x of 100 $[N/mm^2]$ and shear stress τ of 50 $[N/mm^2]$
3. Uniformly distributed longitudinal stress σ_x of 100 $[N/mm^2]$ and shear stress τ of 100 $[N/mm^2]$

The results of the calculated minimum load amplifiers and the amplifiers from EBPlate are given in figures 5.8 to 5.10. The first plate thickness at which local buckling has turned into global buckling is given in the description of the graphs. In the Excel calculation this is the first plate thickness for which

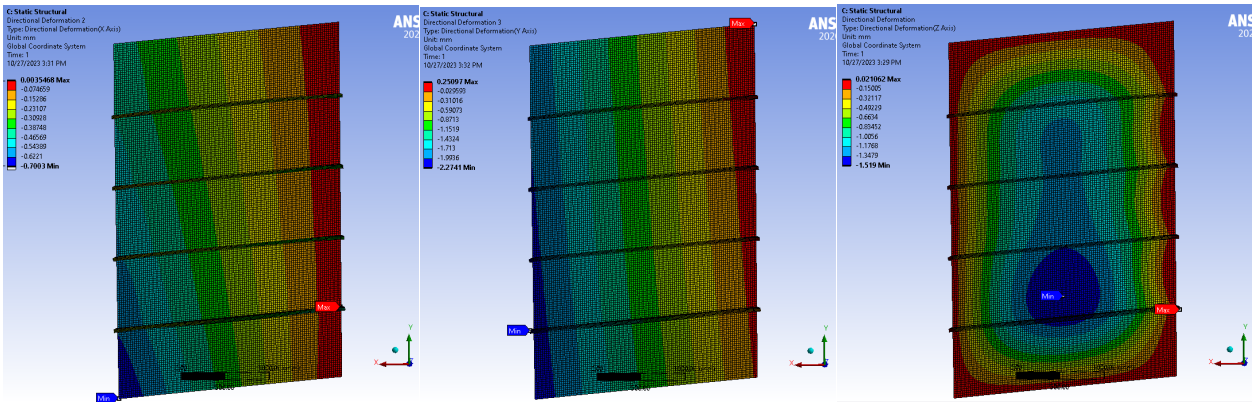

(a) Deformation x component (b) Deformation y component (c) Deformation z component

Figure 5.5

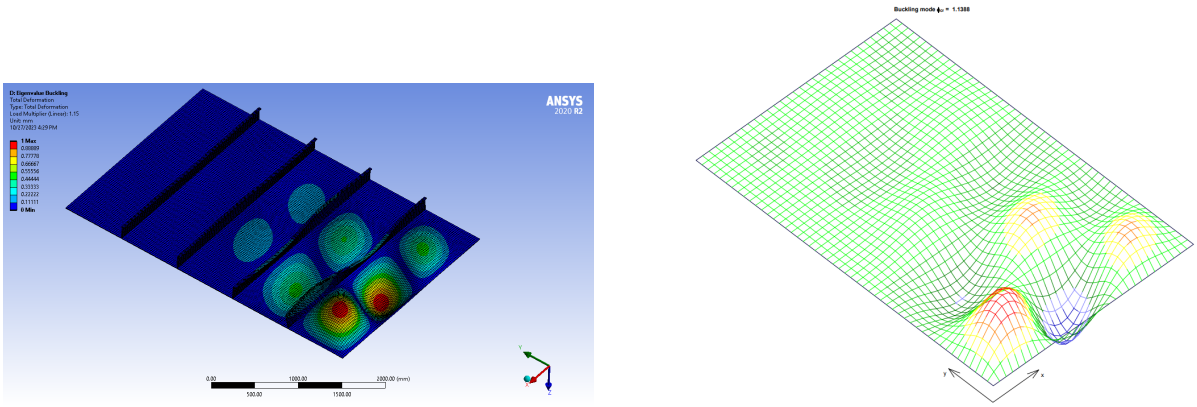

(a) First buckling mode in ANSYS (b) First buckling mode in EBPlate

Figure 5.6

$\alpha_{crit,glob}$ is smaller than $\alpha_{crit,loc}$. In EBPlate a visual inspection of the post processing image was done to assess whether local buckling had changed into global buckling.

It is observed that for loadcase 1 the minimum load amplifier increases exponentially until the point where local buckling becomes global buckling. After this point, the minimum load amplifier decreases, and then seems to increase again. For loadcase 2 and 3 similar phenomena are observed, altough they become less pronounced especially for loadcase 3.

It is also clear that, the EN-1993-1-5 calculation and EBPlate give very similar results for loadcase 1, as the two lines are very close to one another. For loadcase 2 and in larger extent for loadcase 3, the difference is larger. For all loadcases, EN-1993-1-5 surpasses EBPlate at the transition from local to global buckling. Before and after this transition, EN-1993-1-5 gives lower and thus more conservative values than EBPlate.

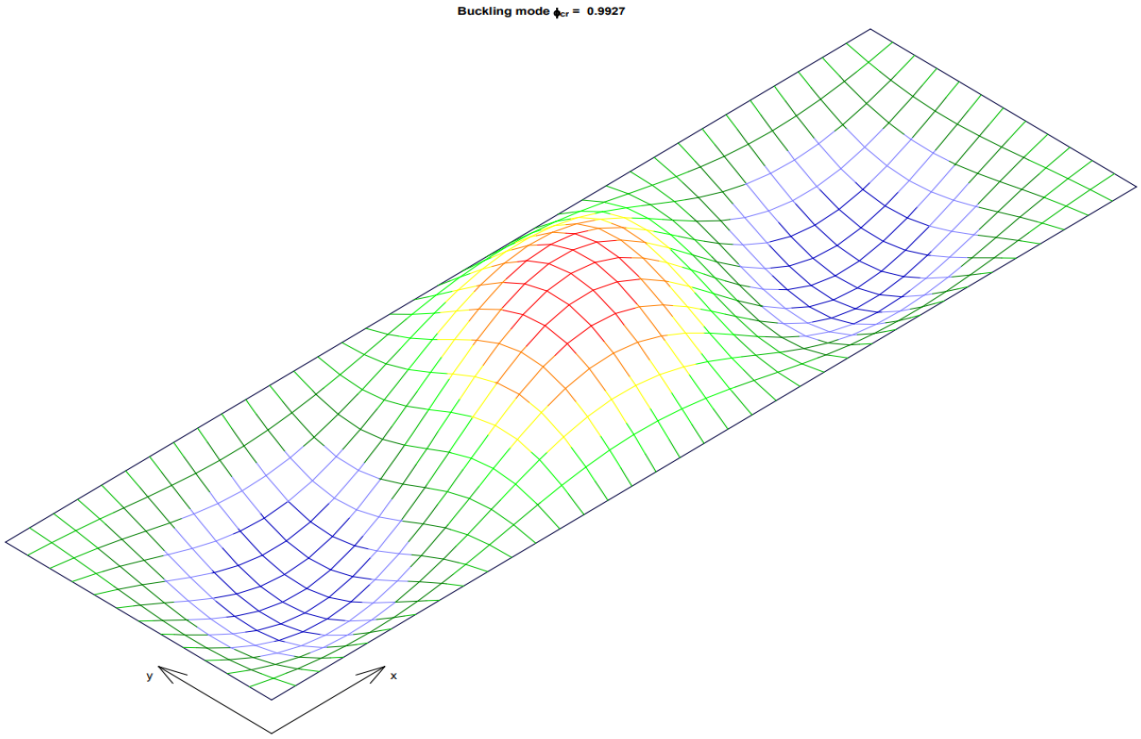

Figure 5.7: First buckling mode of most compressed subpanel in EBPlate

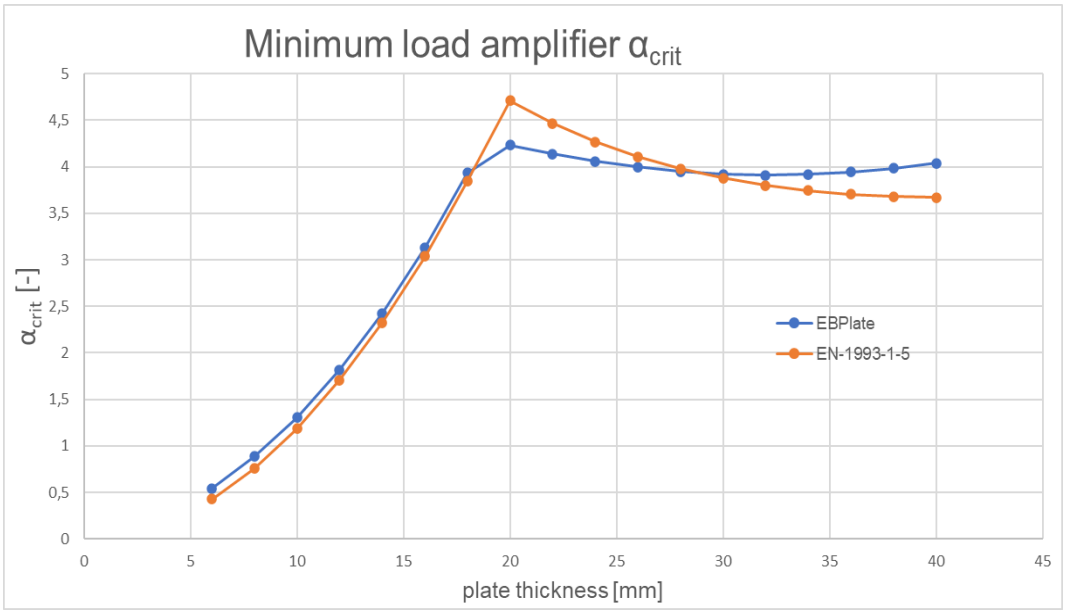

Figure 5.8: Load amplifier EBPlate vs. EN-1993-1-5 for loadcase 1. EN-1993-1-5: t_p = 20 [mm], EBPlate: t_p = 20 [mm]

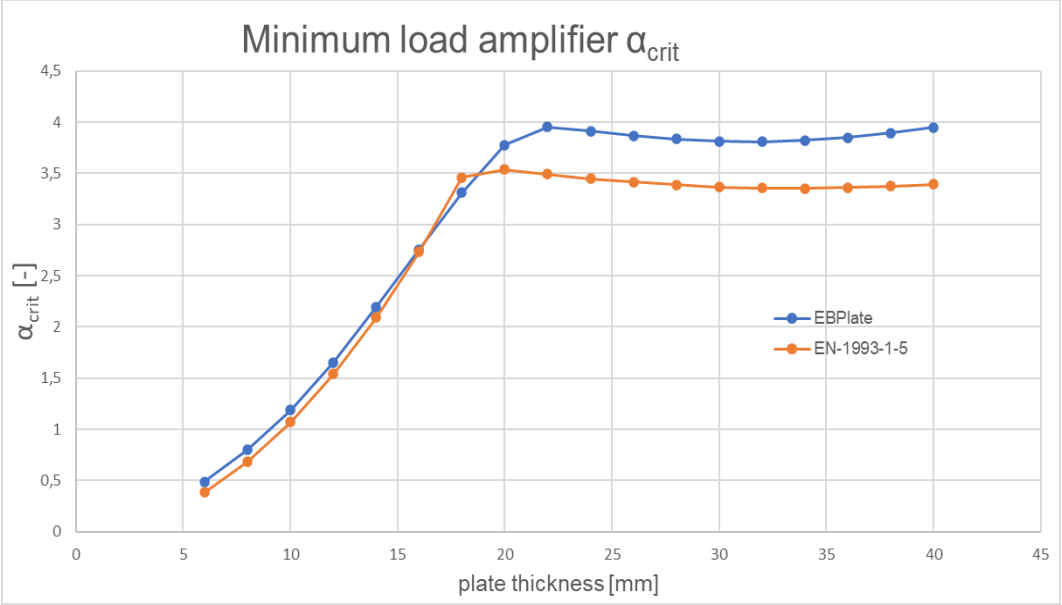

Figure 5.9: Load amplifier EBPlate vs. EN-1993-1-5 for loadcase 2. EN-1993-1-5: t_p = 20 [mm], EBPlate: t_p = 16 [mm]

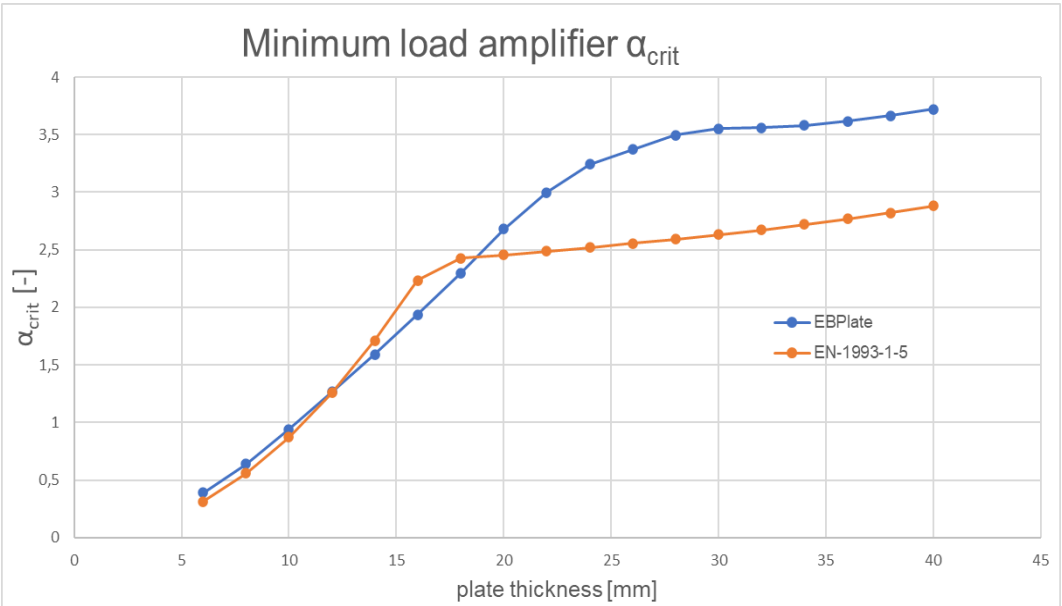

Figure 5.10: Load amplifier EBPlate vs. EN-1993-1-5 for loadcase 3. EN-1993-1-5: t_p = 18 [mm], EBPlate: t_p = 12 [mm]

6

Validation of unity checks

The calculations as described in chapter 4 have been set up in a calculation sheet. With this sheet unity checks of the analysed panel were compared to unity checks obtained from DNV-RP-C201. The DNV-RP-C201 code was not studied in detail during this internship, but is merely used as means of comparison for the developed Eurocode calculation sheets. The DNV-RP-C201 unity checks are in this case obtained from a program called STIPLA. The stiffeners are in this program imported with their real geometric properties as given in appendix E. STIPLA gives multiple unity checks, among which UFp and UFs. The first concerning the plate buckling, the second concerning the stiffener buckling. The UFp can be compared to the unity check from EN-1993-1-5, and UFs to the unity check from EN-1993-1-7.

The panel as described in chapter 3 is studied for four plate thicknesses: t_p = 8 [mm], 10 [mm], 12 [mm] and 14 [mm]. The panel is subjected to an increasing universally distributed longitudinal in-plane stress σ_x. Starting from σ_x = 20 $[N/mm^2]$, the stress is increased with steps of 20 $[N/mm^2]$ until all the unity checks have surpassed the value of 1. The results are given in figure 6.1a until 6.2b. The procedure is also carried out with a shear force of 50 $[N/mm^2]$ applied to the panel, of which the results are given in figure 6.3a until 6.4b. Finally, the verifications are carried out with a shear force of 100 $[N/mm^2]$ applied to the panel, of which results are given in figure 6.5a until 6.6b.

6.1. Loadcase 1

For the cases in which the shear stress is zero, (figure 6.1a until 6.2b), it is observed that the unity checks given by STIPLA and Eurocode are relatively similar. Especially for plate thicknesses 8 [mm] and 10 [mm] this is the case. For all four plate thicknesses Eurocode gives slightly more conservative results for both the stiffener and the plate unity checks compared to DNV. Notable is that DNV UFs (grey line) is not linear, but shows a kink after a certain stress has been surpassed. As DNV-RP-C201 has not been studied in detail it is unknown why this is, but it is clear that EN-1993-1-7 (yellow line) and DNV UFs (grey line) show less difference after the stress where this kink happens. Nevertheless, it is evident that the difference between EN-1993-1-7 and DNV UFs becomes larger for thicker plates. The difference between the unity checks for the plate EN-1993-1-5 (orange line) and DNV UFp (blue line) are quite small for all plate thicknesses, and are actually largest for the thinnest plate with thickness 8 [mm].

6.2. Loadcase 2

For the plates subjected to a shear stress of 50 [MPa], the unity checks for the plates show large similarity (UFp and EN-1993-1-5). For low values of σ_x, EN-1993-1-5 gives more conservative values. For increasing values of σ_x, the difference between the unity checks becomes smaller, and for plate thickness of 12 [mm] they even cross, so that from 120 [MPa] DNV UFp is more conservative than EN-1993-1-5. Because the unity check given by EN-1993-1-7 is not dependent of the shear stress,

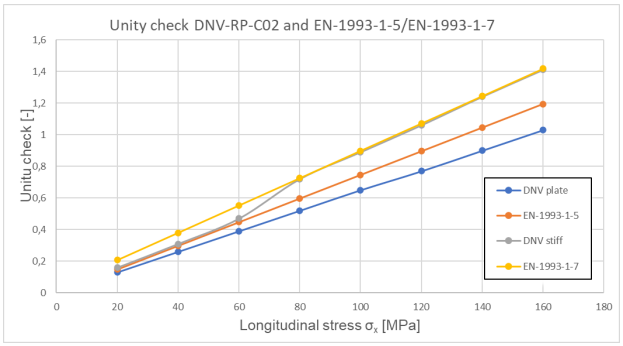

(a) no shear stress, $t_p = 8[mm]$

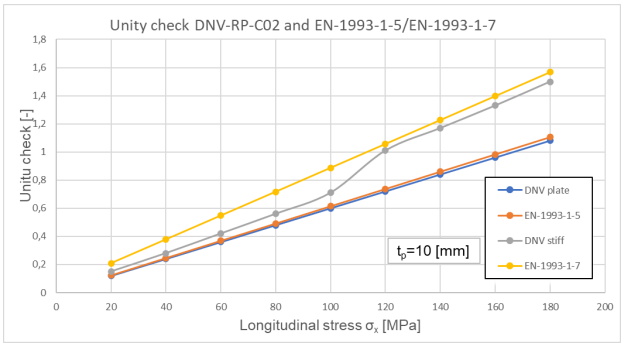

(b) no shear stress, $t_p = 10[mm]$

Figure 6.1

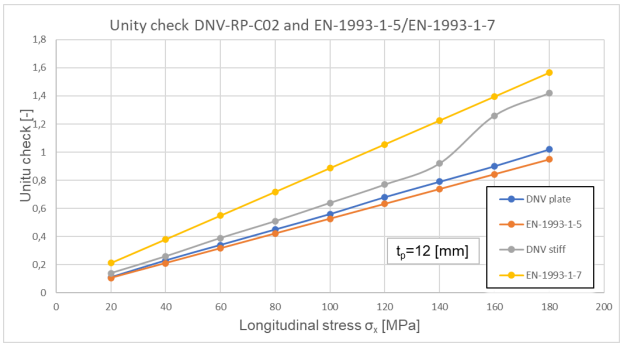

(a) no shear stress, $t_p = 12[mm]$

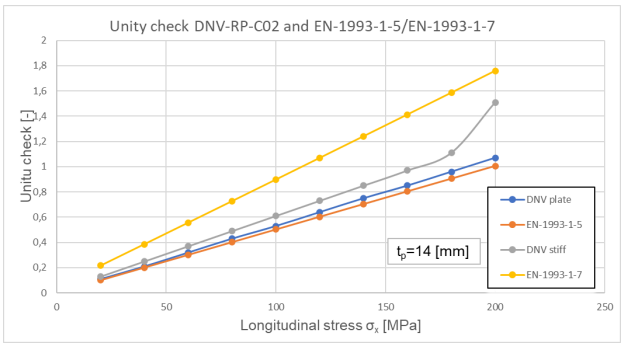

(b) no shear stress, $t_p = 14[mm]$

Figure 6.2

the same lines are plotted as for the case without shear stress. For small plate thicknesses the result is that DNV UFs is more conservative than EN-1993-1-7 by margin. For larger plate thicknesses this effect becomes less pronounced, and for a plate thickness of 12 [mm] EN-1993-1-7 is already the more conservative one of the two unity checks.

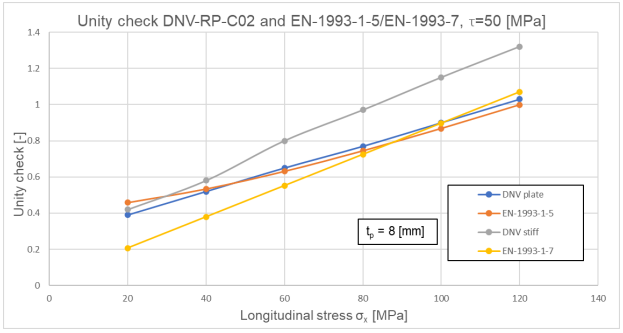

(a) Shear stress $\tau = 50[MPa]$, $t_p = 8[mm]$

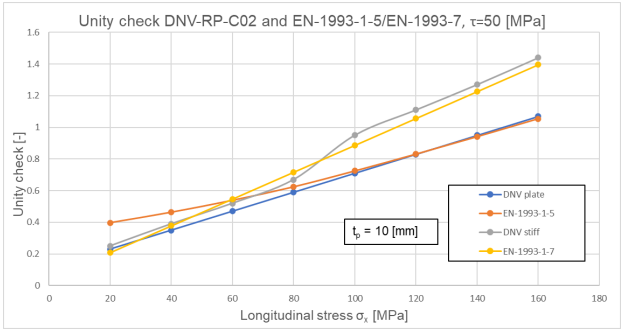

(b) Shear stress $\tau = 50[MPa]$, $t_p = 10[mm]$

Figure 6.3

6.3. Loadcase 3

In the final set of unity checks the panels are subjected to a shear stress of 100 [MPa]. The unity checks for the plate UFp and EN-1993-1-5 again show quite some difference for low longitudinal stress σ_x, similar to the case with a shear stress of 50 [MPa]. This difference again becomes smaller for

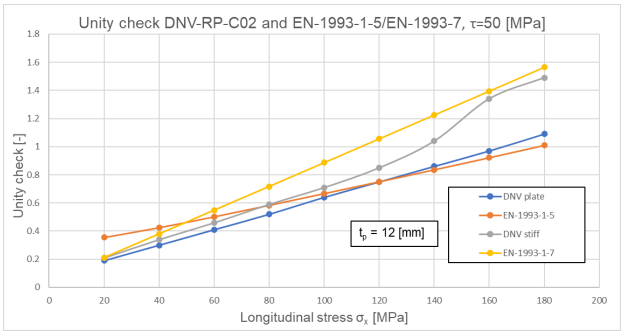

(a) Shear stress $\tau = 50[MPa]$, $t_p = 12[mm]$

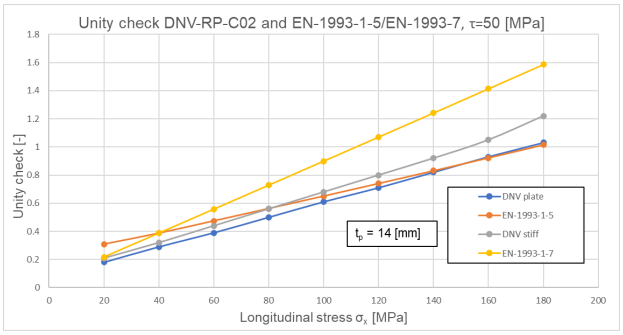

(b) Shear stress $\tau = 50[MPa]$, $t_p = 14[mm]$

Figure 6.4

larger values of σ_x. For a plate thickness of 10 [mm] the lines again cross, after which DNV UFp is more conservative than EN-1993-1-5. As was the case for the shear stress of 50 [MPa], the stiffener unity checks show large differences for small plate thicknesses in which DNV is more conservative. This difference becomes smaller for larger plate thicknesses, so that EN-1993-1-7 gives more conservative values for the unity checks with longitudinal stresses of 120 [MPa] and 140 [MPa].

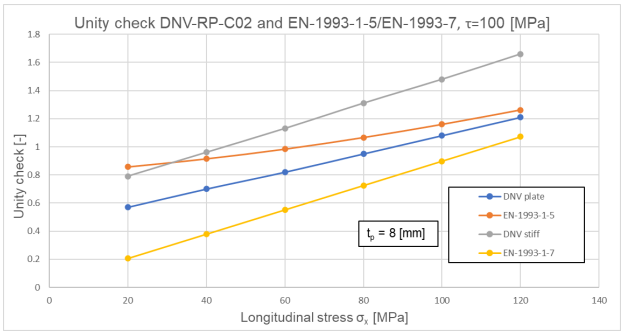

(a) Shear stress $\tau = 100[MPa]$, $t_p = 8[mm]$

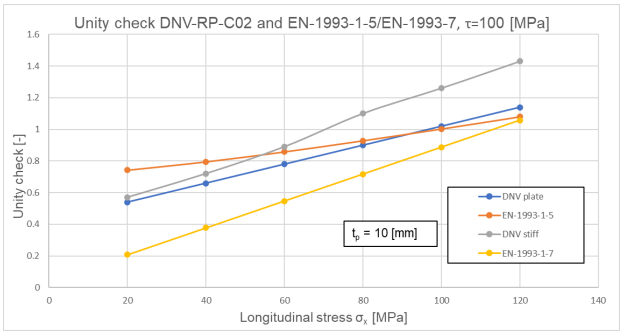

(b) Shear stress $\tau = 100[MPa]$, $t_p = 10[mm]$

Figure 6.5

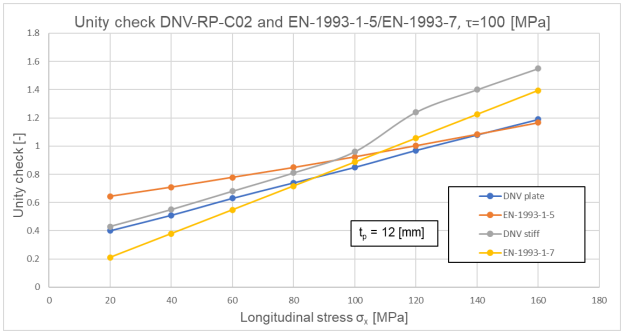

(a) Shear stress $\tau = 100[MPa]$, $t_p = 12[mm]$

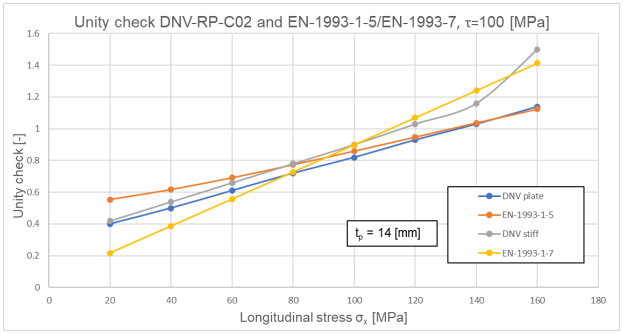

(b) Shear stress $\tau = 100[MPa]$, $t_p = 14[mm]$

Figure 6.6

6.4. STIPLA calculations

The calculation details of the STIPLA software, which is based on the DNV-RP-C201, is given in appendix F. Shown are the analysed panel as described in section 3 under the loads as occurs in the structure, one panel under loadcase 1, and one panel under loadcase 2 (the latter two are included in the graphs above). The STIPLA software gave unity checks for the analysed panel under the stress

state that occurs in the structure of 0.8 (UFs) and 0.69 (UFp). The STIPLA stiffener unity check is higher than the calculated value of 0.504, probably because of the relatively high shear force of 62.3 [MPa]. The plate unity check of 0.69 is very close to the calculated value of 0.681.

7

Conclusion

The results for the unity checks given by Eurocode and DNV are very similar for the case without shear force. For larger plate thicknesses, EN-1993-1-7 becomes significantly more conservative than DNV UFs. In all examined cases, Eurocode gives slightly more conservative results than DNV-RP-C201.

In case shear force is applied, the unity checks given by EN-1993-1-5 and DNV UFp show good similarity. The results converge for higher values of longitudinal stress σ_x. For the unity checks given by EN-1993-1-7 and DNV UFs, this is not the case. For small plate thicknesses, EN-1993-1-7 gives a far lower unity check than DNV UFs. The lines show more similarity for larger plate thicknesses, probably because the shear stress has less influence on the plate if the thickness is larger. The above described phenomena are true for both a shear stress 0f 50 [MPa] and 100 [MPa], although more pronounced in the 100 [MPa] case.

The goal of this internship is to find a calculation method in Eurocodes to verify stiffened panels. More specifically, the following research was formulated:

How can eurocode be used to verify the buckling strength of a stiffened steel panel subjected to bi-axial in-plane normal stress, shear stress and out-of-plane loading?

Including the following sub-questions:

- Which eurocode checks and failure modes are relevant?
- How to validate the acquired results?
- To what extent do the ground truth results and acquired results compare?

The following conclusions are drawn:

- EN-1993-1-5 gives two methods to verify stiffened plated structures: reduced stress method (section 10) and effective width (section 4, 5 and 6). Since a verification of a panel subjected to both biaxial in-plane normal stress and shear stress is desired, the reduced stress method is selected as the most suitable method. A calculation analysis performed taking into account uniformly distributed longitudinal normal stress showed slightly more conservative results for the reduced stress method as compared to the effective width method. This outcome is consistent with relevant literature.

  EN-1993-1-7 5.2.3.4 gives a simplified design model, giving conservative results. The model gives a method to reduce the cross section of a stiffened plate to an equivalent column, and refers to EN-1993-1-1 section 6.3.3 (Uniform members in bending and axial compression). As no alternatives are given in Eurocode to verify plates subjected combinations of in- and out-of-plane loading, this approach is concluded to be the verification strategy to be used.

- The reduced stres method requires a value for the minimum load amplifier (α_{crit}. EN-1993-1-5 gives a method to calculate this value analytically (eq. 10.6). This analytically calculated minimum load amplifier is checked for multiple plate thicknesses under a uniformly distributed longitudinal normal stress and shear stress by making use of EBPlate. In all cases the analytically obtained value for α_{crit} showed good similarity with the EBPlate value. For the panel described in chapter 3 the value for α_{crit} is checked with the analytical formula given in EN-1993-1-5 eq. 10.6, EBPlate and ANSYS, which showed great similarity. Transverse in-plane normal stress was not included in the validation of the minimum load amplifier, for reasons described in section 4.2.2.

  The unity checks are validated by making use of another existing design verification, DNV-RP-C201. The unity checks are calculated making use of EN-1993-1-5 and EN-1993-1-7 for the panel with geometry as described in 3, and compared to the unity checks UFs and UFp given by the program STIPLA, which performs the calculations given in DNV-RP-C201. Better would be to do the validation of unity checks by making use of a finite element software package such as ANSYS. However, due to time restraints this was omitted from the analysis.

- The analytically calculated unity checks obtained from EN-1993-1-5, EN-1993-1-7/EN-1993-1-1 are compared to the unity checks UFp and UFs given by DNV-RP-C201. Very good similarity is found for the loadcase of only longitudinal in-plane normal stress. For larger plate thickness EN-1993-17 is significantly more conservative than DNV-RP-C201 UFs. This is consistent with the statement in EN-1993-1-7 that this concerns a simplified design model that gives conservative estimates.

  In case shear force is applied, the unity checks given by EN-1993-1-5 and DNV UFp show good similarity. The results converge for higher values of longitudinal stress σ_x. For the unity checks given by EN-1993-1-7 and DNV UFs, this is not the case. For small plate thicknesses, EN-1993-1-7 gives a far lower unity check than DNV UFs. The lines show more similarity for larger plate thicknesses, probably because the shear stress has less influence on the plate if the thickness is larger. The above described phenomena are true for both a shear stress 0f 50 [MPa] and 100 [MPa], altough more pronounced in the 100 [MPa] case.

A direct answer to the main research question is not easily given, as a way to verify stiffened panels subjected to the combination of biaxial in-plane normal stress, shear stress and out-of-plane loading is not found in Eurocode. In case only longitudinal in-plane normal stress and out-of-plane loading are concerned, the reduced stress method can be used to find unity checks close to the ones given by the DNV-RP-C201 design code. In case shear stress is added, the unity checks obtained show larger differences compared to DNV-RP-C201, especially the out-of-plane check given by EN-1993-1-7 gives results for plate thicknesses of 8 [mm] and 10 [mm] that do not match up well with the values given by DNV-RP-C201.

8

Recommendation

The verification analysis described in this internship report is used to set up an Excel calculation tool, that calculates unity checks for panels subjected to both in-plane stress and out-of-plane loads. After the execution of the internship, engineers have slightly modified it in layout, in order to make it more presentable to the client. The following recommendations are made for the practical use of this sheet:

- In case a verification analysis is performed on a panel that is subjected to a stress state in which transverse in-plane normal stress (σ_y) is **not** present, the standard calculation approach based on the approach as described in sections 4.2.1 and 4.2.3 can be followed. This analysis completely follows the rules as given in the relevant Eurocodes.
- In case a verification analysis is performed on a panel that is subjected to a stress state in which transverse in-plane normal stress (σ_y) **is** present, a slightly different verification analysis must be followed. In this case, an analytically obtained value for the unity check for global buckling can not be found for reasons described in section 4.2.2. Therefore it is recommended in these cases to do a verification based on local buckling of the normative subpanel (in case of equal dimensions this is the most compressed one, in case of varying dimensions and stresses all subpanels must be checked). In order to guarantee the stiffeners will not buckle, they must be checked to comply with the rules as given in section 9 of EN-1993-1-5. For this local buckling verification the reduction factor ρ_y should be found according to the formulas 4.3 and 4.4 as given in EN-1993-1-5 B.1 and recommended by (Beg et al., 2011, p. 165).
- The verification for the out-of-plane loading in the performed calculations only depends on reduction factor ρ_c and thus only on the amount of longitudinal in-plane normal stress σ_x as described in section 4.2.2. It could be checked whether the results for the unity checks for out-of-plane loading are more similar to the DNV checks in case $\rho_{c,glob}$ as given by equation 4.2 is used instead of the reduction factor ρ_c that is based on the effective width method and thus only depends on longitudinal stress. Especially for panels subjected to high values of shear force this could be a better option. This option however is not possible in case also transverse in-plane normal stress is present for reasons described in section 4.2.2.
- As described in section 2.6 points 8 and 9, the longitudinal stiffeners must fulfill the requirements given in section 9 of EN-1993-1-5 in order for the verification for out-of-plane loading to be valid. Among these are requirements concerning lateral torsion buckling. As observed in the ANSYS first buckling mode (figure 5.6a), some of the stiffeners show some degree of lateral torsion buckling. As already mentioned in this recommendation chapter, a verification of the stiffeners according to EN-1993-1-5 is recommended in order to make sure local buckling is governing the design in case of transverse in-plane normal stress. It is recommended to also subject the stiffeners to this verification in case no transverse stress is present in order to prevent the lateral torsion buckling of the stiffeners.

Bibliography

Ahlstrand, E., Johan Johansson. (2021). *Steel design of plated structural elements - a comparison of the effective width method and the reduced*. https://odr.chalmers.se/items/4e3c8393-9225-41cc-b00c-0c6c7b2d10be

Beg, D., Kuhlmann, U., Davaine, L., & Braun, B. (2011). *Design of plated structures*. ECCS-European Convention for Constructional Steelwork.

Eurocode 3: Design of steel structures — part 1-1: General rules and rules for buildings (Standard). (2005, May). European Committee for Standardization.

Eurocode 3 — design of steel structures — part 1-5: Plated structural elements (Standard). (2006, November). European Committee for Standardization.

Eurocode 3 — design of steel structures — part 1-7: Plated structures subject to out of plane loading (Standard). (2007, July). European Committee for Standardization.

Centre Technique Industriel de la Construction Metallique (CTICM). (n.d.). Centre technique industriel de la construction metallique (cticm). Retrieved October 27, 2023, from https://www.cesdb.com/ebplate.html

Derik, A. M. (2013). *Stiffened plates - reduced stress method*. https://ntnuopen.ntnu.no/ntnu-xmlui/handle/11250/237412

Indriðason, J. P., & Sigmundsson, V. (2015). *Buckling analysis of orthotropic plates stiffened plate and steel sandwich plates*. https://odr.chalmers.se/server/api/core/bitstreams/b839dab3-9761-4c11-85ce-0fe6a36c6575/content

Kleppe, S.-R., Aalberg, A., & Eltvik, L. (2021). Design of stiffened plates subjected to axial compression and transverse load. *ce/papers*, *5*, 1555–1564. https://doi.org/10.1002/cepa.1299

Mensinger, M. (2016). Buckling behavior of stiffened plates under biaxial compression and shear. https://www.researchgate.net/publication/322144815_BUCKLING_BEHAVIOR_OF_STIFFENED_PLATES_UNDER_BIAXIAL_COMPRESSION_AND_SHEAR

Pavlovic, D. M. (2019, May 16). Cie5125-07. Retrieved October 13, 2023, from https://collegeramavideoportal.tudelft.nl/catalogue/cie5125/presentation/71c3e6c58f73442a9203d670b2fc99421d?academicYear=2018-2019-cie5125

renews.biz. (2023). Construction work starts on borwin kappa platform. *renews.biz*. https://renews.biz/86811/construction-work-starts-on-borwin-kappa-platform/

Tankova, D. T. (2023, May). Ciem5240 steel and composite structures. Retrieved October 13, 2023, from https://brightspace.tudelft.nl/d2l/le/content/520156/viewContent/3133212/View

van der Burg, M. (2011). *Plate buckling in design codes the difference between nen 6771 and nen-en 1993-1-5*. https://repository.tudelft.nl/islandora/object/uuid%3Aa642491a-3e90-41d6-a7e3-aacb8586a632

van Dijk, B. (2023). Grootste opdracht ooit van TenneT gaat naar buitenlandse industrie. *Financieel Dagblad*. https://fd.nl/bedrijfsleven/1472208/netbeheerder-tennet-gunt-voor-23-mrd-contracten-voor-windenergie-vanaf-de-noordzee

Zizza, A. (2016). Buckling behaviour of unstiffened and stiffened steel plates under multiaxial stress states. https://elib.uni-stuttgart.de/handle/11682/9011

A

Hand calculation effective width method vs reduced stress method

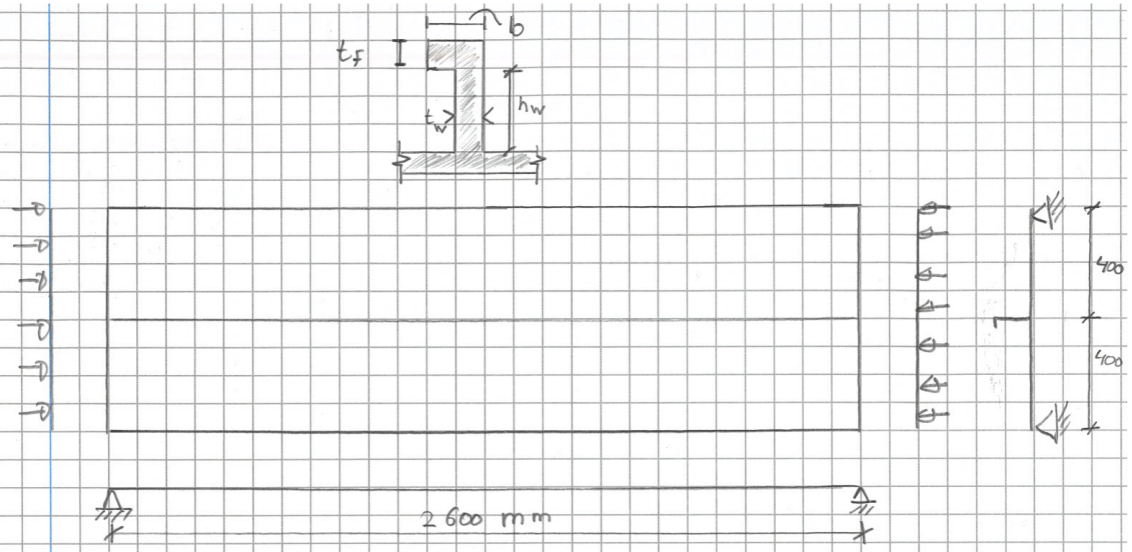

(1) Plate

$$\lambda_p = \frac{b/t}{28.4\,\varepsilon\sqrt{k_\sigma}} = \frac{400/8}{28,4 \cdot 0,8136 \cdot \sqrt{4}} = 1,0819$$

(2) Stiff web

$$\lambda_p = \frac{b/t}{28,4\,\varepsilon\sqrt{k_\sigma}} = \frac{166/11,5}{28,4 \cdot 0,8136 \cdot \sqrt{0,43}} = 0,9527$$

(3) Flange Stiff

$$\lambda_p = \frac{b/t}{28,4 \cdot 0,8136\sqrt{k_\sigma}} = \frac{36,5/14}{28,4 \cdot 0,8136 \cdot \sqrt{0,43}} = 0,17207$$

Stiffener : bulb Flat "180 x 11,5"

h_w = 166 mm

t_w = 11,5 mm

b = 36,5 mm

t_f = 14 mm

$\rho_1 = \rho_2 = \dfrac{\lambda_p - 0{,}055(3+\psi)}{\lambda_p^2} = 0{,}7363$

$\rho_2\ (\text{web}) = \dfrac{\lambda_p - 0{,}055(3+\psi)}{\lambda_p^2} = 0{,}80728$

$\rho_3\ (\text{Flange}) = 1 \quad \text{as} \quad \lambda_p < 0{,}673.$

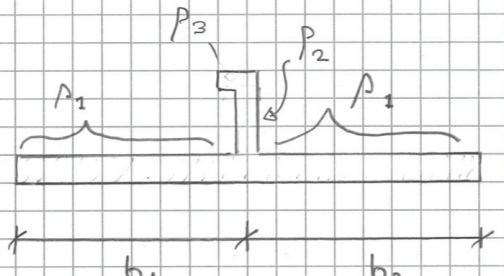

$\psi = 1$

$b_{1,edge} = \dfrac{2}{5-\psi} = 200\ [mm]$

$b_{edge} = \dfrac{2}{5-\psi} \cdot b_2 = 200\ mm$

$\dfrac{3-\psi}{5-\psi} \cdot b_1 = \dfrac{1}{2} b_1 = 200$

$\dfrac{3-\psi}{5-\psi} b_2 = \dfrac{1}{2} b_2 = 200$

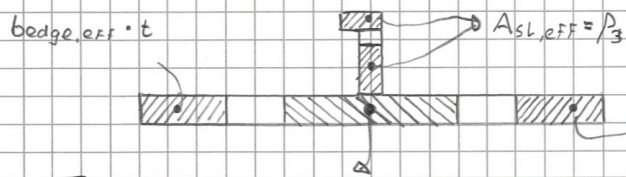

$A_{sl,eff} = \rho_3 \cdot b \cdot t_f + \rho_2 \cdot h_w \cdot t_w = 2052{,}0975$

$b_{edge,eff} \cdot t = 0{,}7363 \cdot 200 \cdot 8$

$\Sigma \rho_{loc}\, b_{c\,loc}\, t = 0{,}7363 \cdot 400 \cdot 8 = 2356{,}16$

$$A_{c,eff,loc} = A_{sl,eff} + \sum_c \rho_{loc} \cdot b_{c,loc} \cdot t$$

$$= 2052,0975 + 2356,16 = 4408,357$$

$$A_{c,eff} = \rho_c \, A_{c,eff,loc} + \sum b_{edge,eff} \cdot t$$

$$\beta_{A,c} = \frac{A_{c,eff,loc}}{A_c} = \frac{4408,357}{5620} = 0,7844$$

$$A_c = 400 \cdot 8 + 166 \cdot 11,5 + 36,5 \cdot 14 = 5620$$

↳ Gross Area of compr. zone of stiffened plate except parts of subpanels supported by adjacent plate

Plate-like behaviour:

$$e_{sl,1} = \frac{\sum A_{sl,1} \cdot e}{\sum A_{sl,1}}$$

$$= \frac{400 \cdot 8 \cdot 4 + 166 \cdot 11,5 \cdot \left(8 + \frac{166}{2}\right) + 36,5 \cdot 14 \cdot (8+166+7)}{5620}$$

$$= 49,6459$$

$$I_{sl,1} = \sum_i \frac{1}{12} \cdot b_i \cdot h_i^3 + A_i \cdot e_i = 30350286 \ mm^4$$

$$a_c = 4,33 \cdot \sqrt[4]{\frac{I_{sl,1} \, b_1^2 \, b_2^2}{t^3 \, b}} = 5081,58 \ mm$$

$$\left(\begin{array}{l} b_1 = b_2 = 400 \\ b = 800 \\ t = 8 \end{array} \right)$$

$$a = 2600 \ mm < a_c \rightarrow$$

$$\sigma_{cr,sl} = \frac{\pi^2 E I_{sl,1}}{A_{sl,1} \, a^2} + \frac{E \, t^3 \, b \, a^2}{4\pi^2 (1-\nu^2) A_{sl,1} \, b_1^2 \, b_2^2}$$

$$\sigma_{cr,sl} = \sigma_{cr,p} = 1768,26 \quad [N/mm^2]$$

$$\lambda_p = \sqrt{\frac{\beta_{A,c} f_y}{\sigma_{cr,p}}} = \sqrt{\frac{0,7844 \cdot 355}{1768,26}} = 0,3968$$

$$\rho = \begin{cases} \dfrac{\lambda_p - 0,055(\psi+3)}{\lambda_p^2} \leq 1 & \lambda_p > 0,673 \\ 1 & \lambda_p \leq 0,673 \end{cases}$$

$$\rho = 1$$

Column-like behaviour:

$$i = \sqrt{\frac{I_{sl,1}}{A_{sl,1}}} = 73,487$$

$$\alpha_e = \alpha + \frac{0,09}{i/e}$$

$\alpha = 0,49$

$i = 73,487$

$e = \max(e_1, e_2) = 60,358$

$e_1 = 60,358$

$e_2 = 45,646$

$\alpha_e = 0,5639$

$$\sigma_{cr,c} = \sigma_{cr,sl} = \frac{\pi^2 E I_{sl,1}}{A_{sl,1} a^2} = 1655,765 \quad N/mm^2$$

$$\bar{\lambda}_c = \sqrt{\frac{\beta_{Ac} f_y}{\sigma_{cr,c}}} = 0,410096$$

$$\Phi = 0,5 \left[1 + \alpha_e \left(\bar{\lambda}_c - 0,2 \right) + \bar{\lambda}_c^2 \right]$$

$$= 0,6433$$

$$\chi_c = \frac{1}{\Phi + \sqrt{\Phi^2 - \bar{\lambda}_c^2}} = 0,87796$$

interaction

$$\xi = \frac{\sigma_{cr,p}}{\sigma_{cr,c}} - 1 = 0,06794$$

$$\rho_c = (\rho_p - \chi_c)\, \xi\, (2 - \xi) + \chi_c$$

$$= 0,89398.$$

$$A_{c,eff} = \rho_c \cdot A_{c,eff,loc} + \sum b_{edge,eff} \cdot t$$

$$= 0,89398 \cdot 4408,357 + 2 \cdot 0,7363 \cdot 200 \cdot 8$$

$$= 6297,244 \ mm^2$$

$$N_{Ed} = 100 \ N/mm^2 \cdot [800 \ mm \cdot 8 \ mm + 166 \cdot 11,5 + 36,5 \cdot 14]$$

$$= 882000$$

$$\eta_1 = \frac{N_{Ed}}{\frac{f_y A_{eff}}{\gamma_{m0}}} = \frac{882000}{\left(\frac{355 \cdot 6297,244}{1}\right)} = 0,3945.$$

reduced stress method

Global buckling:

$\sigma_{x,Ed} = 100$ [MPa]

$\alpha_{ult} \Rightarrow \frac{1}{\alpha_{ult}^2} = \left(\frac{\sigma_{x,Ed}}{f_y}\right)^2 = \left(\frac{100}{355}\right)^2$

$\alpha_{ult} = 3,55$

$\alpha_{cr,x} = \frac{\sigma_{cr,P,x}}{\sigma_{x,Ed}} = \frac{1768,26}{100} = 17,68$

$\frac{1}{\alpha_{cr}} = \frac{1+\psi_x}{4\alpha_{cr,x}} + \sqrt{\left(\frac{1+\psi_x}{4\alpha_{cr,x}}\right)^2} \Rightarrow \alpha_{cr,} = 17,68$

$\bar{\lambda}_p = \sqrt{\frac{\alpha_{ult}}{\alpha_{cr}}} = 0,448$

$\rho_p = 1$ as $\lambda_p < 0,673$.

$\Phi_p = 0,5\left[1 + \alpha_e\left(\bar{\lambda}_p - 0,2\right) + \bar{\lambda}_p^2\right] = 0,6703$

$\chi_c = \frac{1}{\Phi + \sqrt{\Phi_p^2 - \bar{\lambda}_p^2}} = 0,8555$

$\rho_c = (\rho_p - \chi_c)\xi(2-\xi) + \chi_c$

$= (1 - 0,8555)\,0,06794\,(2 - 0,06794) + 0,8555$

$= 0,8745$

local buckling:

$$\sigma_E = \frac{\pi^2 E}{12(1-\nu^2)} \cdot \left(\frac{t}{b}\right)^2 = 75,92 \left[N/mm^2\right]$$

$$k_\sigma = 4$$

$$\sigma_{cr,p} = k_\sigma \cdot \sigma_E = 303,68 \left[N/mm^2\right]$$

$$\alpha_{cr,x} = \frac{\sigma_{cr,p}}{\sigma_{x,Ed}} = 3,0368$$

$$\alpha_{cr} = 3,0368$$

$$\bar{\lambda}_p = \sqrt{\frac{\alpha_{ult}}{\alpha_{cr}}} = 1,0812$$

$$\rho_p = \frac{\bar{\lambda}_p - 0,055(3+\psi)}{\bar{\lambda}_p^2} = 0,7367$$

$$\sigma_{cr,c} = \frac{\pi^2 E t_p^2}{12(1-\nu^2)a^2} = 1,7969 \ N/mm^2$$

$$\xi = \frac{\sigma_{cr,p}}{\sigma_{cr,c}} - 1 \qquad 0 \le \xi \le 1 \qquad \xi = 1$$

$$\Phi = 0,5\left[1 + 0,21(\bar{\lambda}_p - 0,2) + \bar{\lambda}_p^2\right] = 1,177$$

$$\rho_c = (\rho_p - \chi_c)\,\xi\,(2-\xi) + \chi_c$$

$$= (0,7367 - 0,6089) \cdot 1 \cdot 1 + 0,6089 = 0,7367$$

$$\chi_c = \frac{1}{\Phi + \sqrt{\Phi^2 - \bar{\lambda}_p^2}} = 0,6089$$

$$UC = \sqrt{\left(\frac{\sigma_{x,Ed}}{\rho_{cx} \cdot f_y / \gamma_{m1}}\right)^2} \qquad \gamma_{m1} = 1,1$$

$$\rho_{cx} = \min\left(\rho_{c\,loc}, \rho_{c\,glob}\right) = \rho_{c\,loc} = 0,7367$$

$$UC = 0,4206.$$

B

Effective width versus Reduced stress method plots

tp	effwidth	redstress	% diff
20	0.07891	0.08412	6.60627
40	0.15782	0.16824	6.60626
60	0.23672	0.25236	6.60625
80	0.31563	0.33648	6.60625
100	0.39454	0.4206	6.60625
120	0.47345	0.50472	6.60625
140	0.55235	0.58884	6.60625
160	0.63126	0.67296	6.60625
180	0.71017	0.75709	6.60625
200	0.78908	0.84121	6.60625
220	0.86799	0.92533	6.60625
240	0.94689	1.00945	6.60625
260	1.0258	1.09357	6.60625

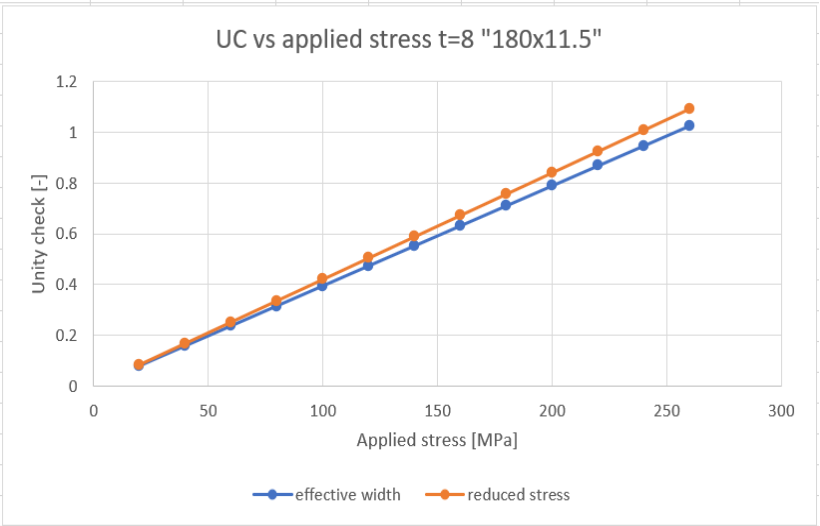

tp	effwidth	redstress	% diff
20	0.0705	0.07189	1.96304
40	0.14101	0.14378	1.96303
60	0.21151	0.21566	1.96303
80	0.28201	0.28755	1.96303
100	0.35252	0.35944	1.96303
120	0.42302	0.43133	1.96302
140	0.49352	0.50321	1.96302
160	0.56403	0.5751	1.96302
180	0.63453	0.64699	1.96302
200	0.70504	0.71888	1.96302
220	0.77554	0.79076	1.96302
240	0.84604	0.86265	1.96302
260	0.91655	0.93454	1.96302
280	0.98705	1.00643	1.96302
300	1.05755	1.07831	1.96302

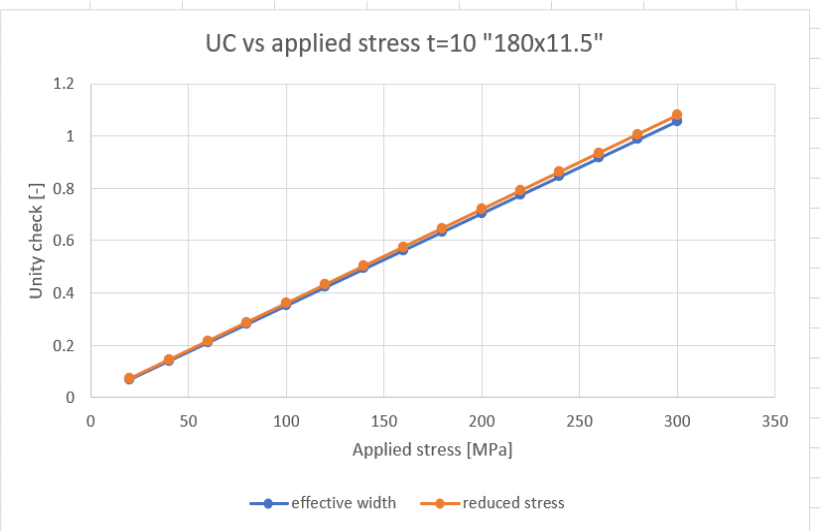

tp	effwidth	redstress	% diff
20	0.06397	0.06861	7.2606
40	0.12794	0.13723	7.26059
60	0.19191	0.20584	7.26059
80	0.25588	0.27446	7.26059
100	0.31985	0.34307	7.26059
120	0.38382	0.41169	7.26059
140	0.44779	0.4803	7.26059
160	0.51176	0.54892	7.26059
180	0.57573	0.61753	7.26059
200	0.6397	0.68615	7.26059
220	0.70367	0.75476	7.26058
240	0.76764	0.82338	7.26058
260	0.83161	0.89199	7.26058
280	0.89558	0.96061	7.26058
300	0.95955	1.02922	7.26058
320	1.02352	1.09784	7.26058

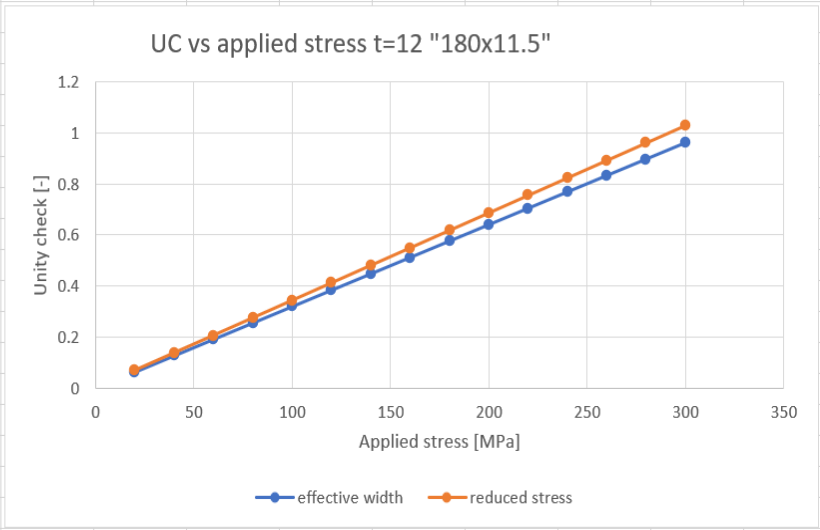

tp	effwidth	redstress	% diff
20	0.06094	0.06665	9.36815
40	0.12188	0.1333	9.36815
60	0.18282	0.19995	9.36814
80	0.24376	0.2666	9.36814
100	0.3047	0.33325	9.36814
120	0.36564	0.39989	9.36814
140	0.42658	0.46654	9.36814
160	0.48752	0.53319	9.36814
180	0.54846	0.59984	9.36814
200	0.6094	0.66649	9.36814
220	0.67034	0.73314	9.36814
240	0.73128	0.79979	9.36814
260	0.79222	0.86644	9.36814
280	0.85316	0.93309	9.36814
300	0.9141	0.99974	9.36814
320	0.97504	1.06639	9.36814
340	1.03598	1.13304	9.36814

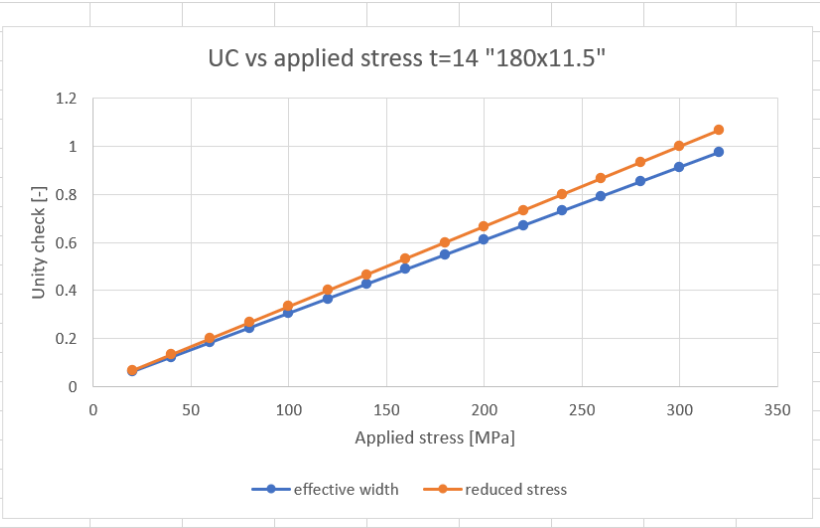

tp	effwidth	redstress	% diff
20	0.08135	0.08412	3.40623
40	0.1627	0.16824	3.40622
60	0.24405	0.25236	3.40622
80	0.3254	0.33648	3.40621
100	0.40675	0.4206	3.40621
120	0.4881	0.50472	3.40621
140	0.56945	0.58884	3.40621
160	0.6508	0.67296	3.40621
180	0.73215	0.75709	3.40621
200	0.8135	0.84121	3.40621
220	0.89485	0.92533	3.40621
240	0.9762	1.00945	3.40621
260	1.05755	1.09357	3.40621

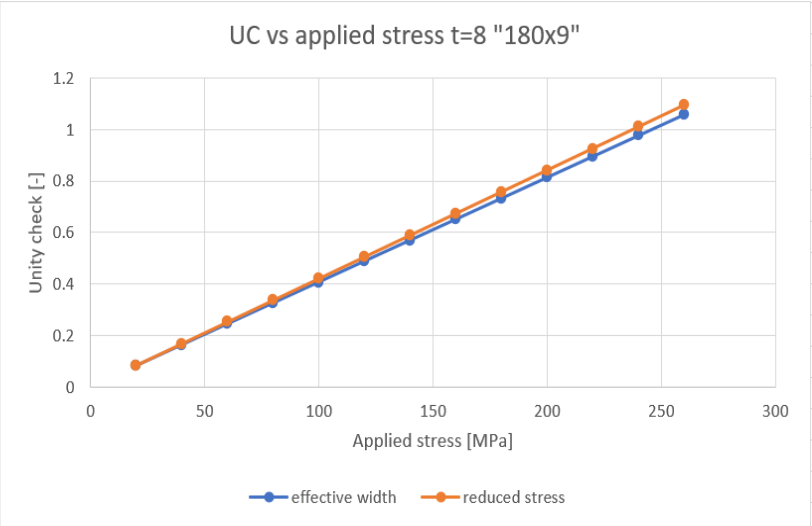

tp	effwidth	redstress	% diff
20	0.07177	0.07189	0.15745
40	0.14355	0.14378	0.15744
60	0.21532	0.21566	0.15744
80	0.2871	0.28755	0.15744
100	0.35887	0.35944	0.15744
120	0.43065	0.43133	0.15743
140	0.50242	0.50321	0.15743
160	0.5742	0.5751	0.15743
180	0.64597	0.64699	0.15743
200	0.71775	0.71888	0.15743
220	0.78952	0.79076	0.15743
240	0.86129	0.86265	0.15743
260	0.93307	0.93454	0.15743
280	1.00484	1.00643	0.15743

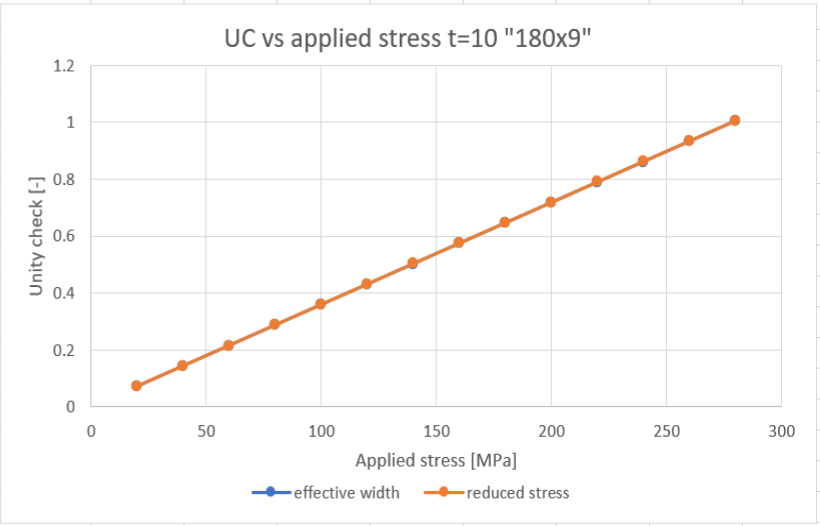

tp	effwidth	redstress	% diff
20	0.06458	0.06844	5.98437
40	0.12916	0.13689	5.98436
60	0.19374	0.20533	5.98436
80	0.25831	0.27377	5.98436
100	0.32289	0.34222	5.98435
120	0.38747	0.41066	5.98435
140	0.45205	0.4791	5.98435
160	0.51663	0.54755	5.98435
180	0.58121	0.61599	5.98435
200	0.64579	0.68443	5.98435
220	0.71037	0.75288	5.98435
240	0.77494	0.82132	5.98435
260	0.83952	0.88976	5.98435
280	0.9041	0.95821	5.98435
300	0.96868	1.02665	5.98435
320	1.03326	1.09509	5.98435

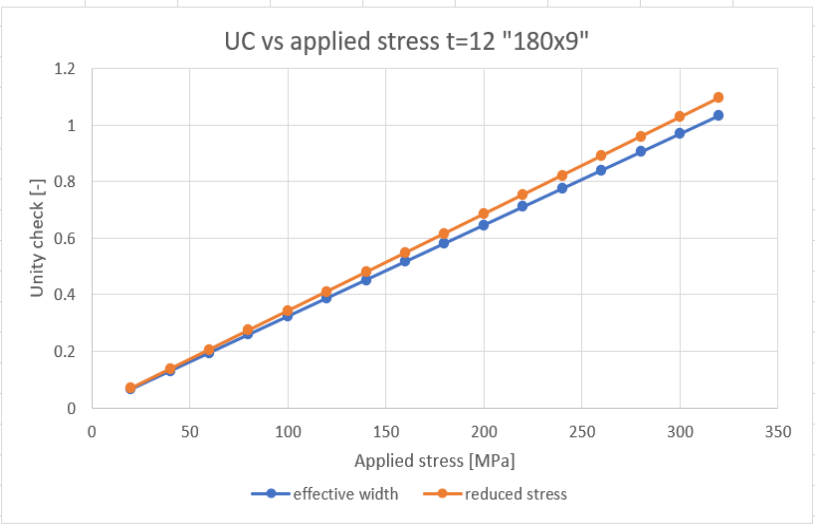

tp	effwidth	redstress	% diff
20	0.06123	0.06621	8.14756
40	0.12245	0.13243	8.14756
60	0.18368	0.19864	8.14756
80	0.2449	0.26486	8.14756
100	0.30613	0.33107	8.14756
120	0.36735	0.39728	8.14755
140	0.42858	0.4635	8.14755
160	0.4898	0.52971	8.14755
180	0.55103	0.59592	8.14755
200	0.61225	0.66214	8.14755
220	0.67348	0.72835	8.14755
240	0.73471	0.79457	8.14755
260	0.79593	0.86078	8.14755
280	0.85716	0.92699	8.14755
300	0.91838	0.99321	8.14755
320	0.97961	1.05942	8.14755
340	1.04083	1.12563	8.14755

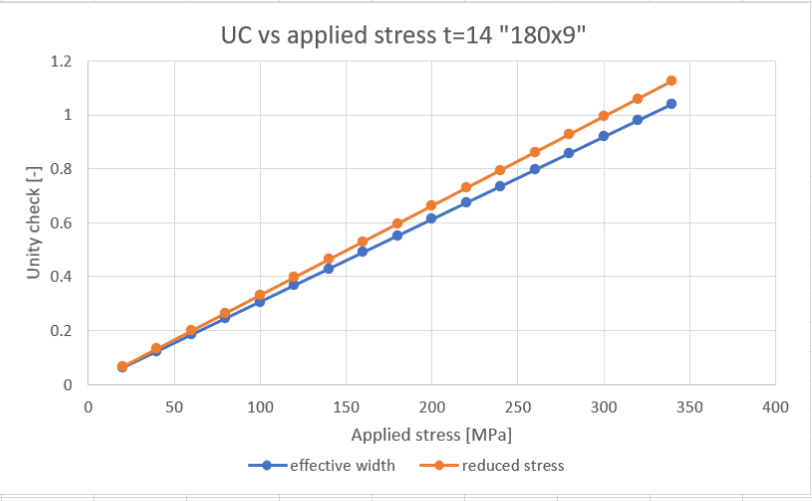

C

Hand calculation reduced stress method longitudinal stress

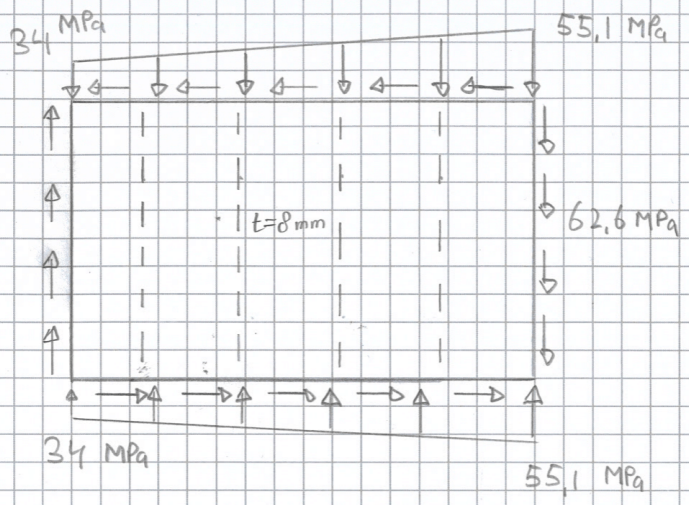

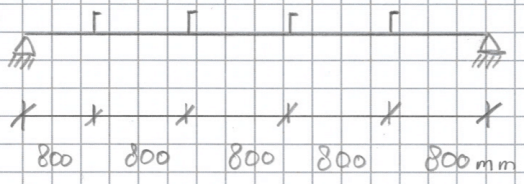

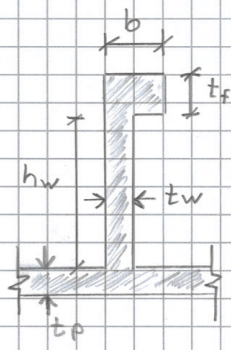

Stiffener: bulb Flat "180 x 9"

h_w	166	[mm]
t_w	9	[mm]
b	34	[mm]
t_f	14	[mm]
I_y	66 109 00	[mm^4]
dx	107,4	[mm]
A	2063	[mm^2]

$$\psi_{glob} = -\frac{34}{55,1} = 0,617 \quad [-]$$

$$\sigma_{cr,p} = k_{\sigma,p} \cdot \sigma_E = k_{\sigma,p} \frac{\pi^2 E}{12(1-\nu^2)} \left(\frac{t}{b}\right)^2$$

$$= 190\,000 \left(\frac{t}{b}\right)^2 \cdot k_{\sigma,p}$$

$$k_{\sigma,p} = \begin{cases} \dfrac{2\left((1+\alpha^2)^2 + \gamma - 1\right)}{\alpha^2 (\psi+1)(1+\delta)} & \text{if } \alpha \leq \sqrt[4]{\gamma} \\ \dfrac{4(1+\sqrt{\gamma})}{(\psi+1)(1+\delta)} & \text{if } \alpha > \sqrt[4]{\gamma} \end{cases}$$

$\psi = 0,617$

$\gamma = \dfrac{I_{sl}}{I_p}$

$\delta = \dfrac{\Sigma A_{sl}}{A_p}$

$\alpha = \dfrac{2600}{4000} = 0,65$

$$I_p = \frac{1}{10,92} b h^3 = \frac{1}{10,92} \cdot 4000 \cdot 8^3 = 1875\,45,78 \text{ mm}^4$$

$$I_{sl} = I_p + A_p \cdot z_p^2 + 4\left[I_{sl} + A_{sl} \cdot z_{sl}^2\right]$$

$$z_p = \frac{4 A_{sl} (dx + 0,5 t_p + A_p \cdot 0}{A_p + 4 A_{sl}}$$

$$= \frac{4 \cdot 2063 \cdot (107,4 + 0,5 \cdot 8)}{4000 \cdot 8 + 4 \cdot 2063} = 22,838 \text{ [mm]}$$

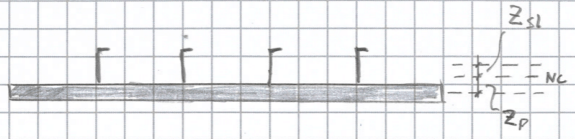

$$z_{sl} = 0,5\, t_p + dx - z_p = 0,5 \cdot 8 + 107,4 - 22,838 = 88,562 \text{ [mm]}$$

$$I_{sl} = 187545,78 + 8 \cdot 4000 \cdot 22,838^2 + 4\left[66\,10900 + 2063 \cdot 88,562^2\right] = 10804\,3837,8 \text{ [mm}^4\text{]}$$

$$\gamma = \frac{I_{sl}}{I_p} = \frac{10804\,3837,8}{187545,78} = 576,093$$

$$\delta = \frac{4 \cdot 2063}{8 \cdot 4000} = 0,2579$$

$$\sqrt[4]{\gamma} = 4,899\,18 > \alpha = 0,64$$

$$k_{\sigma,p} = \frac{2\left((1+\alpha^2)^2 + \gamma - 1\right)}{\alpha^2 (\psi+1)(1+\delta)} = 1343,1$$

$$\sigma_{cr,p} = 1343,1 \cdot 190000 \left(\frac{8}{4000}\right)^2 = 1020,76 \left[\text{N/mm}^2\right]$$

Critical buckling stress σ_{cr}

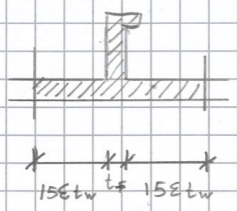

$$15\varepsilon t_w = 15\sqrt{\frac{235}{355}} \cdot 8 = 97,634$$

$$A_{sl,1} = [2 \cdot 97,634 + 9] \cdot 8 + A_{sl}$$
$$= [2 \cdot 97,634 + 9] \cdot 8 + 2063 = 3697,144$$

$$z_{shear} = \frac{A_{sl} \cdot z_{sl} + A_p \cdot z_p}{A_{tot}}$$

$$= \frac{[2 \cdot 97,634 \cdot 8 + 9 \cdot 8] \cdot 0,5 \cdot 8 + 2063\,[107,4 + 8]}{3697,144}$$

$$= 66,16\ [mm]$$

$$I_{sl,1} = \frac{1}{12}[2 \cdot 97,634 + 9] \cdot 8^3 +$$
$$[2 \cdot 97,634 + 9] \cdot 8 \cdot [z_{shear} - 0,5 \cdot 8]^2$$
$$+ 6610900 + 2063\,[8 + 107,4 - z_{shear}]^2$$
$$= 17935631\ [mm^4]$$

$$I_{sl} = 4 \cdot I_{sl,1} = 71742527\ [mm^4]$$

$$\alpha = \frac{2600}{4000} = 0{,}65 < 1$$

$$\rightarrow \quad k_\tau = 4{,}00 + 5{,}34 \left(\frac{h_w}{a}\right)^2 + k_{\tau sl}$$

$$k_{\tau,sl} = 9 \left(\frac{h_w}{a}\right)^2 \sqrt[4]{\left(\frac{I_{sl}}{t^3 h_w}\right)^3}$$

$$= 9 \left(\frac{4000}{2600}\right)^2 \sqrt[4]{\left(\frac{717\,42527}{8^3\,4000}\right)^3}$$

$$= 306{,}726$$

not less than $\frac{2{,}1}{t} \sqrt[3]{\frac{I_{sl}}{h_w}}$

$$= \frac{2{,}1}{8} \sqrt[3]{\frac{717\,42527}{4000}} = 6{,}871 \quad \checkmark$$

$$k_\tau = 4 + 5{,}34 \left(\frac{4000}{2600}\right)^2 + 306{,}727$$

$$= 323{,}365$$

$$\tau_{crit} = \sigma_E \, k_\tau = 190\,000 \left(\frac{8}{4000}\right)^2 \cdot 323{,}365$$

$$= 245{,}76 \quad [N/mm^2]$$

Global buckling of stiffener:

$$\alpha_{ult,k} = \frac{f_y}{\sigma_{v,Ed}} = \frac{355}{121{,}16} = 2{,}93$$

$$\sigma_{v,Ed} = \sqrt{\sigma_{x,Ed}^2 + 3\tau_{Ed}^2} =$$

$$\sqrt{55{,}1^2 + 3 \cdot 62{,}3^2} = 121{,}16 \; [N/mm^2]$$

$$\alpha_{cr,x} = \frac{\sigma_{cr,px}}{\sigma_{x,Ed}} = \frac{1020,76}{55,1} = 18,525$$

$$\alpha_{cr,\tau} = \frac{\tau_{cr}}{\tau_{Ed}} = \frac{245,76}{62,3} = 3,9447$$

$$\frac{1}{\alpha_{cr}} = \frac{1+\psi_x}{4\alpha_{cr,x}} + \sqrt{\left(\frac{1+\psi_x}{4\alpha_{cr,x}}\right)^2 + \frac{1-\psi_x}{2\alpha_{cr,x}^2} + \frac{1}{\alpha_{cr,\tau}^2}}$$

$$= \frac{1+0,617}{4\cdot 18,525} + \sqrt{\left(\frac{1+0,617}{4\cdot 18,525}\right)^2 + \frac{1-0,617}{2\cdot 18,525^2} + \frac{1}{3,9447^2}}$$

$$= 0,27736 \rightarrow \alpha_{cr} = 3,605$$

local buckling

$$\sigma_E = \frac{\pi^2 E}{12(1-\nu^2)}\left(\frac{t}{b}\right)^2 = \frac{\pi^2 210000}{12(1-0,3^2)}\left(\frac{8}{4000}\right)^2$$

$$= 18,98 \quad [N/mm^2]$$

EN-1993-1-5 table 4.1

$$\alpha = \frac{2600}{800} = 3,25$$

$$\psi = \frac{-50,88}{-55,1} = 0,9234$$

$$k_\sigma = \frac{8,2}{1,05+\psi} = 4,155$$

$$\frac{a}{h_w} = \frac{2600}{800} \rightarrow k_\tau = 5,34 + 4,00\left(\frac{800}{2600}\right)^2 + k_{\tau sl}$$

$$k_{\tau sl} = 0$$

$$k_\tau = 5,7187$$

$$\sigma_{cr} = \sigma_E \, k_\sigma = 18,98 \cdot 4,155 = 78,862 \ N/mm^2$$

$$\tau_{cr} = \sigma_E \, k_\tau = 18,98 \cdot 5,7187 = 108,54 \ N/mm^2$$

$$\alpha_{cr,x} = \frac{\sigma_{cr,p,x}}{\sigma_{x,Ed}} = \frac{78,862}{55,1} = 1,4313$$

$$\alpha_{cr,\tau} = \frac{\tau_{cr}}{\tau_{Ed}} = \frac{108,54}{62,3} = 1,7422$$

$$\frac{1}{\alpha_{cr}} = \frac{1+\psi_x}{4\alpha_{cr,x}} + \sqrt{\left(\frac{1+\psi_x}{4\alpha_{cr,x}}\right)^2 + \frac{1-\psi_x}{2\alpha_{cr,x}^2} + \frac{1}{\alpha_{cr,\tau}^2}}$$

$$= \frac{1+0,923}{4 \cdot 1,4313} + \sqrt{\left(\frac{1+0,923}{4 \cdot 1,4313}\right)^2 + \frac{1-0,923}{2 \cdot 1,4313^2} + \frac{1}{1,7422^2}}$$

$$= 1,01992$$

$$\rightarrow \alpha_{cr} = 0,9853$$

global buckling UC

$$\bar{\lambda}_p = \bar{\lambda}_w = \sqrt{\frac{\alpha_{ult}}{\alpha_{cr}}} = \sqrt{\frac{2,93}{3,605}} = 0,901$$

$$\rho_p = \frac{\bar{\lambda}_p - 0,055(3+\psi)}{\bar{\lambda}_p^2} = \frac{0,901 - 0,055(3+0,617)}{0,901^2}$$

$$= 0,864$$

$$\chi_w = \frac{0,83}{\bar{\lambda}_w} = \frac{0,83}{0,901} = 0,921$$

$$\xi = \frac{\sigma_{cr,p}}{\sigma_{cr,c}} - 1$$

$$\sigma_{cr,c} = \frac{\pi^2 E I_{sl,1}}{A_{sl,1}\, a^2} \cdot \frac{\sigma_1}{\sigma_{sl,1}}$$

extrapolate to most compressed point

most compressed stiffener:

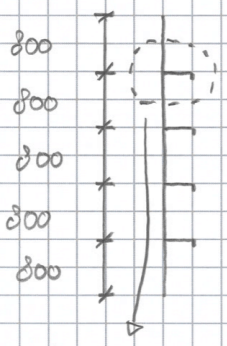

$\psi_1 = 0,923$

$\psi_2 = 0,917$

$\psi_3 = 0,9096$

$\psi_4 = 0,9006$

$\psi_5 = 0,8896$

$$b_{inf} = \frac{3-\psi_1}{5-\psi_1} \cdot 800 = 407,515$$

$$b_{sup} = \frac{2}{5-\psi_2} = 391,875$$

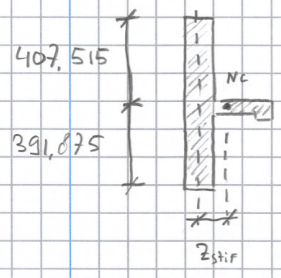

$$z_{stif} = \frac{A_{plate} \cdot 0 + A_{stif} \cdot \left(dx + \frac{1}{2} t_p\right)}{A_{plate} + A_{stif}}$$

$$= \frac{2063\,(107,4 + 0,5 \cdot 8)}{(407,515 + 391,875) \cdot 8 + 2063} = 27,171 \text{ [mm]}$$

$$I_{sl,1} = \frac{1}{12}(407,515 + 391,875)\cdot 8^3 + A_p \cdot z_{stiF}^2 + I_{stiF} + A_{stiF}\left(dx + \frac{1}{2}t_{p,1} - z_{stiF}\right)^2$$

$$= \frac{1}{12}(407,515 + 319,875)\cdot 8^3 + (407,515 + 391,875)\cdot 8 \cdot 27,171^2 + 66\,10900 + 2063\left(107,4 + \frac{1}{2}\cdot 8 - 27,171\right)^2$$

$$= 20600293\ [mm^4]$$

$$\sigma_{cr,c} = \frac{\pi^2 \cdot 210000 \cdot 26002293}{8458,12 \cdot 2600^2} \cdot \frac{55,1}{50,88}$$

$$= 1020,74\ [N/mm^2]$$

$$\xi = \frac{1020,76}{1020,74} - 1 \approx 0 \rightarrow \text{column like behaviour.}$$

$$\rho_c = (\rho_p - \chi_c)\,\xi\,(2 - \xi) + \chi_c$$

$$\chi_c = \frac{1}{\Phi_p + \sqrt{\Phi_p^2 - \bar{\lambda}_p^2}}$$

$$\Phi_p = 0.5\left[1 + \alpha_e\left(\bar{\lambda}_p - 0,2\right) + \bar{\lambda}_p^2\right]$$

$$\alpha_e = \alpha + \frac{0,09}{i/e}$$

$$i = \sqrt{\frac{I_{sl,1}}{A_{sl,1}}} = \sqrt{\frac{26002293}{8458,12}} = 55,446$$

$e = max(e_1 ; e_2)$

$e_1 = 4 + 107,4 - 27,171 = 84,229$

$e_2 = 27,171$

$e = 84,229$

$\alpha_e = 0,49 + \frac{0,09}{55,446/84,229} = 0,6267$

$\Phi_p = 0,5 [1 + 0,6267 (0,901 - 0,2) + 0,901^2] = 1,126$

$\chi_c = \frac{1}{1,126 + \sqrt{1,126^2 - 0,901^2}} = 0,555$

$\rho_c = (0,864 - 0,555) \cdot 0 \cdot (2 - 0) + 0,555$

$= 0,555$

local buckling

$\bar{\lambda}_p = \bar{\lambda}_w = \sqrt{\frac{\alpha_{ult}}{\alpha_{cr}}} = \sqrt{\frac{2,93}{0,9853}} = 1,7244$

$\rho_p = \frac{1,7244 - 0,055 (3 + 0,923)}{1,707^2} = 0,5073$

$\chi_w = \frac{1,37}{0,7 + 1,7244} = 0,565$

as $\bar{\lambda}_w > 1,08$ (EN-1993-1-5 table 5.1)

$$\xi = \frac{\sigma_{cr,p}}{\sigma_{cr,c}} - 1$$

$$\sigma_{cr,c} = \frac{\pi^2 E t_p^2}{12(1-\nu^2)a^2} = \frac{\pi^2\, 210000\, 8^2}{12(1-0{,}3^2)\, 2600^2}$$

$$= 1{,}796 \ N/mm^2$$

$$\xi = \frac{78{,}862}{1{,}796} - 1 = 1 \quad \text{as} \quad 0 \le \xi \le 1.$$

$$\rho_c = (\rho_p - \chi_c)\,\xi\,(2-\xi) + \chi_c$$

$$\chi_c = \frac{1}{\bar{\Phi}_p + \sqrt{\bar{\Phi}_p^2 - \bar{\lambda}_p^2}}$$

$$\bar{\Phi}_p = 0{,}5\left[1 + \alpha(\bar{\lambda}_p - 0{,}2) + \bar{\lambda}_p^2\right]$$

$$= 0{,}5\left[1 + 0{,}21(1{,}7244 - 0{,}2) + 1{,}7244^2\right]$$

$$= 2{,}1469$$

$$\chi_c = \frac{1}{2{,}1469 + \sqrt{2{,}1469^2 - 1{,}7244^2}} = 0{,}2919$$

$$\rho_c = (0{,}5073 - 0{,}2919)\,1\,(2-1) + 0{,}2919$$

$$= 0{,}5073$$

$$\rho_x = \min\left(\rho_{c,loc} ; \rho_{c,glob}\right)$$

$$= \min\left(0,5073 ; 0,555\right) = 0,5073$$

$$\chi_w = \min\left(\chi_{loc} ; \chi_{glob}\right) = \min\left(0,565 ; 0,921\right)$$

$$= 0,565$$

$$UC = \sqrt{\left(\frac{\sigma_{x,Ed}}{\rho_x f_y / \gamma_{m1}}\right)^2 + 3\left(\frac{\tau_{Ed}}{\chi_w f_y / \gamma_{m1}}\right)^2}$$

$$= \sqrt{\left(\frac{55,1}{0,5073 \cdot 355/1,1}\right)^2 + 3\left(\frac{62,3}{0,565 \cdot 355/1,1}\right)^2}$$

$$= \underline{0,681}$$

D

Hand calculation out-of-plane loading

1

Out of plane loading

column - like behaviour

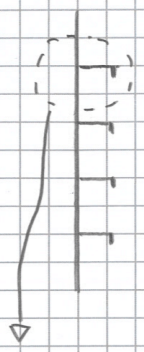

$\psi_1 = 0,923$, $k_\sigma = 4,155$, $\bar{\lambda}_p = 2,123$ $\rho = 0,423$

$\psi_2 = 0,917$, $k_\sigma = 4,169$, $\bar{\lambda}_p = 2,12$ $\rho = 0,424$

$\psi_3 = 0,9096$

$\psi_4 = 0,9006$

$\psi_5 = 0,8896$

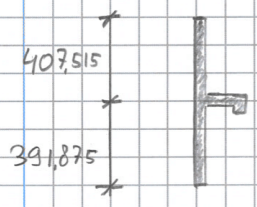

$\sigma_{cr,c} = 1020,74$ N/mm^2

$i = 55,46$

$e = 84,229$

$\alpha_e = 0,6267$

$$\bar{\lambda}_c = \sqrt{\frac{\beta_{Ac} f_y}{\sigma_{cr,c}}}$$

$$\beta_{Ac} = \frac{A_{sl,2eff}}{A_{sl,2}}$$

$A_{sl,2eff} = 8 \cdot [172,437 + 166,087] +$

$111,723 \cdot 9 + 34 \cdot 14 = 4189,7$

2

$$b_{1\,inF,eFF} = \frac{3-\psi_1}{5-\psi_1}\, b_{1\,eFF} = \frac{3-\psi_1}{5-\psi_1} \cdot \rho_1 \cdot b_1$$

$$= \frac{3-0,923}{5-0,923} \cdot 0,423 \cdot 800 = 172,437\ [mm]$$

$$b_{2,\,supp,eFF} = \frac{2}{5-\psi_2} \cdot b_{2\,eFF} = \frac{2}{5-\psi_2} \cdot \rho_2 \cdot b_2$$

$$= 166,087\ [mm]$$

Stiffener: web and Flange

Web $\psi = 1$ always $\rightarrow$ $k_\sigma = 0,43$

$$\bar{\lambda}_p = \frac{b/t}{28,4\,\varepsilon\sqrt{k_\sigma}} = 1,2173$$

$b = 166$

$t = 9$

$$\rho = \frac{\bar{\lambda}_p - 0,055\,(\psi+3)}{\bar{\lambda}_p^{\,2}} = 0,673$$

$$b_{eFF} = \rho \cdot b = 111,723\ [mm]$$

Flange $\psi = 1$ $\rightarrow$ $k_\sigma = 0,43$

$\bar{\lambda}_p = 0,16028$

$\rho = 1$

$b_{eFF} = \rho \cdot b = 34\ [mm]$.

3

$$A_{sl,2} = 8 \cdot [407,515 + 391,875] + 2063$$

A_{sl} (Area stiffener)

$$A_{sl,2} = 8458,11$$

$$\beta_{Ac} = \frac{4189,7}{8458,11} = 0,4953$$

$$\bar{\lambda}_c = \sqrt{\frac{\beta_{Ac} \cdot f_y}{\sigma_{cr,c}}} = 0,41506$$

$$\phi = 0,5 [\alpha_e (\bar{\lambda}_c - 0,2) + \bar{\lambda}_c^2] = 0,6535$$

$$\chi_c = \frac{1}{\phi - \sqrt{\phi^2 - \bar{\lambda}_c^2}} = 0,8633$$

plate - like buckling

$$\bar{\lambda}_p = \sqrt{\frac{\beta_{Ap} \cdot f_y}{\sigma_{cr,p}}} \qquad \sigma_{cr,p} = 1020,74 \ N/mm^2$$

$$\beta_{Ac} = \frac{A_{c,eff,loc}}{A_c} = \frac{16788,73}{33826,16} = 0,496$$

$$\bar{\lambda}_p = 0,4155$$

$$\rho_p = 1 \quad \text{as} \quad \bar{\lambda}_p < 0,673$$

4

interaction

$$\xi = \frac{\sigma_{cr,p}}{\sigma_{cr,c}} - 1 \approx 0$$

$$\rho_c = (\rho_p - \chi_c)\,\xi\,(2 - \xi) + \chi_c = 0,8633$$

most compressed stiffener can be checked according to:

$$A_i := \rho_c \left[A_{sl,eff} + \sum \rho_{pan,i}\, b_{pan,i}\, t_{pan,i} \right]$$

$$= 0,86338 \left[111,723 \cdot 9 + 34 \cdot 14 + 172,437 \cdot 8 + 166,087 \cdot 8 \right] = 3617,015 \ mm^2.$$

$h_w = 111,723$ [mm]

$t_w = \rho_c \cdot 9 = 7,77$ [mm]

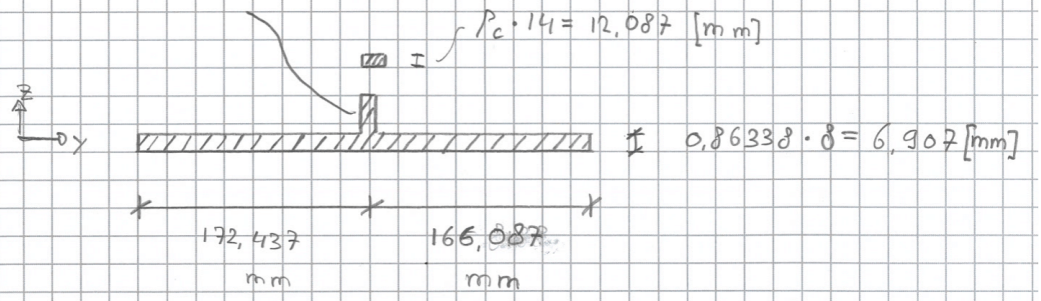

$I_y = 18649991$ [mm^4]

$I_z = 22456523,74$ [mm^4]

5

$$N_{Rk} = A_{eff} \cdot f_y = 3617{,}015\ [mm^2] \cdot 355\ [N/mm^2]$$
$$= 1284040{,}27\ [N]$$

$$M_{y,Rk} = W_{y\,eff\,min} \cdot f_y = 435516317\ [Nmm]$$

$$M_{z,Rk} = W_{z\,eff\,min} \cdot f_y = 468751169\ [Nmm]$$

$$N_{cr,y} = \frac{\pi^2 E I_y}{L_{cr}} = 5718089{,}83\ [N]$$

$$N_{cr,z} = \frac{\pi^2 E I_z}{L_{cr}} = 6885173{,}25\ [N]$$

$$\bar{\lambda}_z = \sqrt{\frac{N_{Rk}}{N_{cr,z}}} = 0{,}43185$$

$$\Phi_z = 0{,}5\left[1 + 0{,}49\,(\bar{\lambda}_z - 0{,}2) + \bar{\lambda}_z^2\right]$$
$$= 0{,}65$$

$$\chi_z = \frac{1}{\Phi_z + \sqrt{\Phi_z^2 - \lambda_z^2}} = 0{,}88$$

EN-1993-1-1 table A.2 ?

$$C_{my} = 1 + 0{,}03\,\frac{N_{Ed}}{N_{cr,y}} = 1{,}0022$$

$$C_{mz} = 0{,}79 + 0{,}21 \cdot \psi + 0{,}36\,(\psi - 0{,}33)\,\frac{N_{Ed}}{N_{cr,z}} = 1{,}0149$$

6

$$C_{m,LT} = 1$$

$$\mu_y = \frac{1 - \frac{N_{Ed}}{N_{cr,y}}}{1 - \chi_y} = 0,989 \quad (\chi_y = 0,863)$$

$$\mu_z = \frac{1 - \frac{N_{Ed}}{N_{cr,z}}}{1 - \chi_z \frac{N_{Ed}}{N_{cr,z}}} = 0,992$$

$$k_{yy} = C_{my} C_{mLT} \frac{\mu_y}{1 - \frac{N_{Ed}}{N_{cr,y}}} = 1,071$$

$$k_{yz} = C_{mz} \frac{\mu_y}{1 - \frac{N_{Ed}}{N_{cr,z}}} = 1,070$$

$$k_{zy} = C_{my} C_{mLT} \frac{\mu_z}{1 - \frac{N_{Ed}}{N_{cr,y}}} = 1,074$$

$$k_{zz} = C_{mz} \frac{\mu_z}{1 - \frac{N_{Ed}}{N_{cr,z}}} = 1,073$$

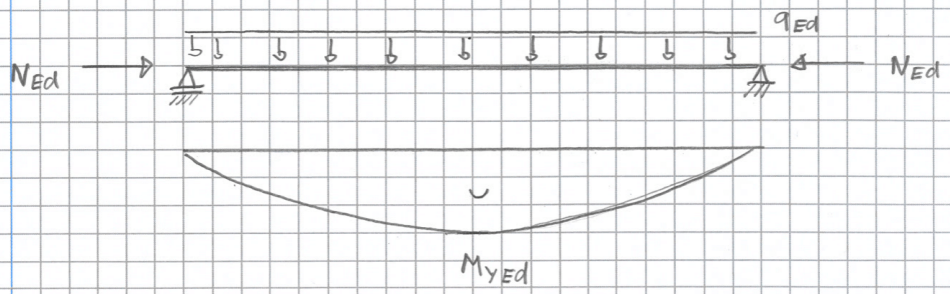

$$M_{y,Ed} = \frac{1}{8}\left[\left(391,875 + 407,515\right)\cdot 0,002\left[\frac{N}{mm^2}\right]\right] \cdot 2600^2 = 1350969 \; [Nmm]$$

$M_{z,Ed}$:

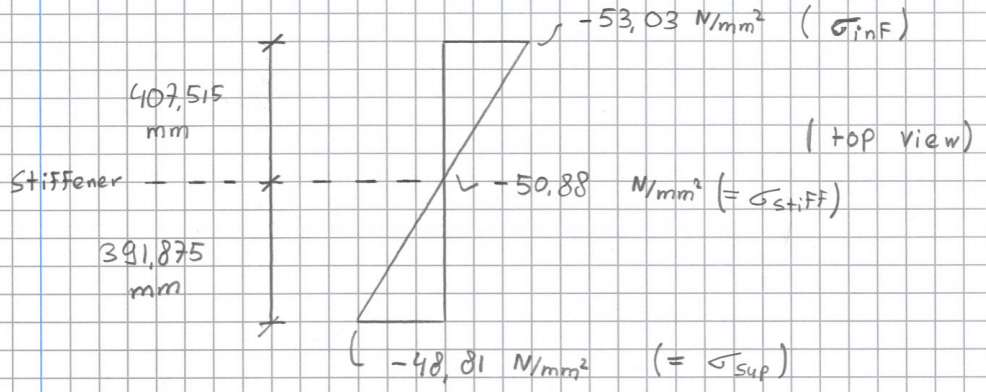

$$M_{z,Ed} = \frac{1}{2}\left(\sigma_{stiff} - \sigma_{inF}\right)\cdot 407,515 \cdot t_p \cdot \frac{2}{3}\cdot 407,515 + \frac{1}{2}\left(\sigma_{sup} - \sigma_{stiff}\right)\cdot 391,875 \cdot t_p \cdot \frac{2}{3}\cdot 391,875 = 1798476,57 \; [Nmm]$$

$$\frac{N_{Ed}}{\frac{\chi_y N_{Rk}}{\gamma_{m1}}} + k_{yy}\frac{M_{y,Ed}}{\chi_{LT}\frac{M_{yRk}}{\gamma_{m1}}} + k_{yz}\frac{M_{z,Ed}}{\frac{M_{z,Rk}}{\gamma_{m1}}} = 0,504$$

$$\frac{N_{Ed}}{\frac{\chi_z N_{Rk}}{\gamma_{m1}}} + k_{zy}\frac{M_{y,Ed}}{\chi_{LT}\frac{M_{yRk}}{\gamma_{m1}}} + k_{zz}\frac{M_{z,Ed}}{\frac{M_{zRk}}{\gamma_{m1}}} = 0,496$$

E

Bulb flat data

Section	b mm	t mm	c mm	d mm	r mm	G kg/m	A cm2	U m2/m	dx mm	dy mm	Ix cm4	Iy cm4	Zx cm3	Zy cm3	rx cm	ry cm	Zy cm6/10	J cm4
160x7	160	7.0	22.0	22.2	6.0	11.46	14.58	0.365	96.7	6.5	371.10	5.85	38.4	9.0	5.05	0.63	1.11	3.65
160x8	160	8.0	22.0	22.2	6.0	12.72	16.18	0.367	95.1	6.8	409.27	6.54	43.0	9.7	5.03	0.64	1.15	4.57
160x9	160	9.0	22.0	22.2	6.0	13.97	17.78	0.370	93.7	7.1	446.70	7.31	47.7	10.3	5.01	0.64	1.19	5.73
160x10	160	10.0	22.0	22.2	6.0	15.30	19.34	0.371	92.6	7.5	481.31	8.15	52.0	10.9	4.99	0.65	1.22	7.12
160x11	160	11.0	22.0	22.2	6.0	16.49	20.94	0.373	91.7	7.9	517.81	9.09	56.5	11.5	4.97	0.66	1.26	8.86
160x11.5	160	11.5	22.0	22.2	6.0	17.30	21.74	0.374	91.3	8.1	535.93	9.60	58.7	11.9	4.96	0.66	1.29	9.85
180x8	180	8.0	25.0	25.5	7.0	14.80	18.83	0.412	109.0	7.4	606.55	9.89	55.6	13.3	5.67	0.72	2.41	6.24
180x9	180	9.0	25.0	25.5	7.0	16.22	20.63	0.414	107.4	7.7	661.09	10.92	61.6	14.1	5.66	0.73	2.47	7.57
180x10	180	10.0	25.0	25.5	7.0	17.63	22.40	0.416	106.0	8.1	711.72	12.03	67.1	14.9	5.64	0.73	2.52	9.15
180x11	180	11.0	25.0	25.5	7.0	19.04	24.20	0.418	104.8	8.4	764.60	13.25	72.9	15.7	5.62	0.74	2.60	11.13
180x11.5	180	11.5	25.0	25.5	7.0	19.70	25.10	0.419	104.3	8.6	790.81	13.90	75.8	16.1	5.61	0.74	2.64	12.26
200x8.5	200	8.5	28.0	28.8	8.0	17.80	22.63	0.458	122.2	8.2	901.07	15.06	73.7	18.3	6.31	0.82	4.71	9.20
200x9	200	9.0	28.0	28.8	8.0	18.57	23.63	0.459	121.3	8.4	939.14	15.75	77.4	18.8	6.30	0.82	4.76	10.00
200x10	200	10.0	28.0	28.8	8.0	20.14	25.60	0.460	119.7	8.7	1010.47	17.18	84.4	19.8	6.28	0.82	4.83	11.78
200x11	200	11.0	28.0	28.8	8.0	21.71	27.60	0.463	118.3	9.0	1084.33	18.75	91.7	20.8	6.27	0.82	4.95	14.01
200x11.5	200	11.5	28.0	28.8	8.0	22.50	28.60	0.464	117.6	9.2	1120.89	19.57	95.3	21.3	6.26	0.83	5.02	15.28
200x12	200	12.0	28.0	28.8	8.0	23.28	29.60	0.465	117.0	9.4	1157.23	20.43	98.9	21.8	6.25	0.83	5.09	16.65
220x9	220	9.0	31.0	32.1	9.0	21.00	26.78	0.504	135.5	9.1	1290.48	22.01	95.2	24.3	6.94	0.91	8.61	13.17
220x10	220	10.0	31.0	32.1	9.0	22.77	28.94	0.505	133.7	9.3	1387.89	23.86	103.8	25.5	6.92	0.91	8.72	15.16
220x11	220	11.0	31.0	32.1	9.0	24.50	31.14	0.507	132.0	9.7	1488.07	25.83	112.7	26.8	6.91	0.91	8.90	17.65
220x11.5	220	11.5	31.0	32.1	9.0	25.30	32.24	0.509	131.2	9.8	1537.57	26.87	117.2	27.4	6.91	0.91	8.99	19.06
220x12	220	12.0	31.0	32.1	9.0	26.22	33.34	0.510	130.5	10.0	1586.73	27.94	121.6	28.0	6.90	0.92	9.10	20.60
230x11	230	11.0	32.5	33.75	9.5	25.06	32.97	0.530	138.9	10.0	1724.98	30.05	124.2	30.1	7.23	0.95	11.69	19.81
240x9.5	240	9.5	34.0	35.4	10.0	24.40	31.23	0.549	148.9	9.9	1787.40	31.12	120.0	31.4	7.57	1.00	14.83	18.25
240x10	240	10.0	34.0	35.4	10.0	25.50	32.43	0.550	147.9	10.0	1854.67	32.30	125.4	32.2	7.56	1.00	14.94	19.46
240x10.5	240	10.5	34.0	35.4	10.0	26.40	33.63	0.551	146.9	10.2	1921.25	33.52	130.8	33.0	7.56	1.00	15.06	20.78
240x11	240	11.0	34.0	35.4	10.0	27.39	34.83	0.552	145.9	10.3	1987.20	34.78	136.2	33.8	7.55	1.00	15.19	22.22
240x11.5	240	11.5	34.0	35.4	10.0	28.30	36.03	0.554	145.1	10.5	2052.60	36.06	141.5	34.5	7.55	1.00	15.33	23.79
240x12	240	12.0	34.0	35.4	10.0	29.27	37.23	0.555	144.3	10.6	2117.50	37.39	146.8	35.2	7.54	1.00	15.48	25.49
260x10	260	10.0	37.0	38.7	11.0	28.35	36.05	0.595	162.3	10.7	2421.72	42.80	149.2	39.9	8.20	1.09	24.54	24.85
260x11	260	11.0	37.0	38.7	11.0	30.39	38.65	0.597	160.1	11.0	2593.45	45.86	162.0	41.8	8.19	1.09	24.87	27.91
260x12	260	12.0	37.0	38.7	11.0	32.43	41.25	0.600	158.2	11.3	2762.00	49.07	174.6	43.6	8.18	1.09	25.25	31.50
260x13	260	13.0	37.0	38.7	11.0	34.40	43.85	0.602	156.5	11.6	2927.94	52.45	187.0	45.3	8.17	1.09	25.69	35.69
280x10.5	280	10.5	40.0	42.0	12.0	32.40	41.22	0.641	175.7	11.6	3210.10	57.50	182.7	49.7	8.82	1.18	39.05	33.16
280x11	280	11.0	40.0	42.0	12.0	33.50	42.62	0.642	174.5	11.7	3318.79	59.39	190.2	50.8	8.82	1.18	39.27	34.90
280x12	280	12.0	40.0	42.0	12.0	35.70	45.42	0.645	172.4	11.9	3532.99	63.29	205.0	53.0	8.82	1.18	39.77	38.84
280x13	280	13.0	40.0	42.0	12.0	37.90	48.22	0.647	170.5	12.2	3743.56	67.37	219.6	55.1	8.81	1.18	40.34	43.42
300x11	300	11.0	43.0	45.3	13.0	36.70	46.73	0.687	189.1	12.4	4175.43	75.68	220.8	60.9	9.45	1.27	60.10	43.42
300x12	300	12.0	43.0	45.3	13.0	39.09	49.73	0.690	186.7	12.7	4443.49	80.39	238.0	63.5	9.45	1.27	60.72	47.73
300x13	300	13.0	43.0	45.3	13.0	41.44	52.73	0.692	184.6	12.9	4706.64	85.27	254.9	66.1	9.45	1.27	61.45	52.71
320x11.5	320	11.5	46.0	48.6	14.0	41.20	52.59	0.733	202.5	13.3	5342.16	97.86	263.8	73.7	10.08	1.36	89.86	55.95
320x12	320	12.0	46.0	48.6	14.0	42.60	54.19	0.735	201.3	13.4	5506.76	100.69	273.6	75.3	10.08	1.36	90.25	58.38
320x12.5	320	12.5	46.0	48.6	14.0	43.80	55.79	0.736	200.1	13.5	5669.75	103.58	283.4	76.8	10.08	1.36	90.68	60.99
320x13	320	13.0	46.0	48.6	14.0	45.09	57.39	0.737	199.0	13.6	5831.26	106.51	293.1	78.3	10.08	1.36	91.15	63.79
320x13.5	320	13.5	46.0	48.6	14.0	46.30	58.94	0.737	198.0	13.7	5977.59	109.44	301.9	79.7	10.07	1.36	91.35	66.51
320x14	320	14.0	46.0	48.6	14.0	47.60	60.54	0.738	197.0	13.9	6136.58	112.48	311.5	81.1	10.07	1.36	91.89	69.71
340x12	340	12.0	49.0	52.0	15.0	46.20	58.78	0.780	216.0	14.1	6736.30	124.57	311.9	88.2	10.70	1.46	131.02	71.06
340x12.5	340	12.5	49.0	52.0	15.0	47.50	60.48	0.781	214.7	14.2	6934.97	127.98	323.1	89.9	10.71	1.45	131.53	73.88
340x13	340	13.0	49.0	52.0	15.0	48.86	62.18	0.782	213.5	14.3	7131.73	131.44	334.1	91.7	10.71	1.45	132.09	76.91
340x14	340	14.0	49.0	52.0	15.0	51.50	65.54	0.784	211.3	14.6	7504.42	138.47	355.2	95.0	10.70	1.45	132.97	83.29
340x15	340	15.0	49.0	52.0	15.0	54.20	68.94	0.786	209.2	14.8	7886.99	145.80	377.0	98.3	10.70	1.45	134.41	90.88
370x12.5	370	12.5	53.5	56.9	16.5	53.10	67.79	0.848	236.9	15.4	9184.55	172.23	387.8	112.1	11.64	1.59	221.07	97.62
370x13	370	13.0	53.5	56.9	16.5	54.70	69.64	0.850	235.5	15.5	9444.05	176.62	401.0	114.2	11.64	1.59	221.76	101.01
370x14	370	14.0	53.5	56.9	16.5	57.60	73.30	0.851	233.0	15.7	9936.79	185.49	426.5	118.5	11.64	1.59	222.83	108.11
370x15	370	15.0	53.5	56.9	16.5	60.50	77.00	0.854	230.7	15.9	10440.07	194.68	452.5	122.6	11.64	1.59	224.72	116.55
370x16	370	16.0	53.5	56.9	16.5	63.50	80.70	0.857	228.6	16.1	10935.90	204.14	478.4	126.6	11.64	1.59	226.88	126.04
400x13	400	13.0	58.0	61.9	18.0	60.80	77.43	0.918	257.9	16.6	12234.74	232.34	474.5	139.7	12.57	1.73	357.80	131.25
400x14	400	14.0	58.0	61.9	18.0	63.96	81.38	0.919	255.1	16.8	12872.91	243.41	504.7	145.0	12.58	1.73	358.96	139.13
400x15	400	15.0	58.0	61.9	18.0	67.10	85.38	0.922	252.5	17.0	13521.89	254.79	535.5	150.1	12.58	1.73	361.32	148.48
400x16	400	16.0	58.0	61.9	18.0	70.20	89.38	0.925	250.2	17.2	14160.53	266.45	566.1	154.9	12.59	1.73	364.08	158.97
430x14	430	14.0	62.5	66.8	19.5	70.60	89.78	0.987	277.5	18.0	16366.61	313.68	589.9	174.7	13.50	1.87	559.02	177.41
430x15	430	15.0	62.5	66.8	19.5	73.90	94.08	0.990	274.6	18.1	17189.22	327.65	626.0	180.8	13.52	1.87	561.76	187.72
430x17	430	17.0	62.5	66.8	19.5	80.70	102.68	0.995	269.6	18.5	18794.22	356.44	697.1	192.5	13.53	1.86	569.01	212.09
430x18	430	18.0	62.5	66.8	19.5	83.90	106.98	0.998	267.4	18.8	19579.84	371.35	732.2	197.9	13.53	1.86	573.41	226.30
430x19	430	19.0	62.5	66.8	19.5	87.40	111.28	1.001	265.4	19.0	20355.95	386.65	767.0	203.4	13.52	1.86	578.26	241.98
430x20	430	20.0	62.5	66.8	19.5	90.80	115.58	1.004	263.5	19.3	21123.62	402.40	801.6	208.6	13.52	1.87	583.53	259.20

F

STIPLA details

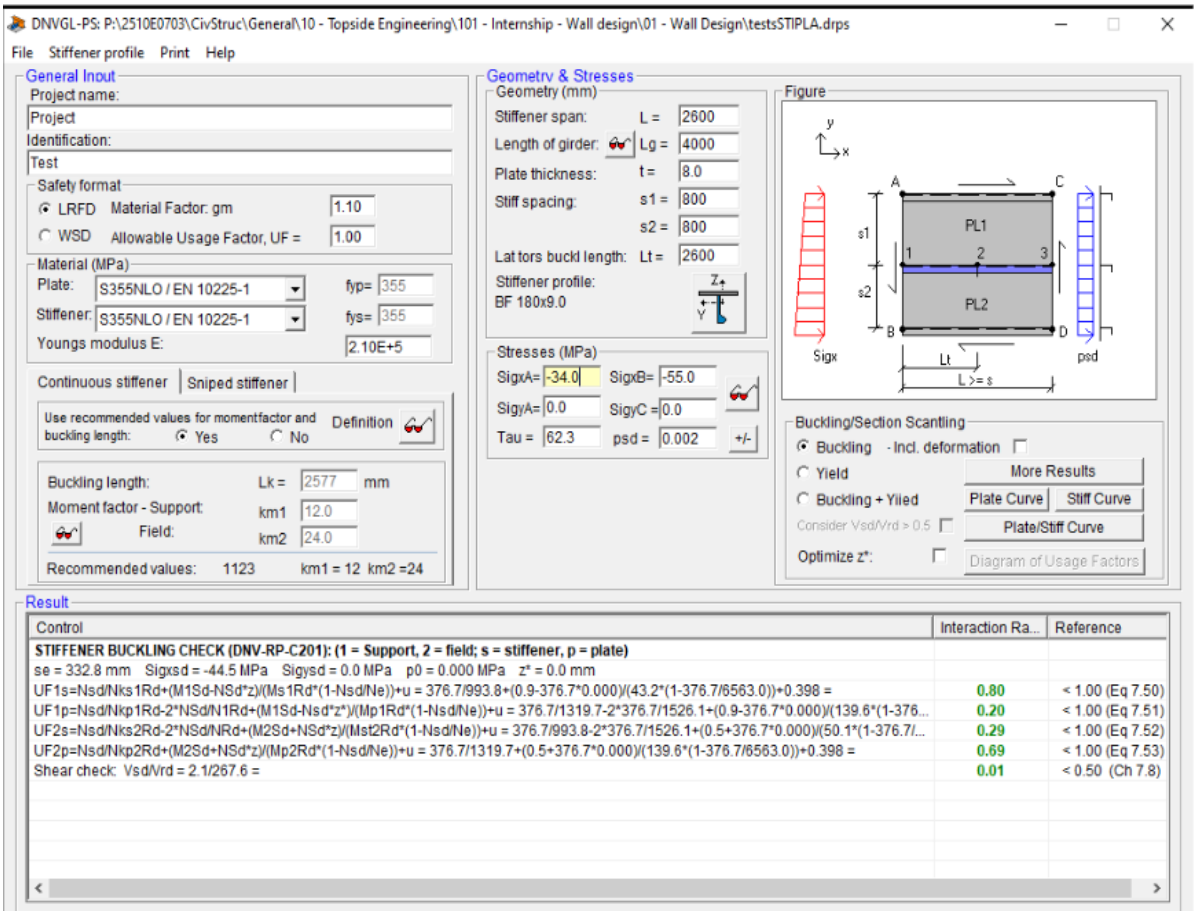
DNVGL-PS: P:\2510E0703\CivStruc\General\10 - Topside Engineering\101 - Internship - Wall design\01 - Wall Design\testsSTIPLA.drps
File Stiffener profile Print Help
General Inout
Project name:
Project
Identification:
Test
Safety format
LRFD Material Factor: gm 1.10
WSD Allowable Usage Factor, UF = 1.00
Material (MPa)
Plate: S355NLO / EN 10225-1 fyp= 355
Stiffener: S355NLO / EN 10225-1 fys= 355
Youngs modulus E: 2.10E+5
Continuous stiffener Sniped stiffener
Use recommended values for momentfactor and buckling length: Yes No Definition
Buckling length: Lk = 2577 mm
Moment factor - Support: km1 12.0
Field: km2 24.0
Recommended values: 1123 km1 = 12 km2 =24
Geometry & Stresses
Geometry (mm)
Stiffener span: L = 2600
Length of girder: Lg = 4000
Plate thickness: t = 8.0
Stiff spacing: s1 = 800
s2 = 800
Lat tors buckl length: Lt = 2600
Stiffener profile:
BF 180x9.0
Stresses (MPa)
SigxA= -34.0 SigxB= -55.0
SigyA= 0.0 SigyC = 0.0
Tau = 62.3 psd = 0.002 +/-
Figure
y
x
A
C
PL1
1
2
3
s1
s2
PL2
B
D
Sigx
psd
Lt
L >= s
Buckling/Section Scantling
Buckling - Incl. deformation
Yield
Buckling + Yiled
Consider Vsd/Vrd > 0.5
Optimize z*:
More Results
Plate Curve
Stiff Curve
Plate/Stiff Curve
Diagram of Usage Factors
Result
Control
Interaction Ra...
Reference
STIFFENER BUCKLING CHECK (DNV-RP-C201): (1 = Support, 2 = field; s = stiffener, p = plate)
se = 332.8 mm Sigxsd = -44.5 MPa Sigysd = 0.0 MPa p0 = 0.000 MPa z* = 0.0 mm
UF1s=Nsd/Nks1Rd+(M1Sd-NSd*z)/(Ms1Rd*(1-Nsd/Ne))+u = 376.7/993.8+(0.9-376.7*0.000)/(43.2*(1-376.7/6563.0))+0.398 = 0.80 < 1.00 (Eq 7.50)
UF1p=Nsd/Nkp1Rd-2*NSd/N1Rd+(M1Sd-Nsd*z*)/(Mp1Rd*(1-Nsd/Ne))+u = 376.7/1319.7-2*376.7/1526.1+(0.9-376.7*0.000)/(139.6*(1-376... 0.20 < 1.00 (Eq 7.51)
UF2s=Nsd/Nks2Rd-2*NSd/NRd+(M2Sd+NSd*z)/(Mst2Rd*(1-Nsd/Ne))+u = 376.7/993.8-2*376.7/1526.1+(0.5+376.7*0.000)/(50.1*(1-376.7/... 0.29 < 1.00 (Eq 7.52)
UF2p=Nsd/Nkp2Rd+(M2Sd+NSd*z)/(Mp2Rd*(1-Nsd/Ne))+u = 376.7/1319.7+(0.5+376.7*0.000)/(139.6*(1-376.7/6563.0))+0.398 = 0.69 < 1.00 (Eq 7.53)
Shear check: Vsd/Vrd = 2.1/267.6 = 0.01 < 0.50 (Ch 7.8)

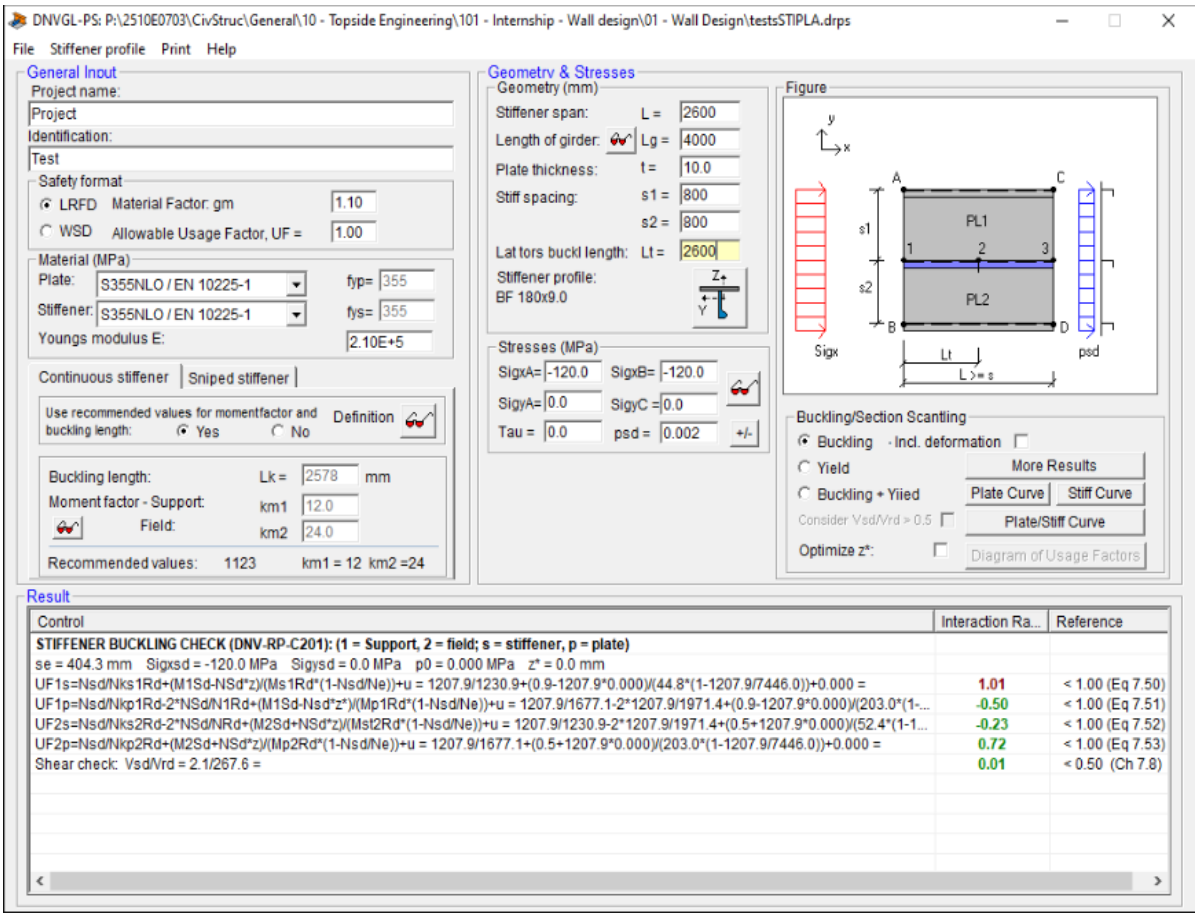
DNVGL-PS: P:\2510E0703\CivStruc\General\10 - Topside Engineering\101 - Internship - Wall design\01 - Wall Design\testsSTIPLA.drps
File Stiffener profile Print Help
General Input
Project name:
Project
Identification:
Test
Safety format
LRFD Material Factor: gm 1.10
WSD Allowable Usage Factor, UF = 1.00
Material (MPa)
Plate: S355NLO / EN 10225-1 fyp= 355
Stiffener: S355NLO / EN 10225-1 fys= 355
Youngs modulus E: 2.10E+5
Continuous stiffener Sniped stiffener
Use recommended values for momentfactor and buckling length: Yes No Definition
Buckling length: Lk = 2578 mm
Moment factor - Support: km1 12.0
Field: km2 24.0
Recommended values: 1123 km1 = 12 km2 =24
Geometry & Stresses
Geometry (mm)
Stiffener span: L = 2600
Length of girder: Lg = 4000
Plate thickness: t = 10.0
Stiff spacing: s1 = 800
s2 = 800
Lat tors buckl length: Lt = 2600
Stiffener profile:
BF 180x9.0
Stresses (MPa)
SigxA= -120.0 SigxB= -120.0
SigyA= 0.0 SigyC = 0.0
Tau = 0.0 psd = 0.002 +/-
Figure
y
x
A
C
PL1
s1
1
2
3
s2
PL2
B
D
Sigx
Lt
L >= s
psd
Buckling/Section Scantling
Buckling Incl. deformation
Yield
Buckling + Yiied
Consider Vsd/Vrd > 0.5
Optimize z*:
More Results
Plate Curve
Stiff Curve
Plate/Stiff Curve
Diagram of Usage Factors
Result
Control
Interaction Ra...
Reference
STIFFENER BUCKLING CHECK (DNV-RP-C201): (1 = Support, 2 = field; s = stiffener, p = plate)
se = 404.3 mm Sigxsd = -120.0 MPa Sigysd = 0.0 MPa p0 = 0.000 MPa z* = 0.0 mm
UF1s=Nsd/Nks1Rd+(M1Sd-NSd*z)/(Ms1Rd*(1-Nsd/Ne))+u = 1207.9/1230.9+(0.9-1207.9*0.000)/(44.8*(1-1207.9/7446.0))+0.000 = 1.01 < 1.00 (Eq 7.50)
UF1p=Nsd/Nkp1Rd-2*NSd/N1Rd+(M1Sd-Nsd*z*)/(Mp1Rd*(1-Nsd/Ne))+u = 1207.9/1677.1-2*1207.9/1971.4+(0.9-1207.9*0.000)/(203.0*(1-... -0.50 < 1.00 (Eq 7.51)
UF2s=Nsd/Nks2Rd-2*NSd/NRd+(M2Sd+NSd*z)/(Mst2Rd*(1-Nsd/Ne))+u = 1207.9/1230.9-2*1207.9/1971.4+(0.5+1207.9*0.000)/(52.4*(1-1... -0.23 < 1.00 (Eq 7.52)
UF2p=Nsd/Nkp2Rd+(M2Sd+NSd*z)/(Mp2Rd*(1-Nsd/Ne))+u = 1207.9/1677.1+(0.5+1207.9*0.000)/(203.0*(1-1207.9/7446.0))+0.000 = 0.72 < 1.00 (Eq 7.53)
Shear check: Vsd/Vrd = 2.1/267.6 = 0.01 < 0.50 (Ch 7.8)

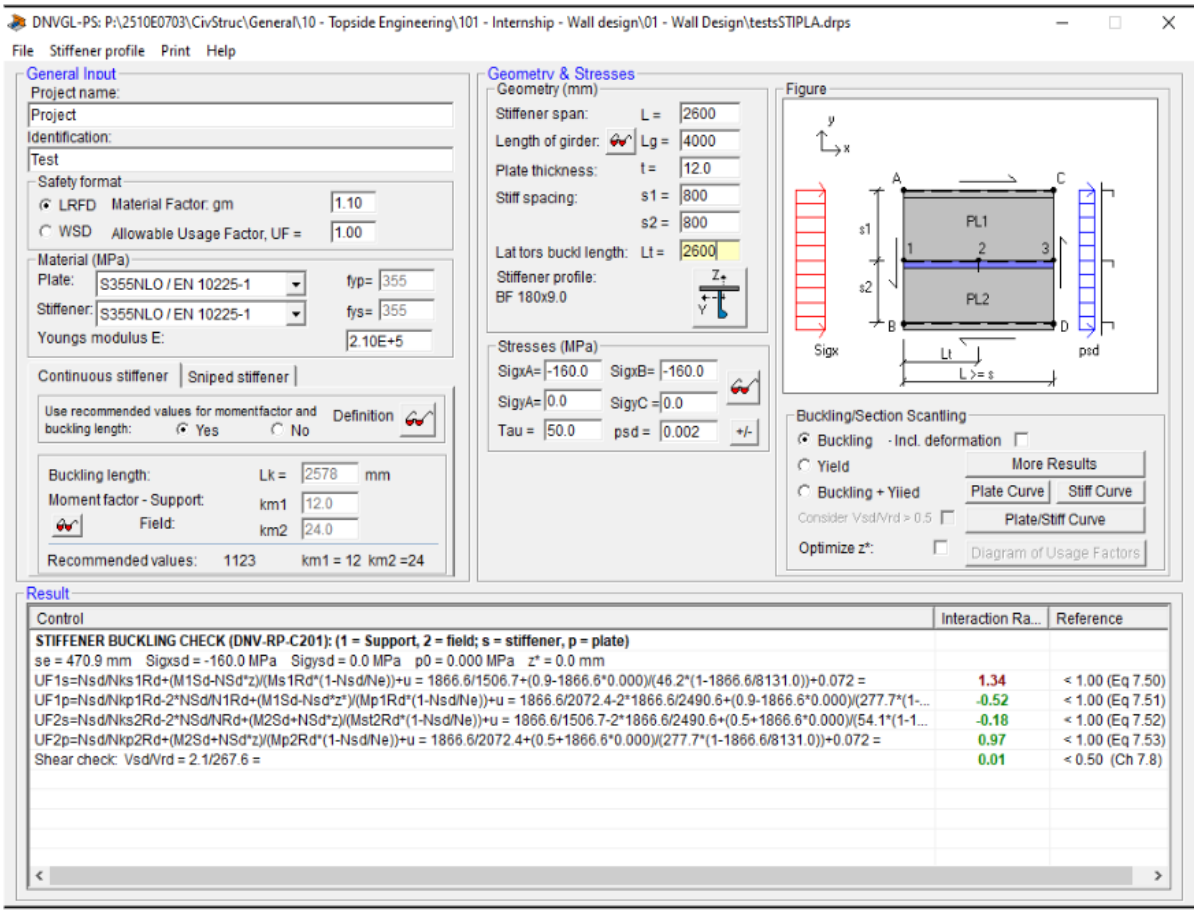
DNVGL-PS: P:\2510E0703\CivStruc\General\10 - Topside Engineering\101 - Internship - Wall design\01 - Wall Design\testsSTIPLA.drps
File Stiffener profile Print Help
General Input
Project name:
Project
Identification:
Test
Safety format
LRFD Material Factor: gm 1.10
WSD Allowable Usage Factor, UF = 1.00
Material (MPa)
Plate: S355NLO / EN 10225-1 fyp= 355
Stiffener: S355NLO / EN 10225-1 fys= 355
Youngs modulus E: 2.10E+5
Continuous stiffener Sniped stiffener
Use recommended values for momentfactor and buckling length: Yes No Definition
Buckling length: Lk = 2578 mm
Moment factor - Support: km1 12.0
Field: km2 24.0
Recommended values: 1123 km1 = 12 km2 =24
Geometry & Stresses
Geometry (mm)
Stiffener span: L = 2600
Length of girder: Lg = 4000
Plate thickness: t = 12.0
Stiff spacing: s1 = 800
s2 = 800
Lat tors buckl length: Lt = 2600
Stiffener profile:
BF 180x9.0
Stresses (MPa)
SigxA= -160.0 SigxB= -160.0
SigyA= 0.0 SigyC = 0.0
Tau = 50.0 psd = 0.002
Figure
PL1
PL2
s1
s2
Sigx
psd
Lt
L >= s
Buckling/Section Scantling
Buckling Incl. deformation
Yield
Buckling + Yiled
Consider Vsd/Vrd > 0.5
Optimize z*:
More Results
Plate Curve
Stiff Curve
Plate/Stiff Curve
Diagram of Usage Factors
Result
Control
Interaction Ra...
Reference
STIFFENER BUCKLING CHECK (DNV-RP-C201): (1 = Support, 2 = field; s = stiffener, p = plate)
se = 470.9 mm Sigxsd = -160.0 MPa Sigysd = 0.0 MPa p0 = 0.000 MPa z* = 0.0 mm
UF1s=Nsd/Nks1Rd+(M1Sd-NSd*z)/(Ms1Rd*(1-Nsd/Ne))+u = 1866.6/1506.7+(0.9-1866.6*0.000)/(46.2*(1-1866.6/8131.0))+0.072 = 1.34 < 1.00 (Eq 7.50)
UF1p=Nsd/Nkp1Rd-2*NSd/N1Rd+(M1Sd-Nsd*z*)/(Mp1Rd*(1-Nsd/Ne))+u = 1866.6/2072.4-2*1866.6/2490.6+(0.9-1866.6*0.000)/(277.7*(1-... -0.52 < 1.00 (Eq 7.51)
UF2s=Nsd/Nks2Rd-2*NSd/NRd+(M2Sd+NSd*z)/(Mst2Rd*(1-Nsd/Ne))+u = 1866.6/1506.7-2*1866.6/2490.6+(0.5+1866.6*0.000)/(54.1*(1-1... -0.18 < 1.00 (Eq 7.52)
UF2p=Nsd/Nkp2Rd+(M2Sd+NSd*z)/(Mp2Rd*(1-Nsd/Ne))+u = 1866.6/2072.4+(0.5+1866.6*0.000)/(277.7*(1-1866.6/8131.0))+0.072 = 0.97 < 1.00 (Eq 7.53)
Shear check: Vsd/Vrd = 2.1/267.6 = 0.01 < 0.50 (Ch 7.8)